

Ortho-phenyl dialkylphosphonium sulfonate compounds: two rotamers in equilibrium

Emmanuelle Martin-Mothes, Emmanuel Puig, Laure Vendier, Christian Bijani, Mary Grellier
and Sébastien Bontemps*

CNRS, LCC (Laboratoire de Chimie de Coordination), 205 route de Narbonne, BP 44099, F-31077 Toulouse
Cedex 4, France and Université de Toulouse, UPS, INPT, F-31077 Toulouse Cedex 4, France

Table of Contents

NMR and IR Spectra of compound 1	2
NMR and IR Spectra of compound 2	13
NMR and IR Spectra of compound 3	22
NMR and IR Spectra of compound 4	34
Dynamic exchange between the exo and endo form in solution for 1-3.....	40
X-Ray Analyses and Structural Figures	46
References.....	48

NMR and IR Spectra of compound 1

emoL0017.4.fid
P31_DECOPPLE_H1
EMM172 - Vérification apres RMN du solide

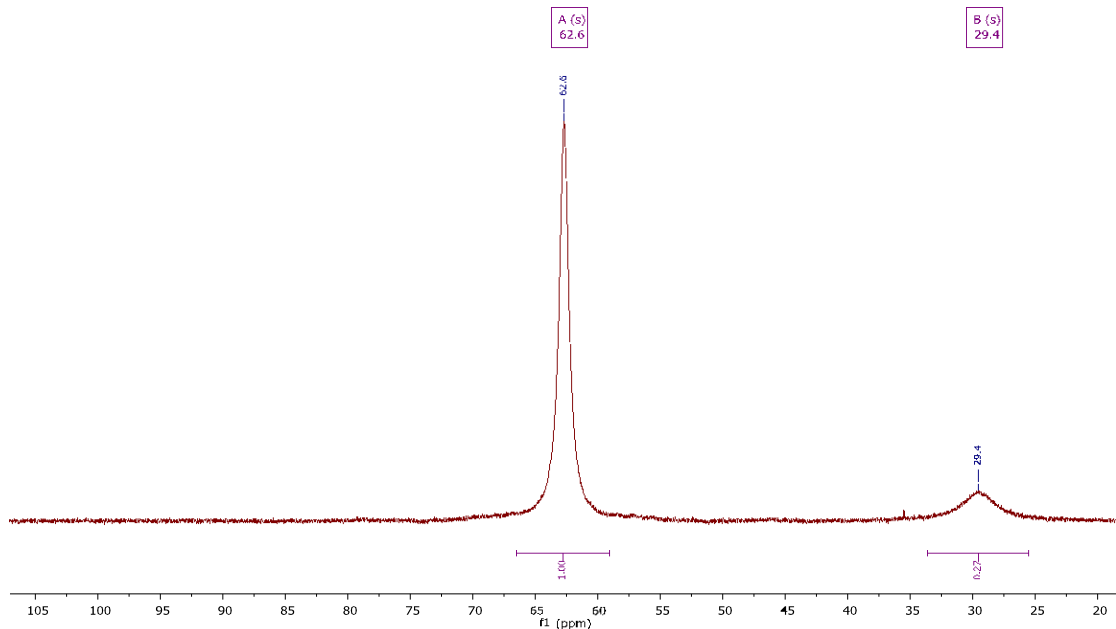


Figure S1. $^{31}\text{P}\{\text{H}\}$ NMR spectrum for compound 1 at 298 K in CD_2Cl_2

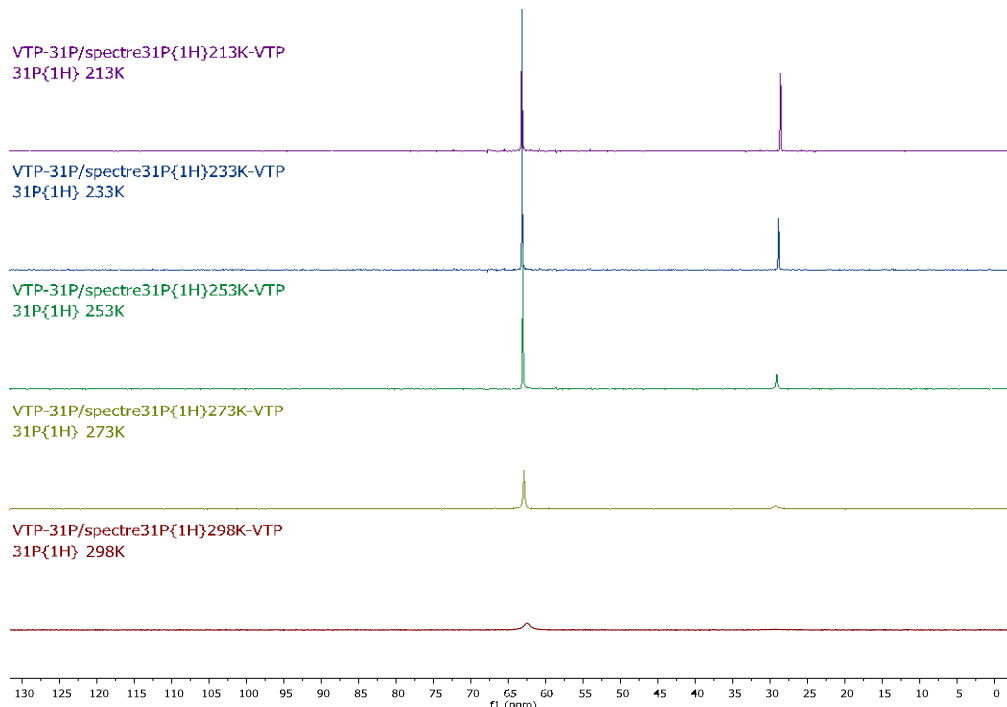


Figure S2. Variable temperature $^{31}\text{P}\{\text{H}\}$ NMR spectra for compound 1 from 298 K to 213 K in CD_2Cl_2

osbG170609.5.fid
 Sample: EMM172
 Probc: 3.2mm Vr = 16kHz
 31P CP

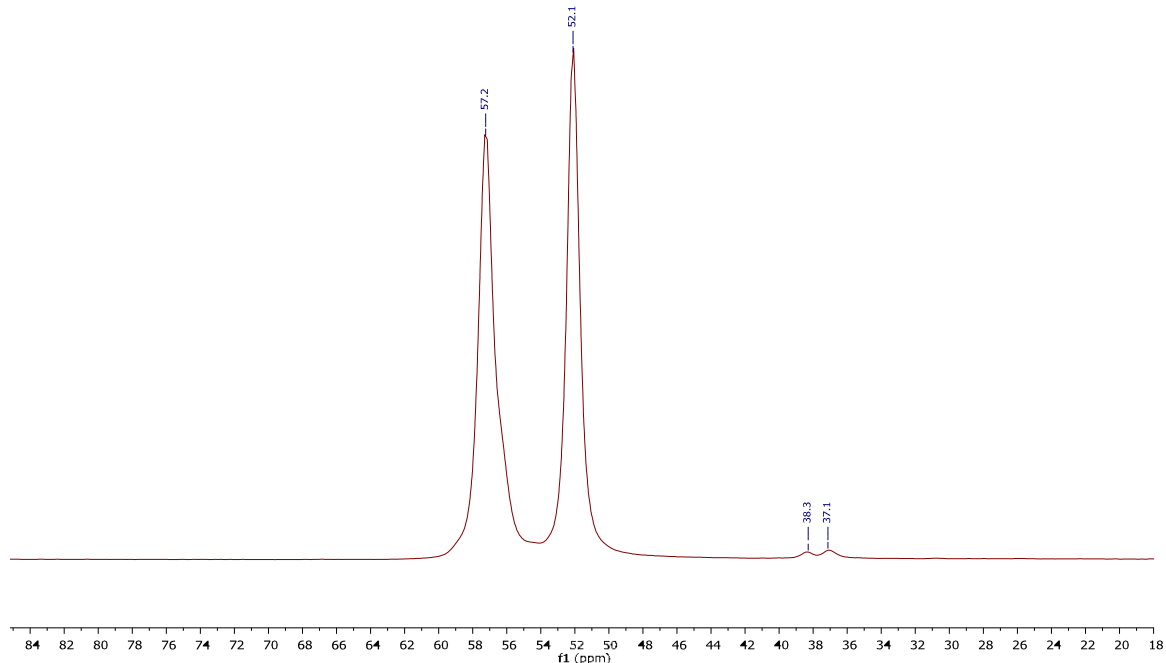


Figure S3. Solid state CPMAS ^{31}P NMR spectrum for compound 1

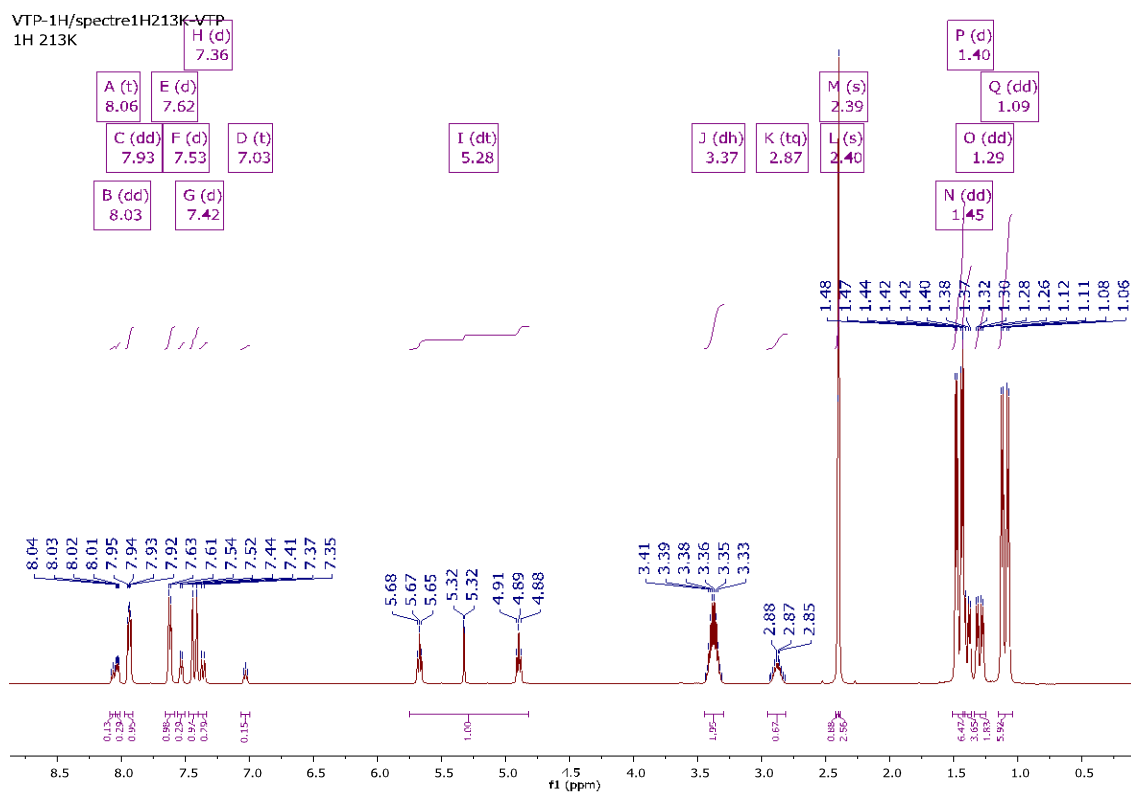


Figure S4. ^1H NMR spectrum for compound 1 at 213 K in CD_2Cl_2

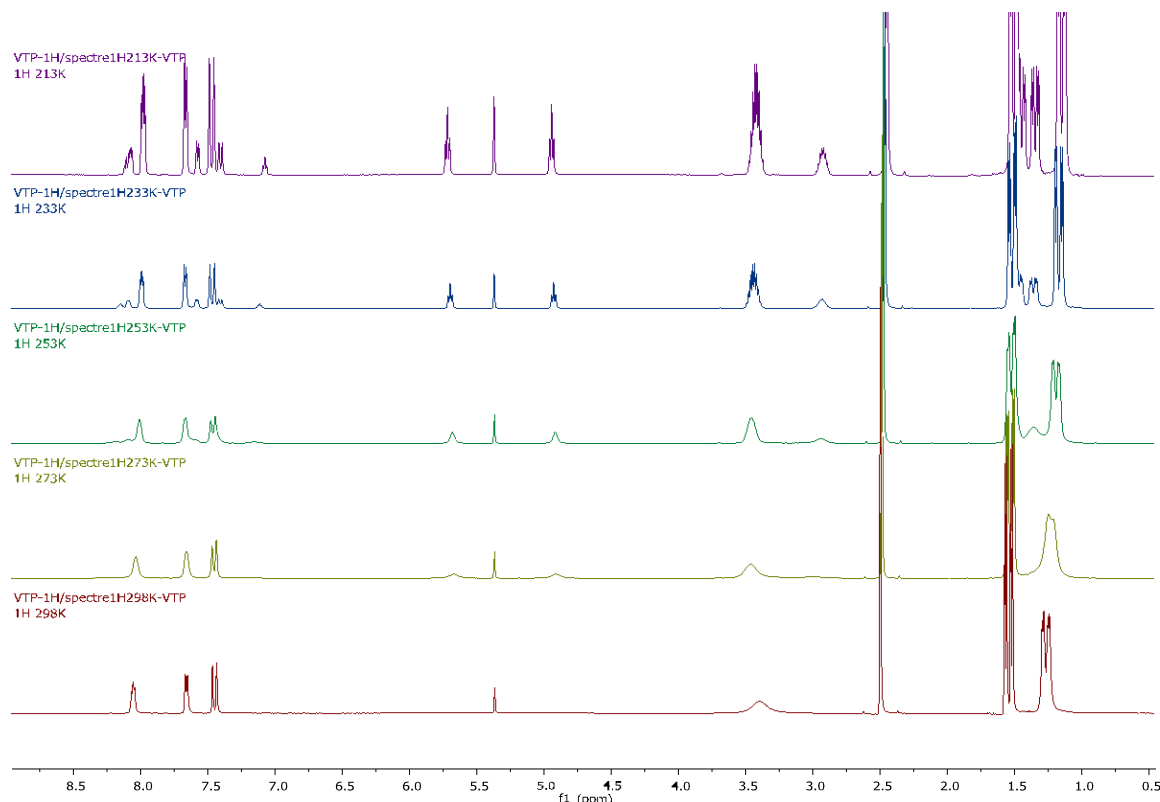


Figure S5. Variable temperature ^1H NMR spectra for compound **1** from 298 K to 213 K in CD_2Cl_2

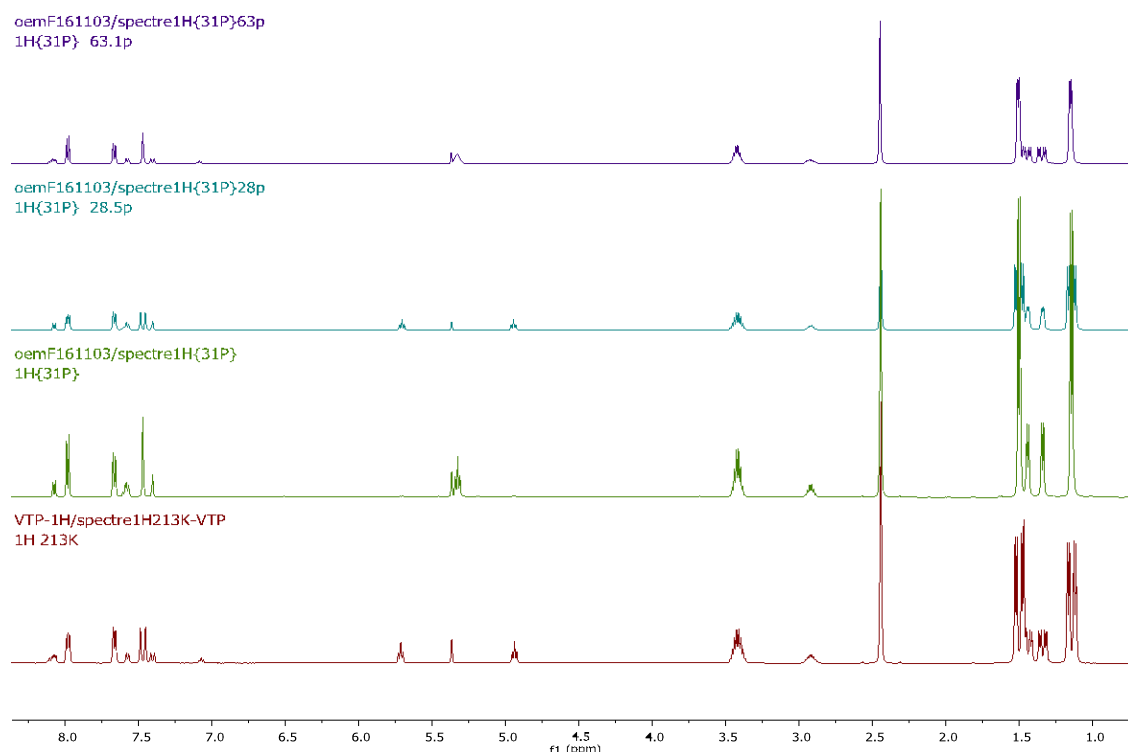


Figure S6. ^1H NMR analysis of compound **1** at 213 K in CD_2Cl_2 , from bottom to top: no ^{31}P decoupling, broad band ^{31}P decoupling, selective ^{31}P decoupling at 28 ppm, selective ^{31}P decoupling at 63 ppm.

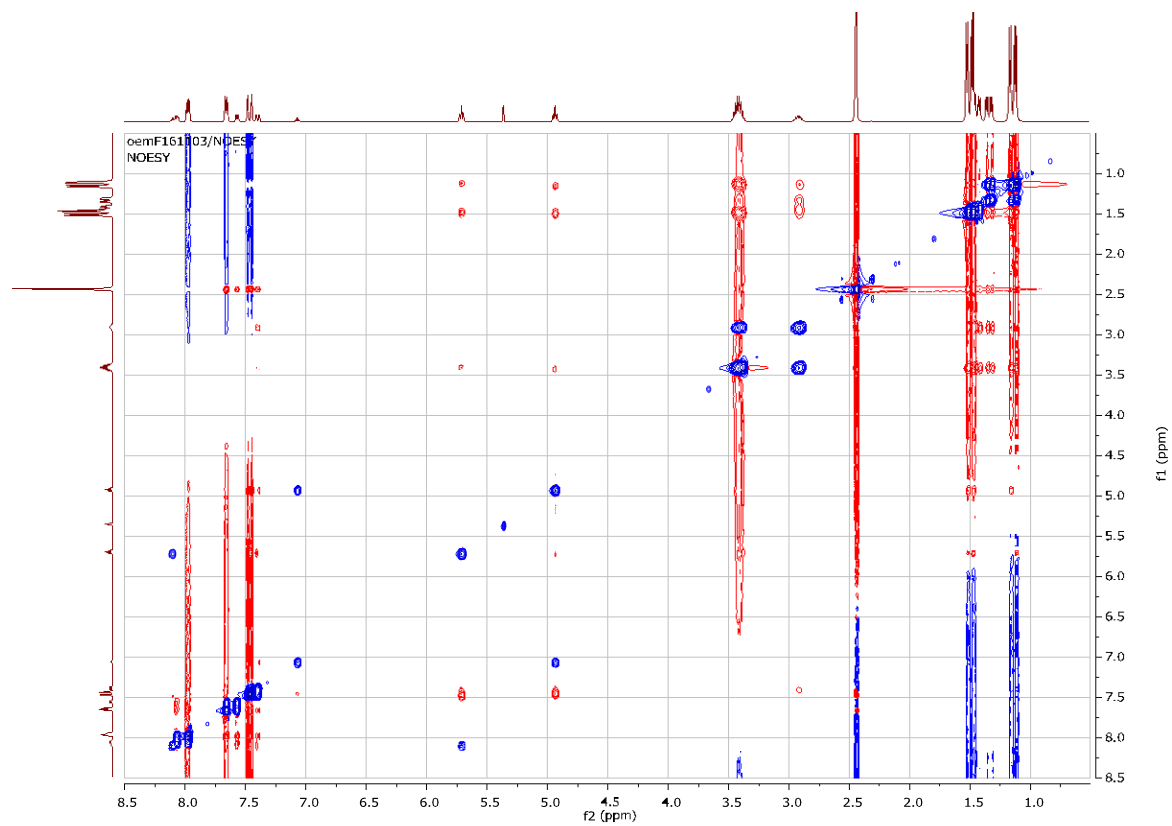


Figure S7. NOESY $^1\text{H}/^1\text{H}$ spectrum for compound **1** at 213 K in CD_2Cl_2

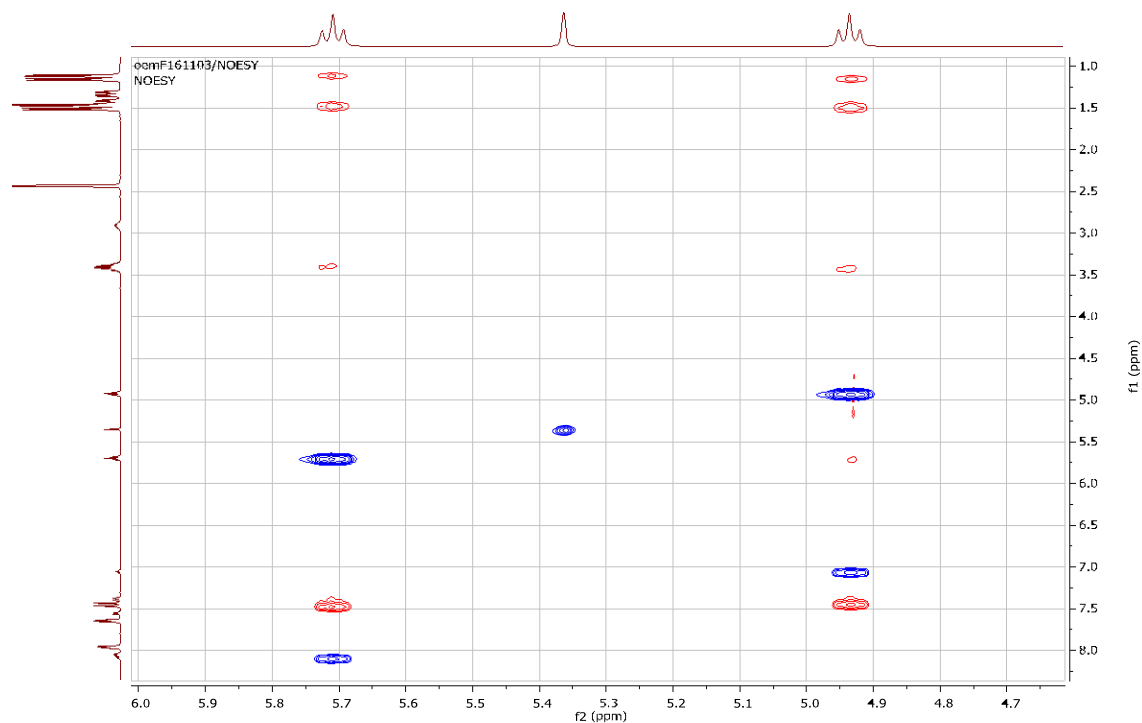


Figure S8. NOESY $^1\text{H}/^1\text{H}$ spectrum for compound **1** at 213 K, zoom on H-P form **1** in CD_2Cl_2

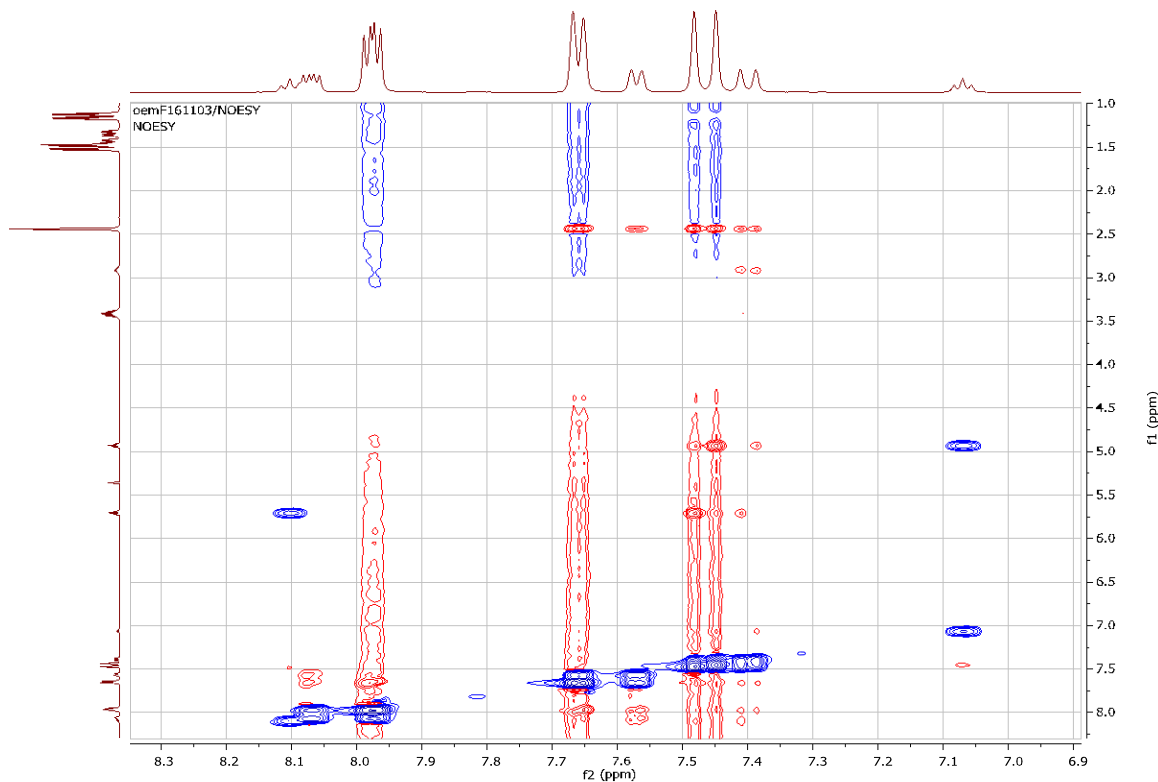


Figure S9. NOESY $^1\text{H}/^1\text{H}$ spectrum for compound **1** at 213 K, zoom on H-P form 2 in CD_2Cl_2

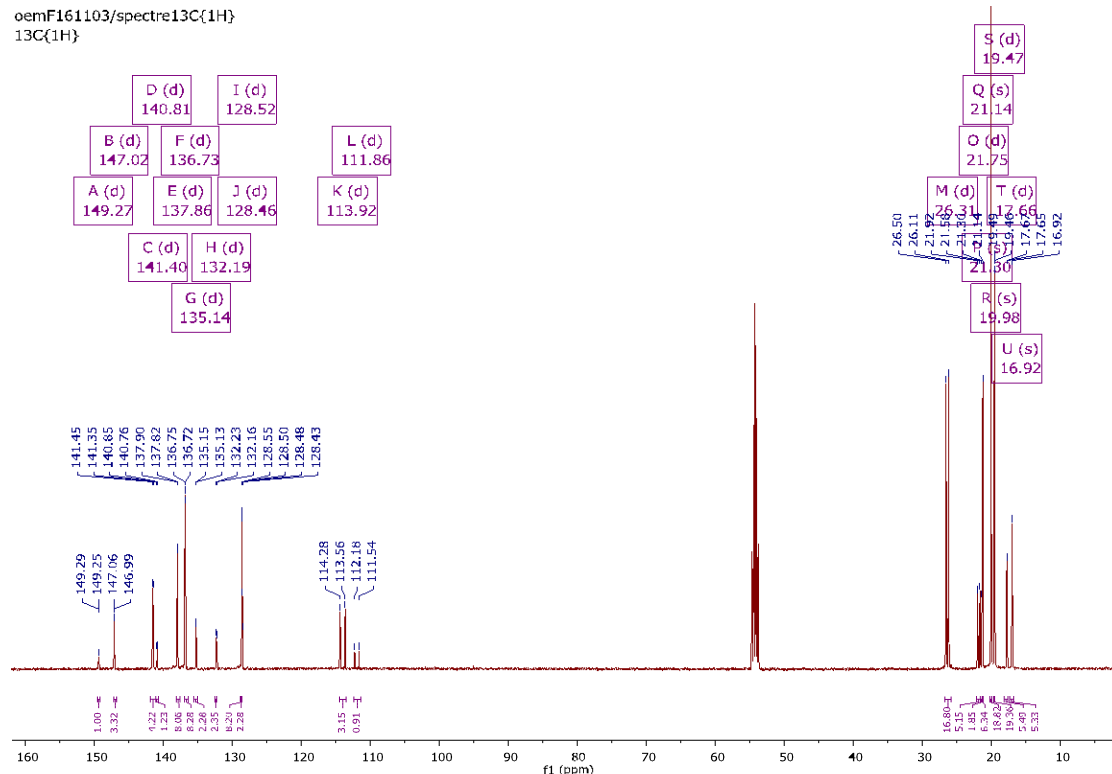


Figure S10. $^{13}\text{C}\{^1\text{H}\}$ NMR spectrum of compound **1** at 213 K in CD_2Cl_2

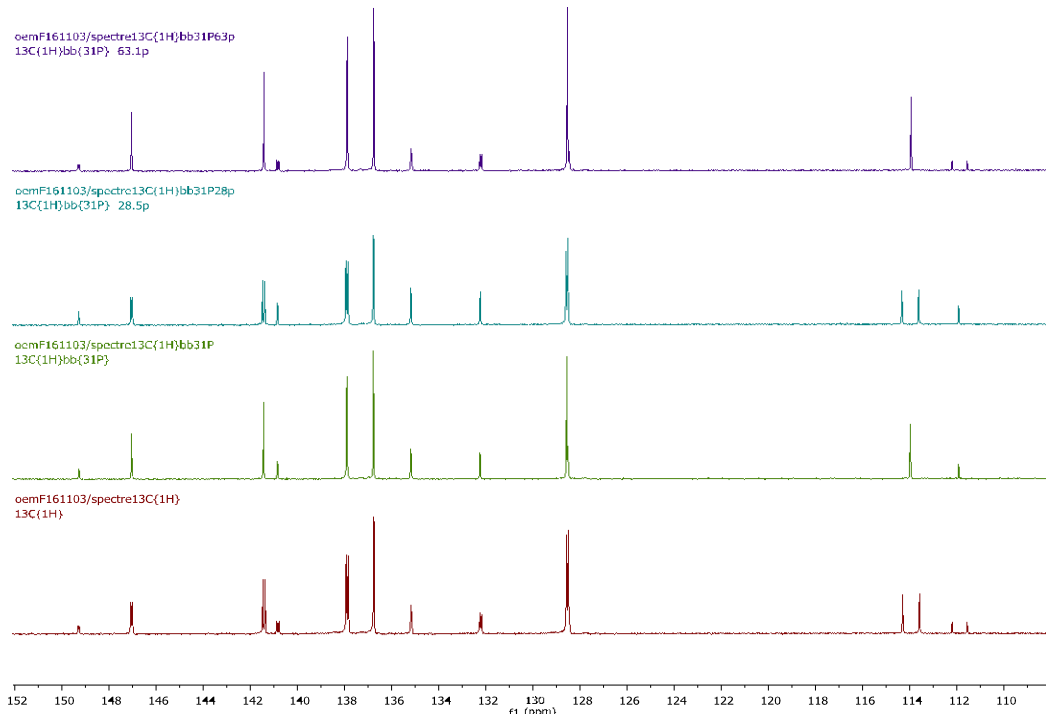


Figure S11. $^{13}\text{C}\{^1\text{H}\}$ NMR analysis of compound **1** at 213 K in CD_2Cl_2 , from bottom to top: no ^{31}P decoupling, broad band ^{31}P decoupling, selective ^{31}P decoupling at 28.5 ppm, selective ^{31}P decoupling at 63.1 ppm.

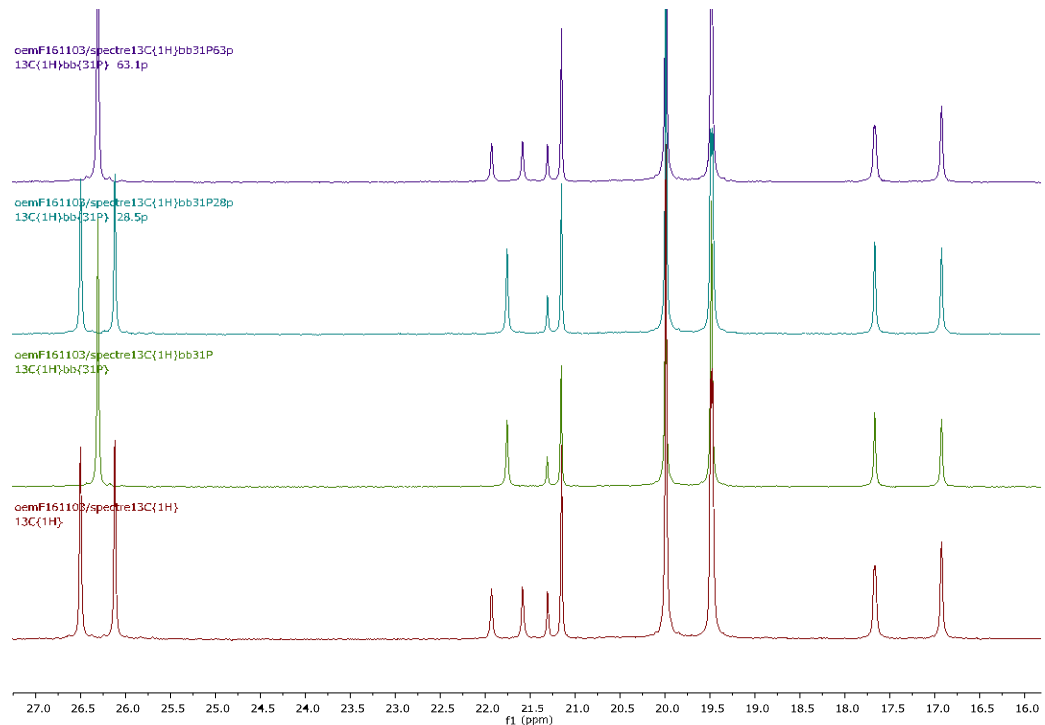


Figure S12. $^{13}\text{C}\{^1\text{H}\}$ NMR analysis of compound **1** at 213 K in CD_2Cl_2 , from bottom to top: no ^{31}P decoupling, broad band ^{31}P decoupling, selective ^{31}P decoupling at 28.5 ppm, selective ^{31}P decoupling at 63.1 ppm, 27.5 to 16.0 ppm window.

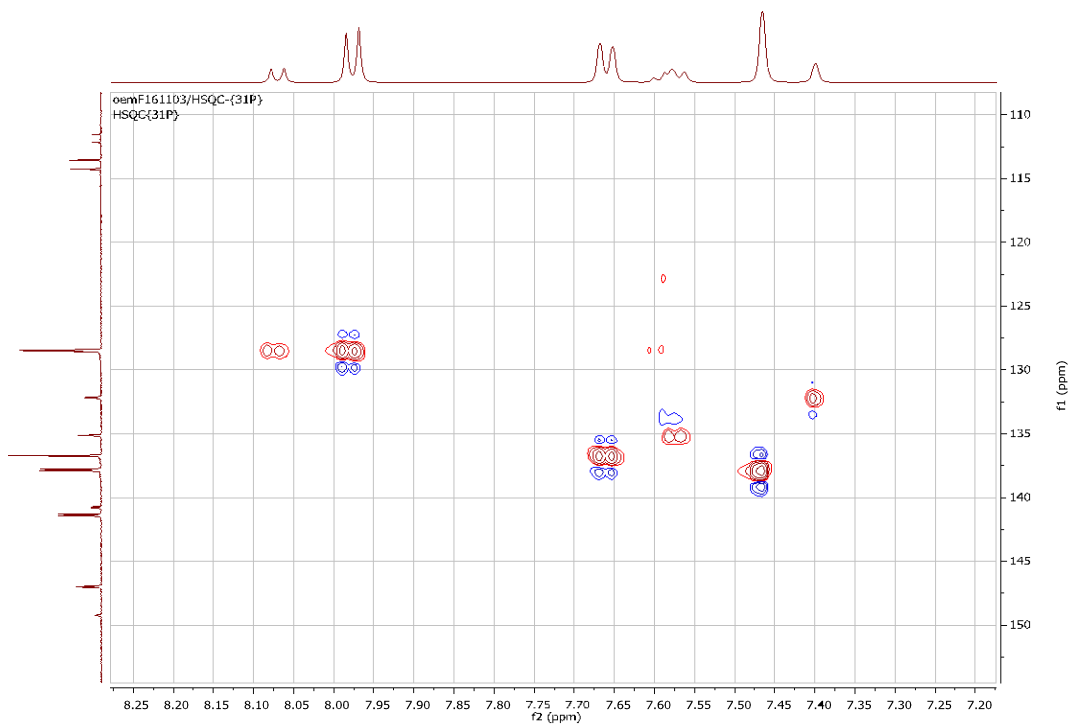


Figure S13. ^1H / $^{13}\text{C}\{^1\text{H}\}$ NMR HSQC experiment at 213 K for compound **1**, zoom 1 in CD_2Cl_2

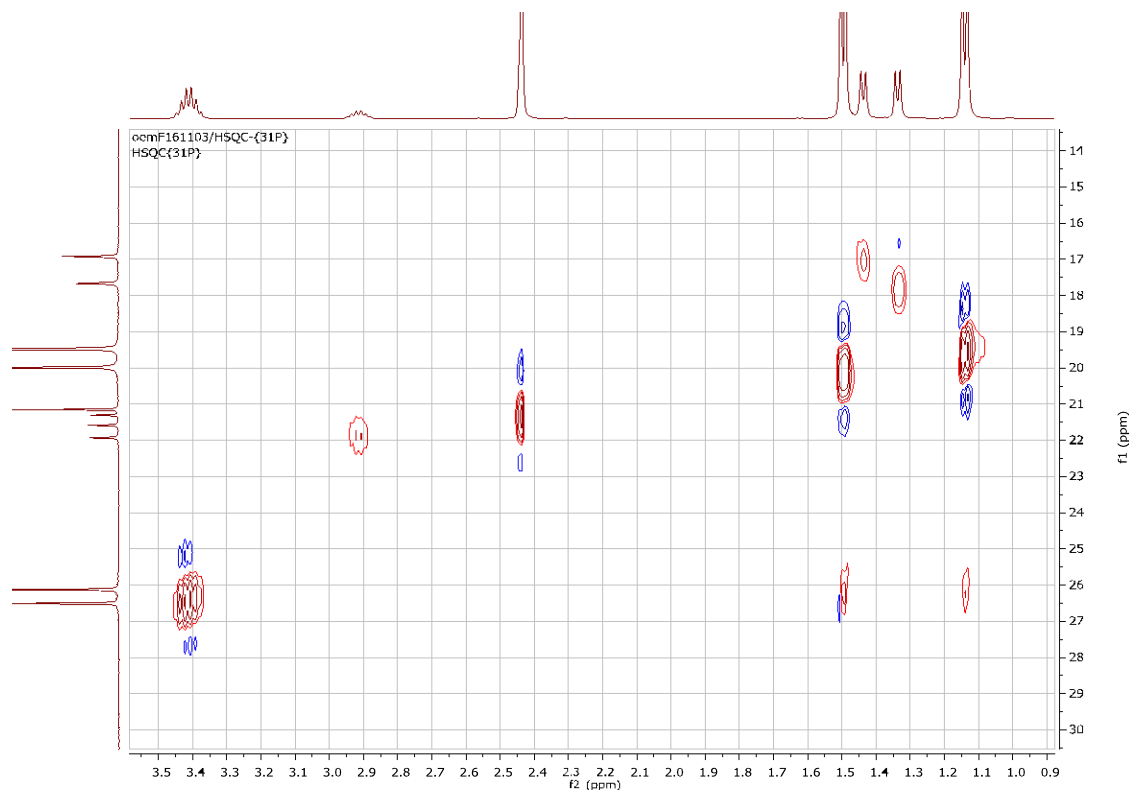


Figure S14. ^1H / $^{13}\text{C}\{^1\text{H}\}$ NMR HSQC experiment at 213 K for compound **1**, zoom 2 in CD_2Cl_2

emoL0019.2.fid
H1_INI
EMM183 : K[PO-iPr]

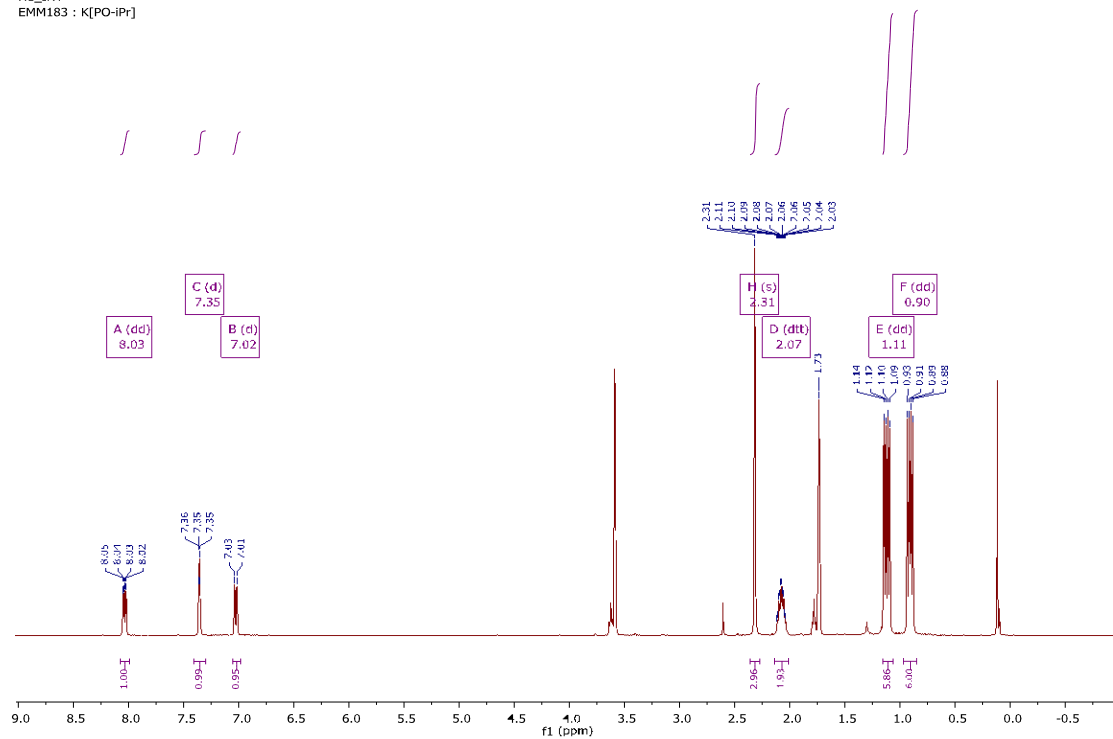


Figure S15. ^1H NMR spectrum for compound **K[PO-iPr]** at 298 K in $\text{THF}-\text{d}_8$

emoL0019.3.fid
P31_DECOPPLE_H1
EMM183 : K[PO-iPr]

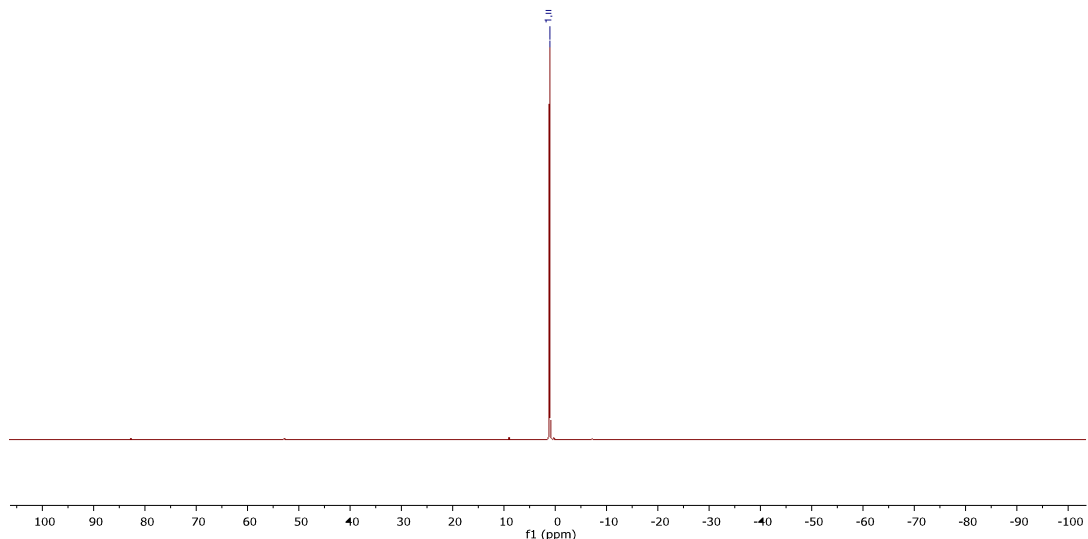


Figure S16. $^{31}\text{P}\{^1\text{H}\}$ NMR spectrum for compound **K[PO-iPr]** at 298 K in $\text{THF}-\text{d}_8$

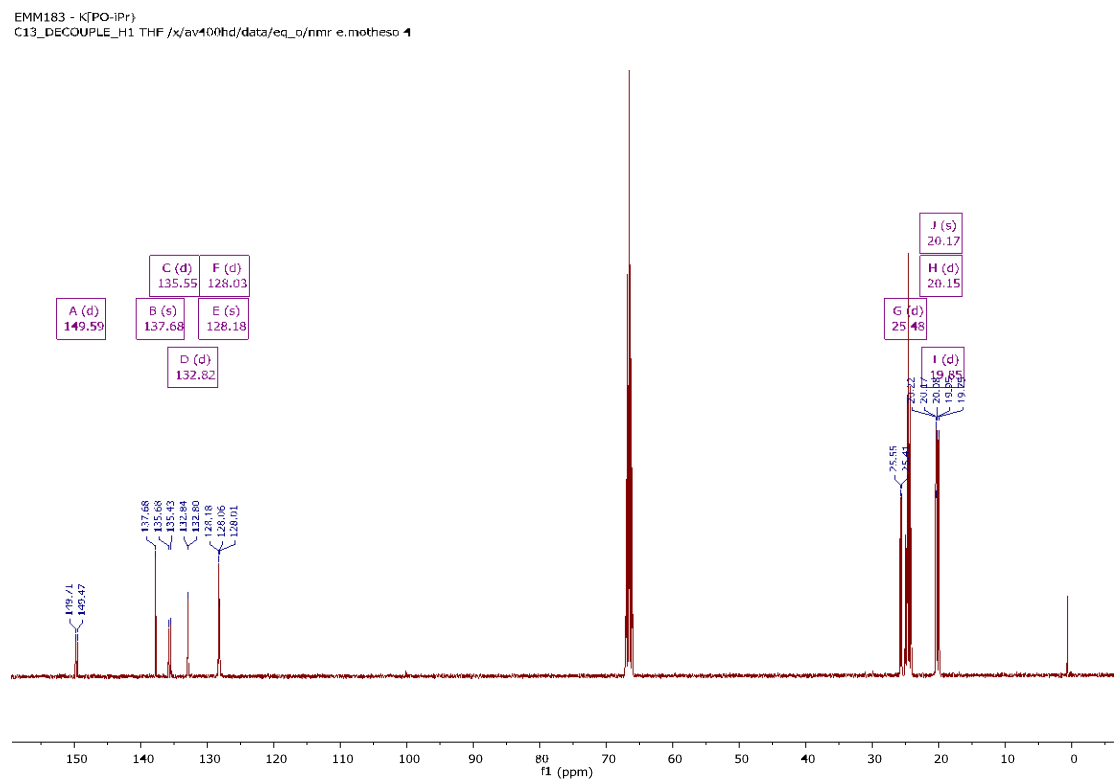


Figure S17. $^{13}\text{C}\{^1\text{H}\}$ NMR spectrum for compound **K[PO-iPr]** at 298 K in THF- d_8

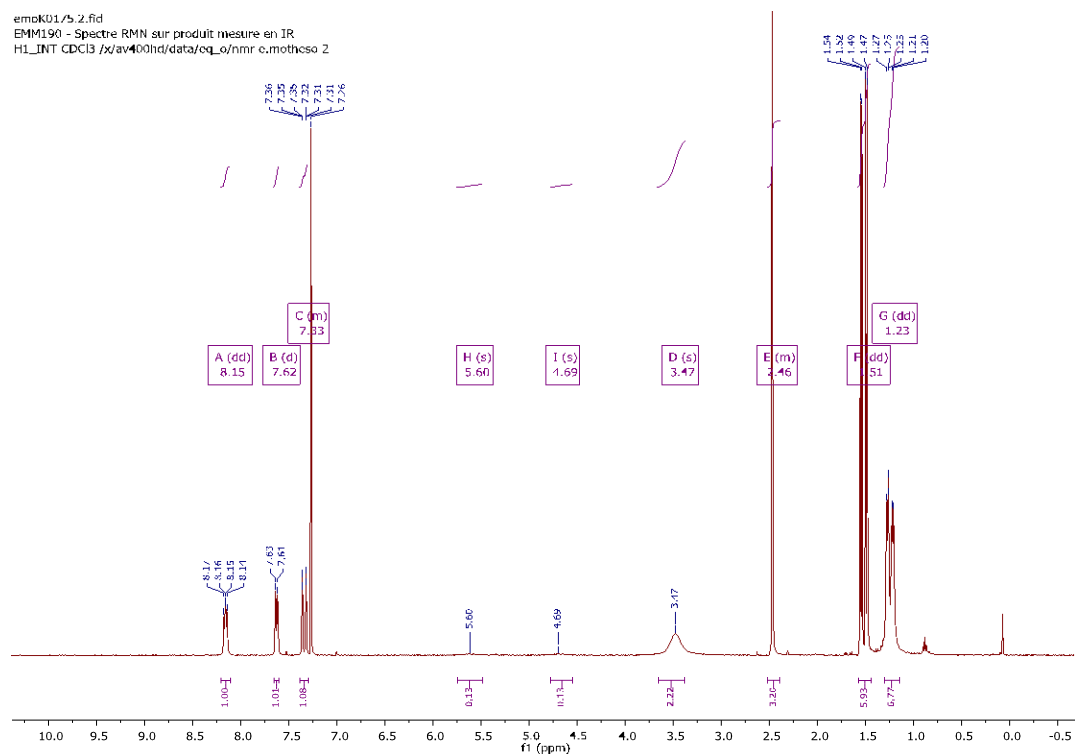


Figure S18. ^1H NMR spectrum for compound D[PO-iPr] at 298 K in CDCl_3

emoK0175.3.fid
EMM190 - Spectre RMN sur produit mesuré en 63.13 s
P31_DECUPLE_H1 CDCl₃ /x/av400hd/data/eq_o/nmr e.mothoso 2

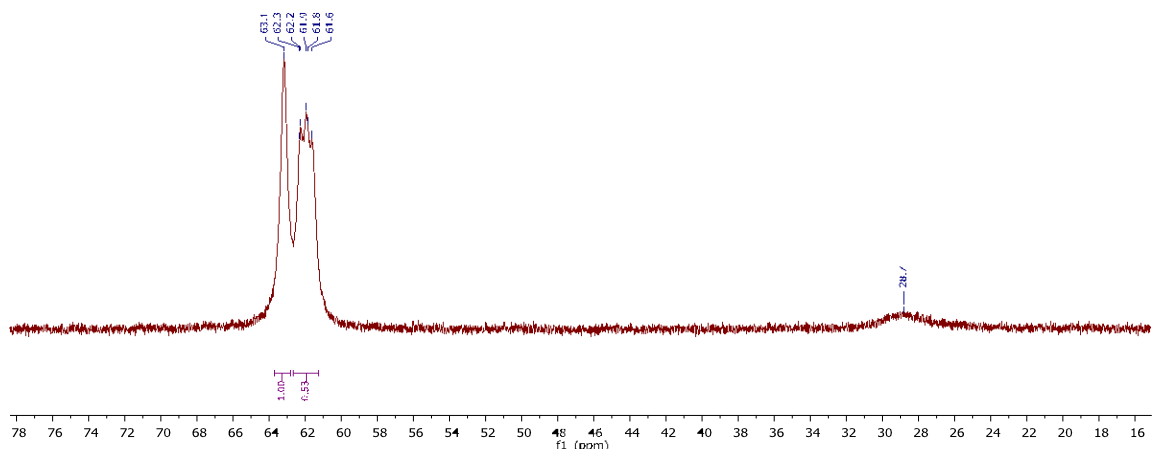
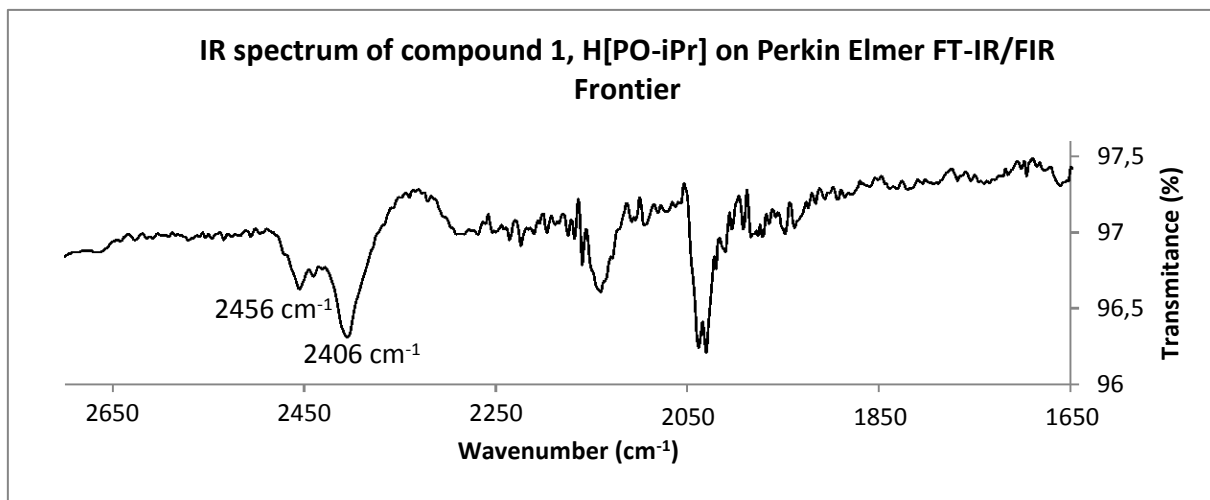
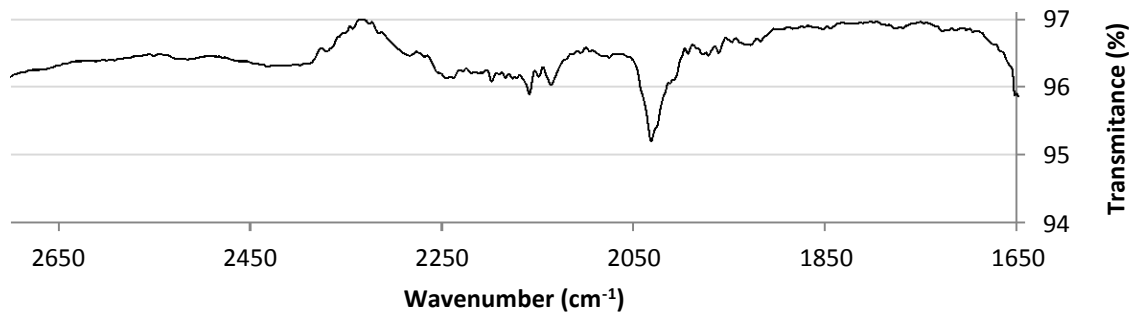


Figure S19. ³¹P{¹H} NMR spectrum for compound D[PO-iPr] at 298 K in CDCl₃



IR spectrum of K[PO-iPr] on Perkin Elmer FT-IR/FIR Frontier (100 scans)



IR spectrum of a mixture of $^2\text{H}[\text{PO-iPr}]$ et $^1\text{H}[\text{PO-iPr}]$ on Perkin Elmer FT-IR/FIR Frontier

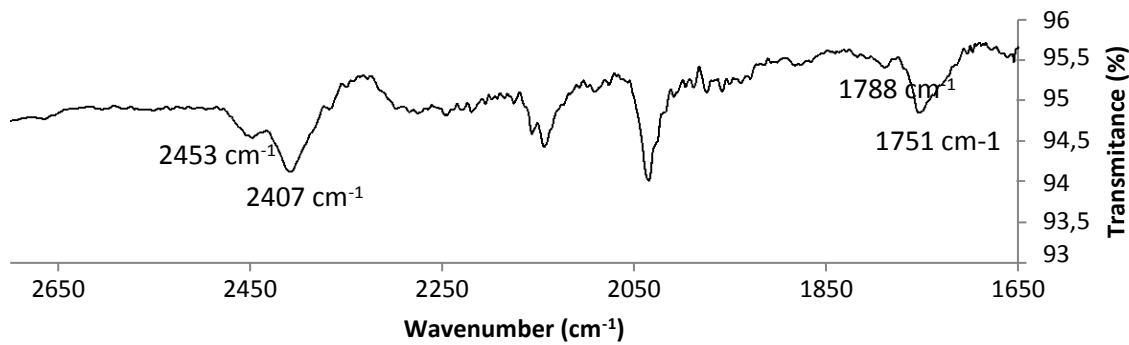


Figure S20. Powder ATR IR for compound 1.

NMR and IR Spectra of compound 2

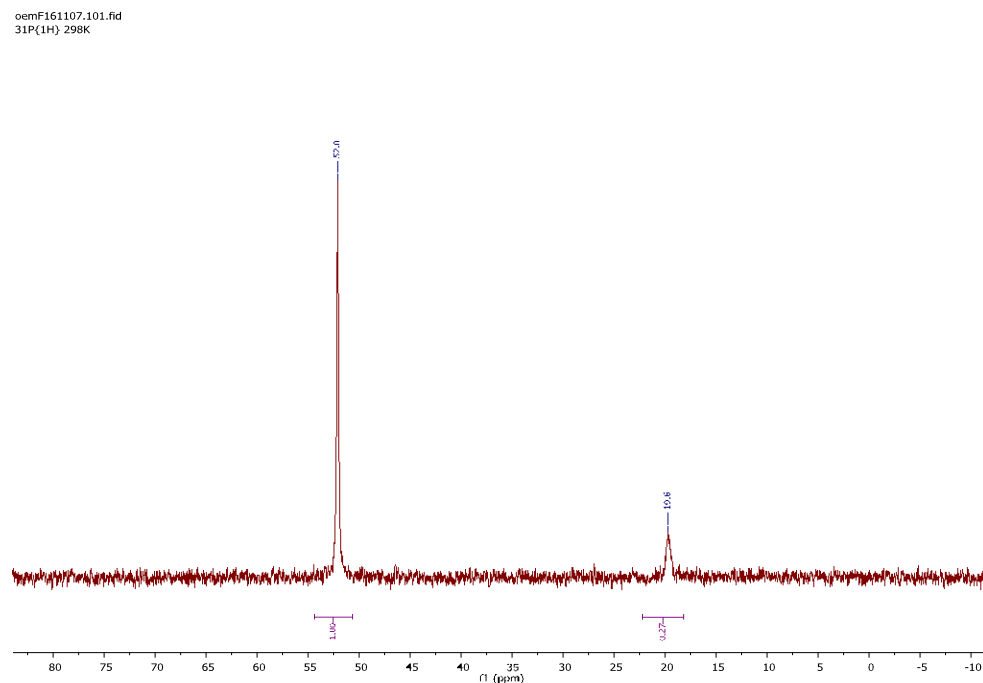


Figure S21. $^{31}\text{P}\{^1\text{H}\}$ NMR spectrum for compound 2 at 298 K in CD_2Cl_2

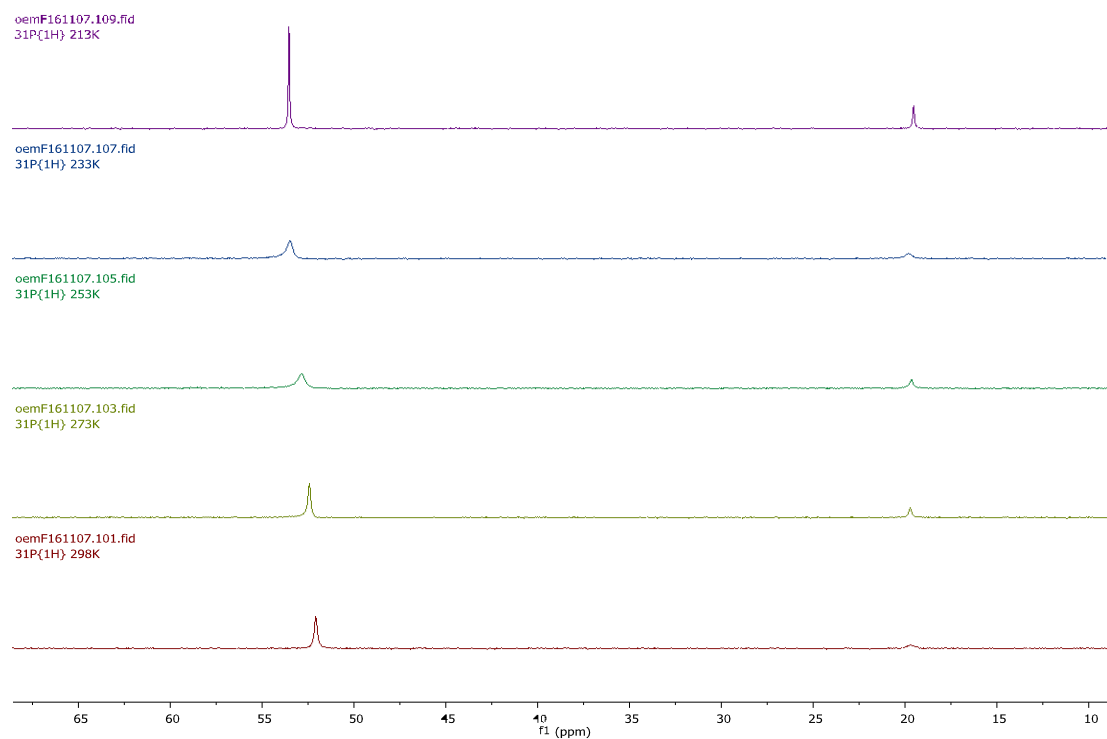


Figure S22. Variable temperature $^{31}\text{P}\{^1\text{H}\}$ NMR spectra for compound 2 from 298 K to 213 K in CD_2Cl_2

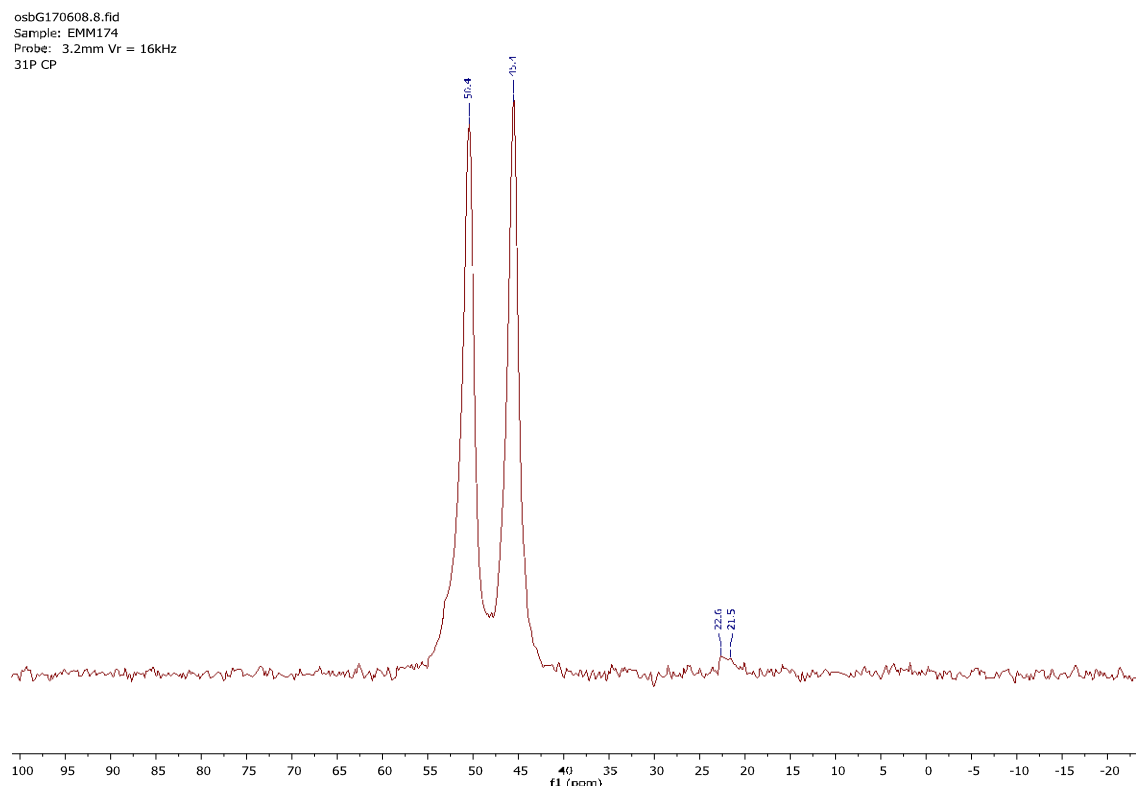


Figure S23. Solid state CPMAS ^{31}P NMR spectrum for compound 2

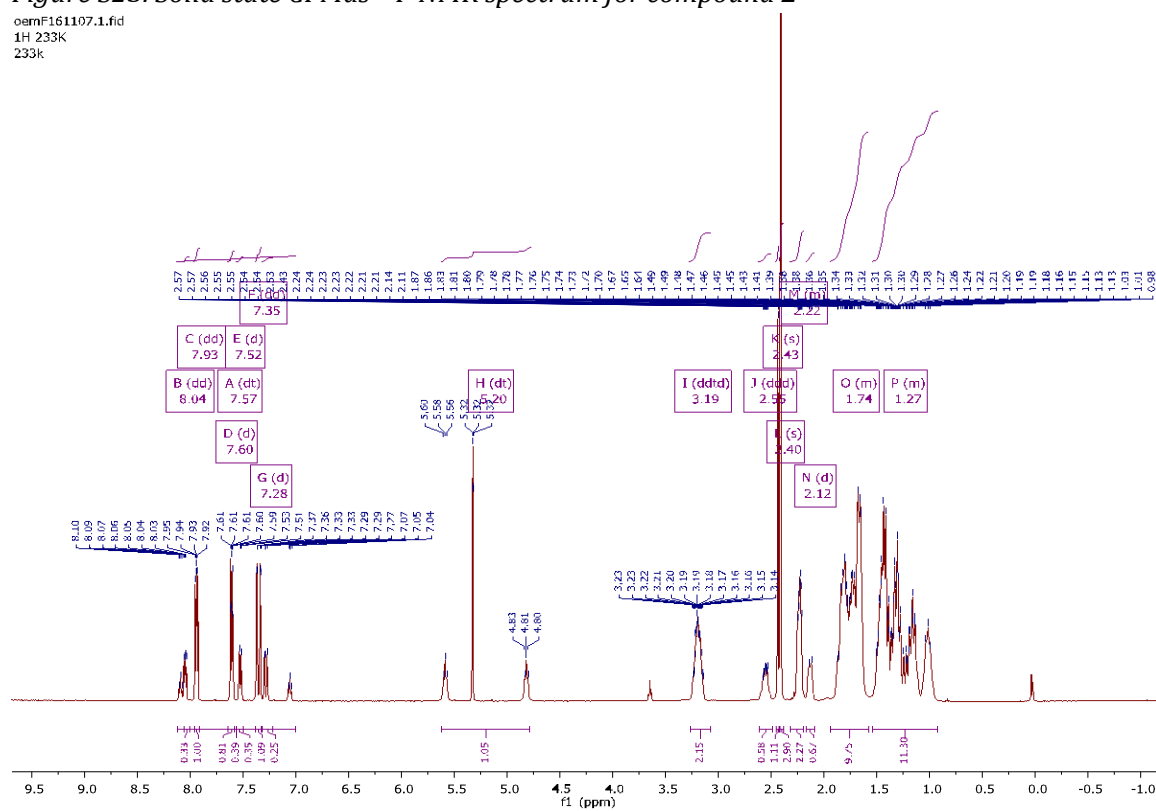


Figure S24. ^1H NMR spectrum for compound **2** at 233 K in CD_2Cl_2

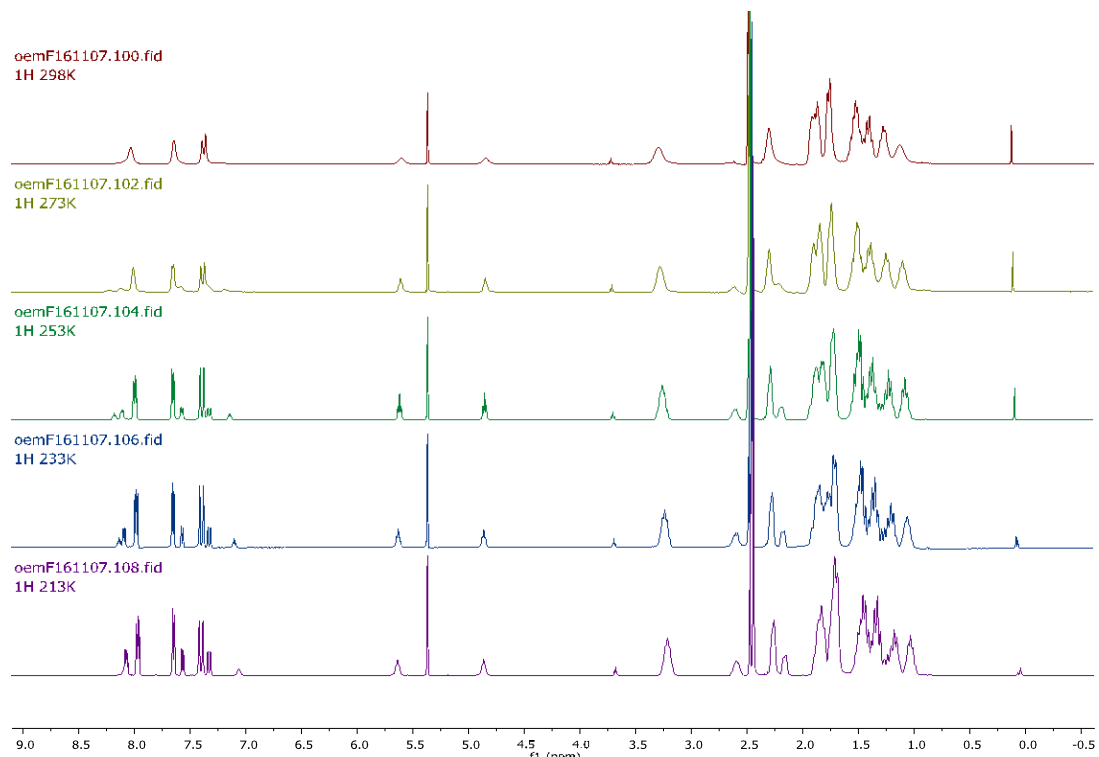


Figure S25. Variable temperature ^1H NMR spectra for compound **2** from 298 K to 213 K in CD_2Cl_2

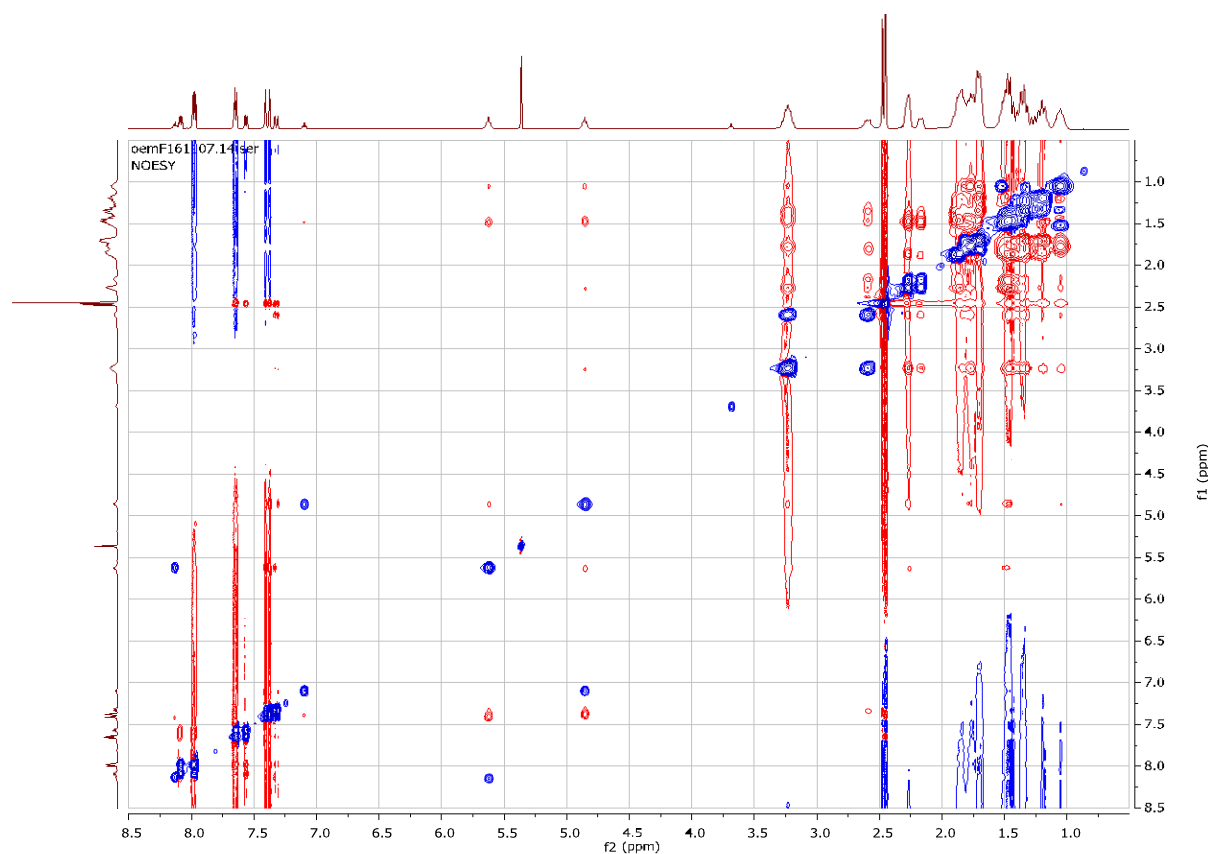


Figure S26. NOESY $^1\text{H}/^1\text{H}$ spectrum for compound **2** at 233 K in CD_2Cl_2

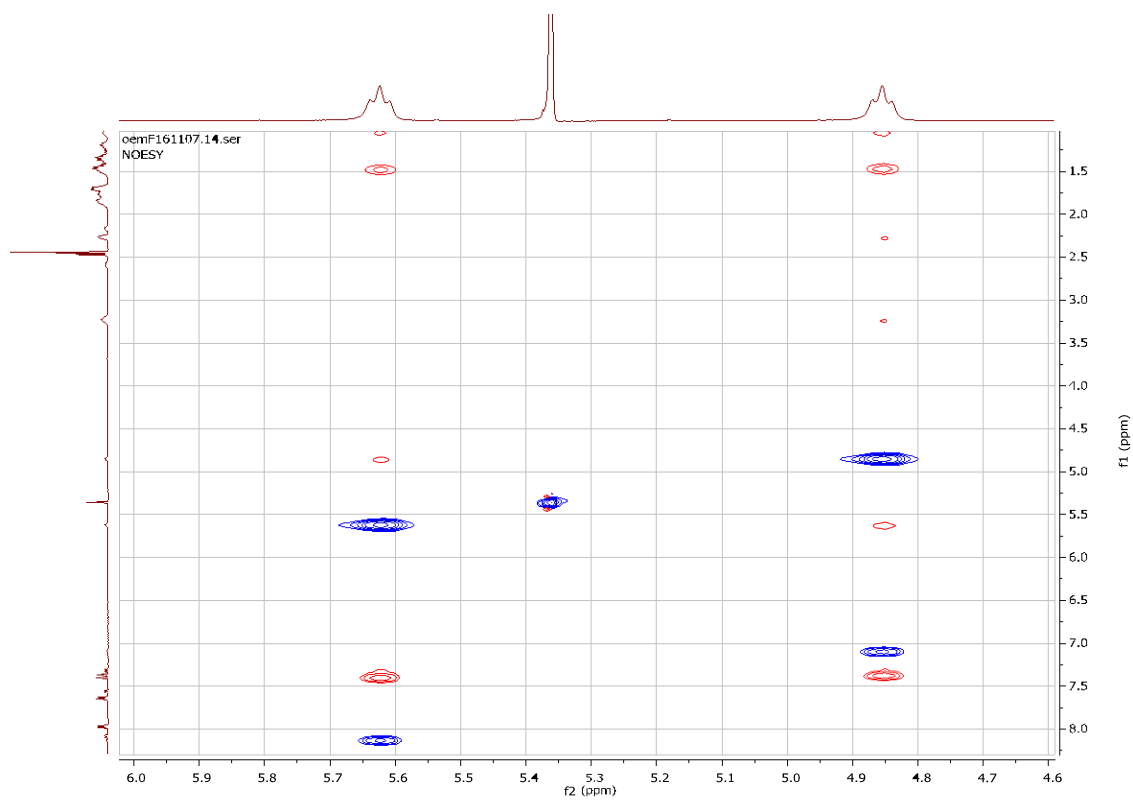


Figure S27. NOESY $^1\text{H}/^1\text{H}$ spectrum for compound **2** at 233 K, zoom on H-P form 1 in CD_2Cl_2

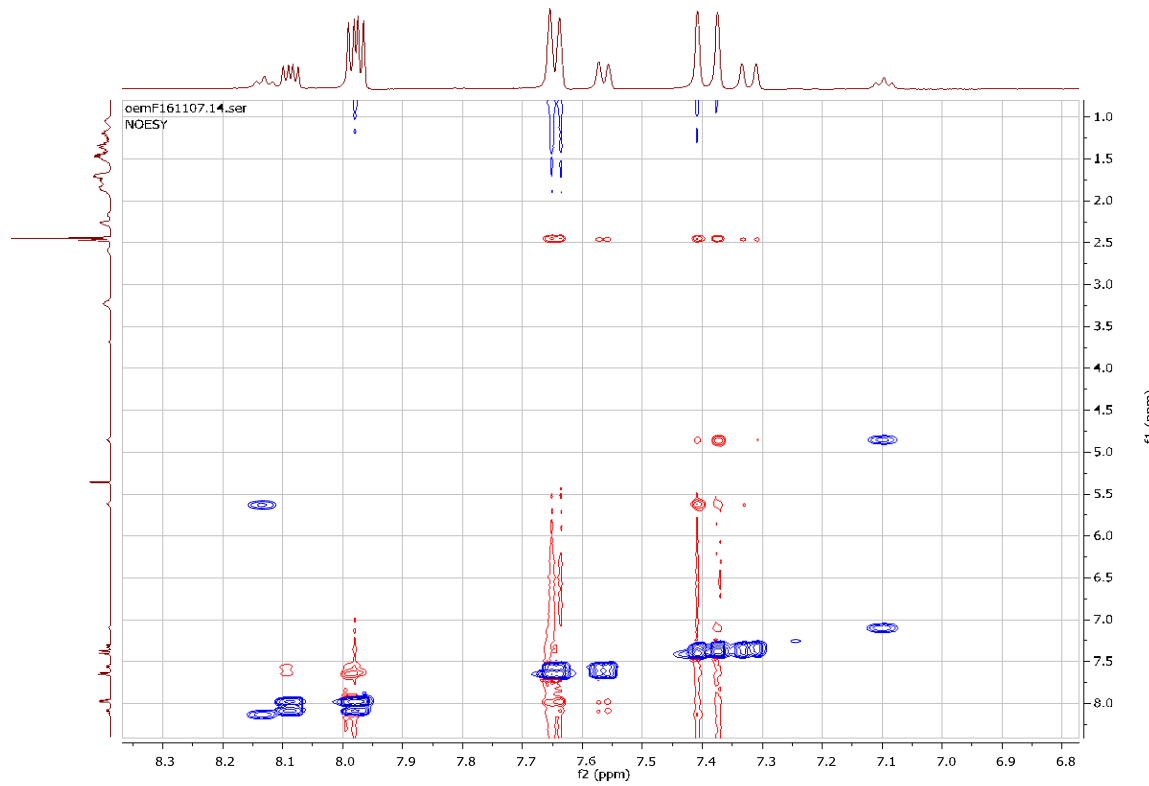


Figure S28. NOESY $^1\text{H}/^1\text{H}$ spectrum for compound **2** at 233 K, zoom on H-P form 2 in CD_2Cl_2

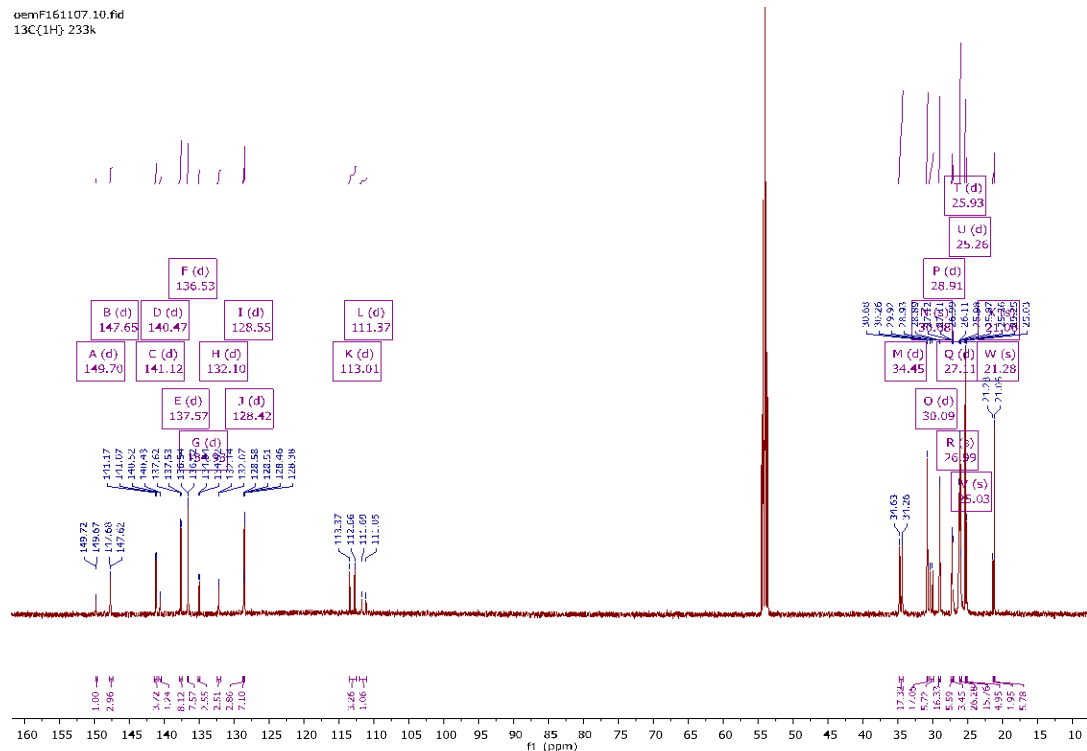


Figure S29. $^{13}\text{C}\{^1\text{H}\}$ NMR spectrum of compound **2** at 213 K in CD_2Cl_2

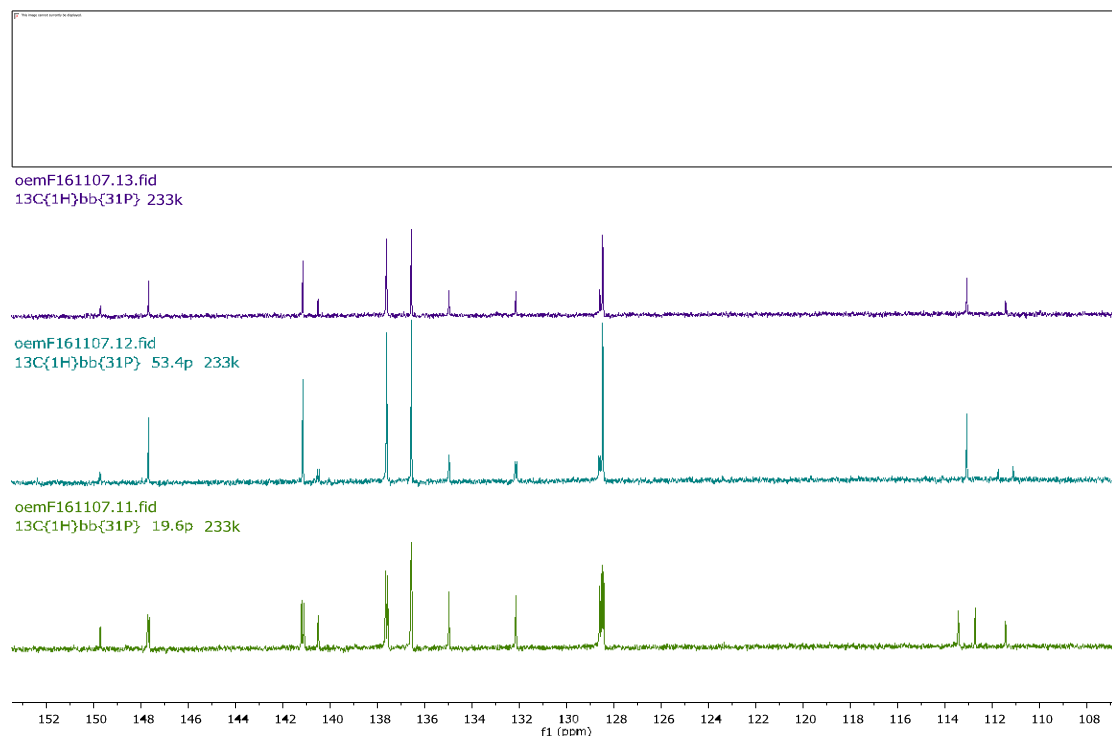


Figure S30. $^{13}\text{C}\{^1\text{H}\}$ NMR analysis of compound **2** at 233 K in CD_2Cl_2 , from top to bottom: no ^{31}P decoupling, broad band ^{31}P decoupling, selective ^{31}P decoupling at 53.4 ppm, selective ^{31}P decoupling at 19.6 ppm, 153 to 107 ppm window.

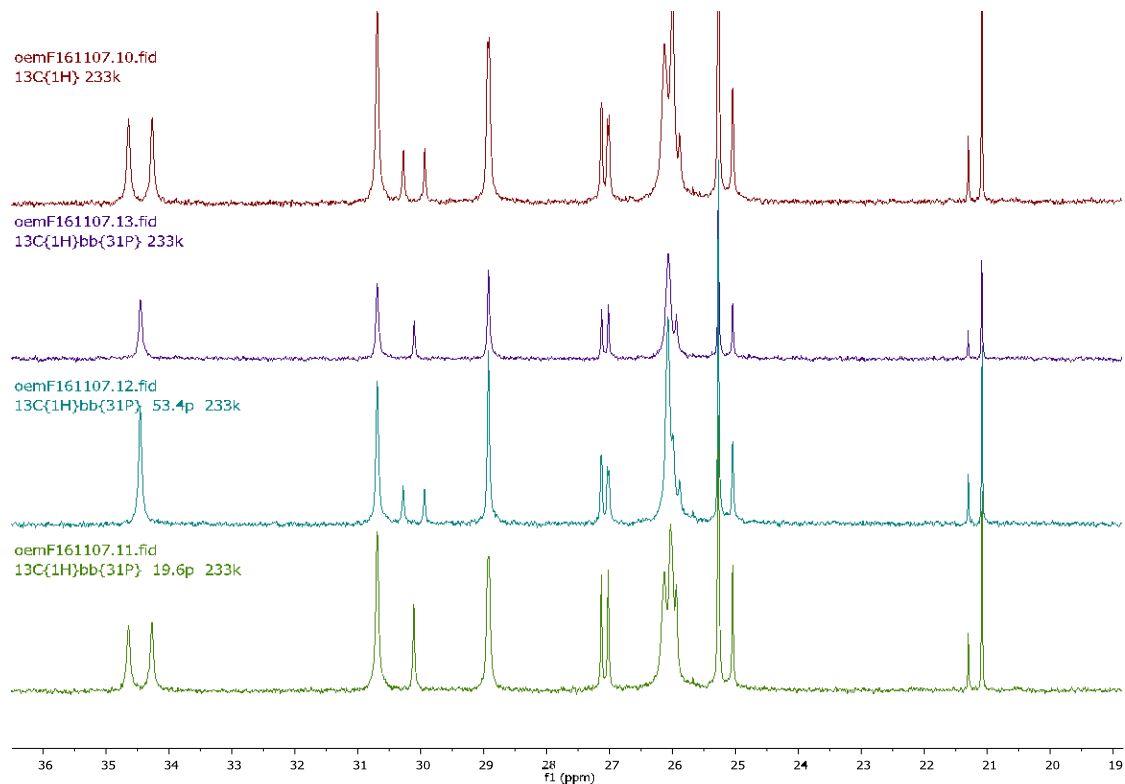


Figure S31. $^{13}\text{C}\{^1\text{H}\}$ NMR analysis of compound **2** at 233 K in CD_2Cl_2 , from top to bottom: no ^{31}P decoupling, broad band ^{31}P decoupling, selective ^{31}P decoupling at 53.4 ppm, selective ^{31}P decoupling at 19.6 ppm, 36 to 19 ppm window.

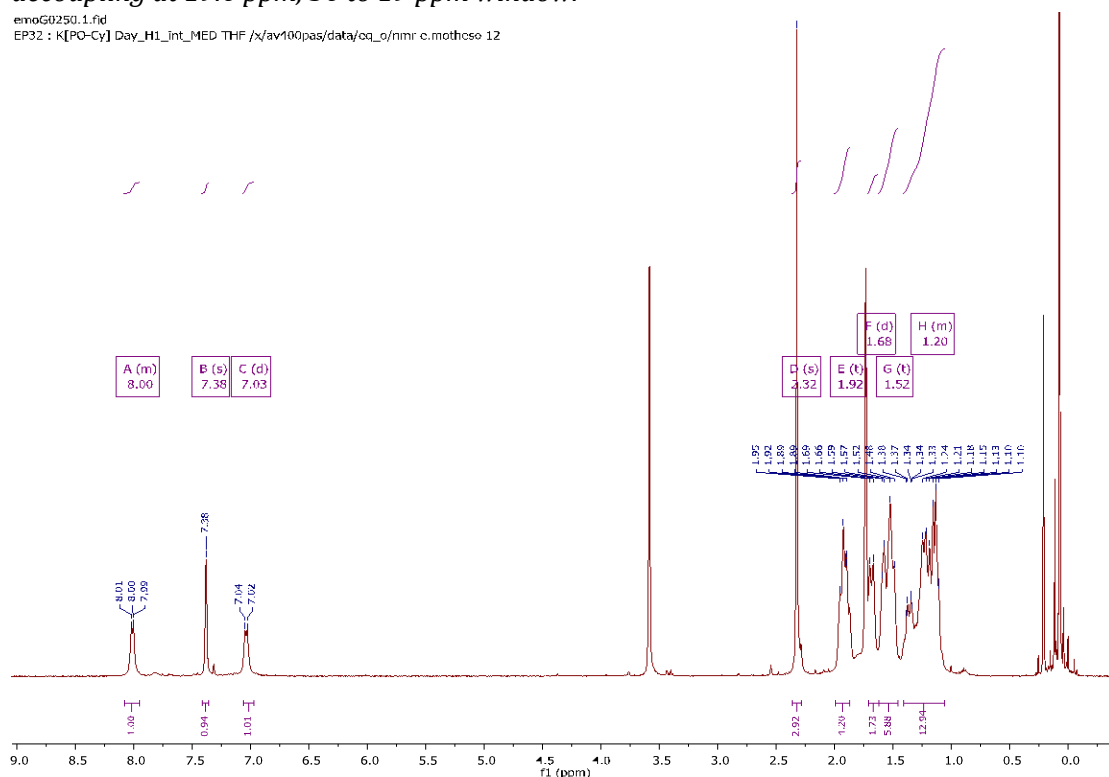


Figure S32. ^1H NMR spectrum for compound **K[PO-Cy]** at 298 K in $\text{THF}-d_8$

emoG0250.2.fid
EP32 : K[PO-Cy]
Day_P31_DECOPPLE_H1_MED THF /x/av400pas/data/eq_o/nmr e.mothess 12

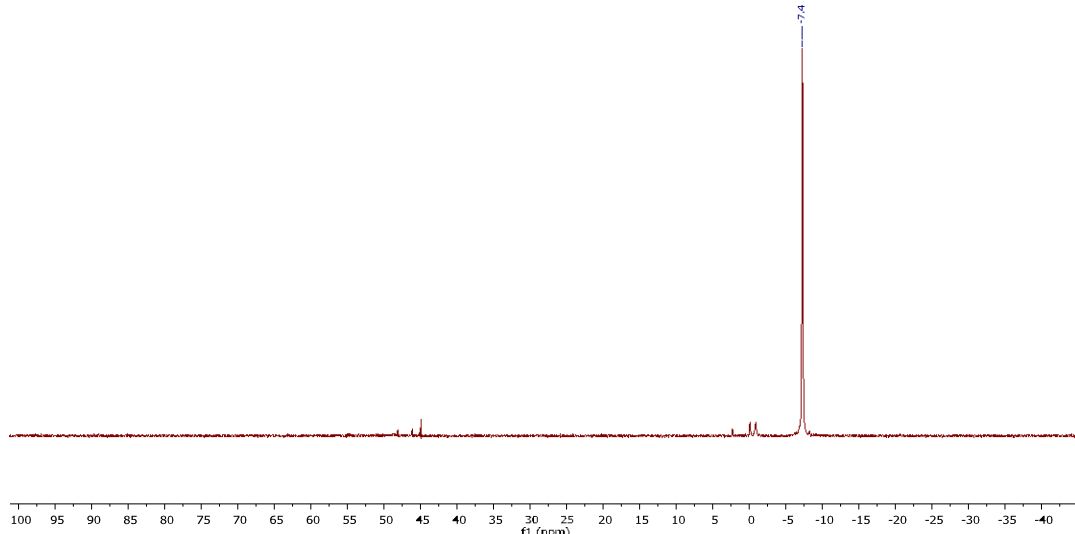


Figure S33. $^{31}\text{P}\{\text{H}\}$ NMR spectrum for compound **K[PO-Cy]** at 298 K in THF- d_8

EMM205 - K[PO-Cy]
C13_DECOPPLE_H1 THF /x/av400hd/data/eq_o/nmr e.mothess 4

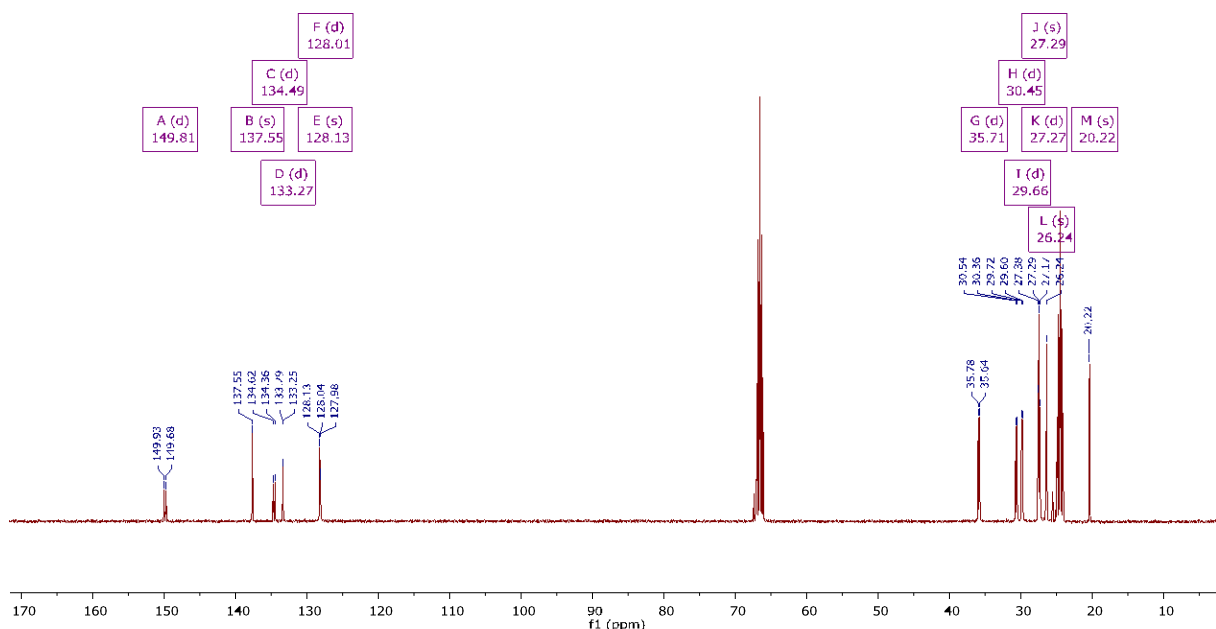


Figure S34. $^{13}\text{C}\{\text{H}\}$ NMR spectrum for compound **K[PO-Cy]** at 298 K in THF- d_8

emoG0287.1.fid
EMM188 - D[PO-Cy]
Day_H1_int_MED CD₂Cl₂ /x/av400pas/data/eq_o/nmr e.mothoso 13

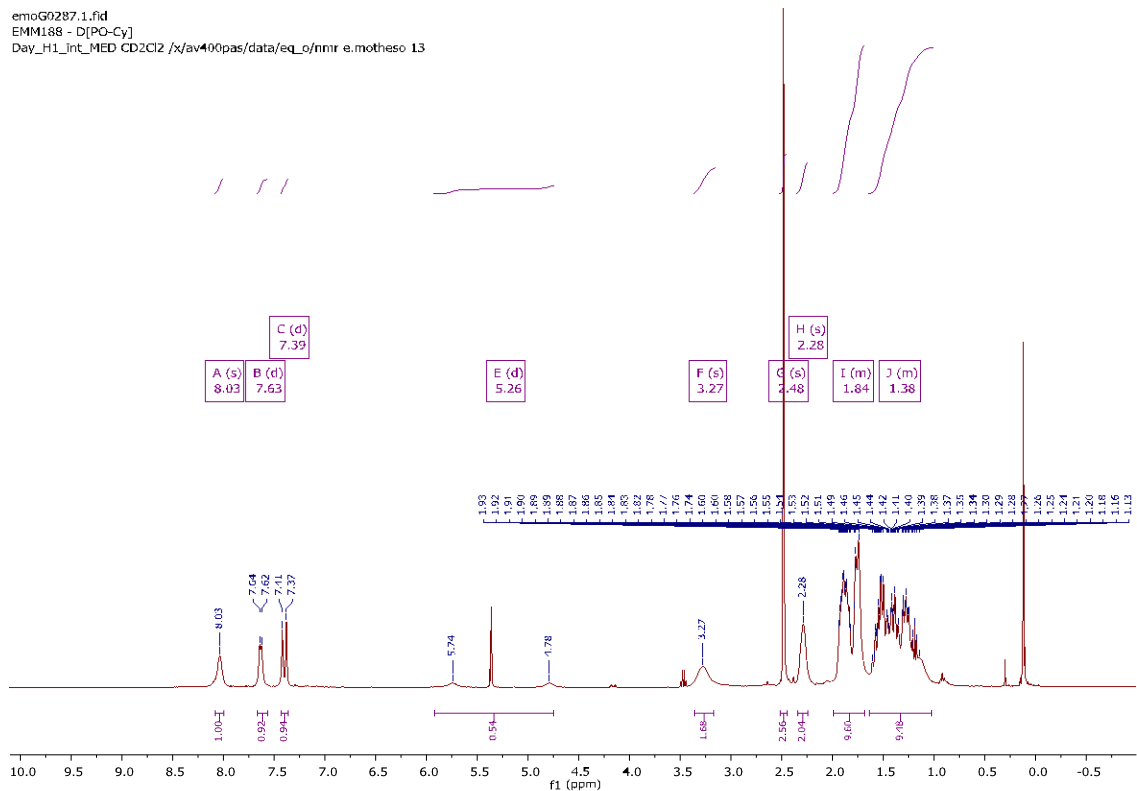


Figure S35. ^1H NMR spectrum for compound **D[PO-Cy]** at 298 K in CD_2Cl_2

emoG0287.2.fid
EMM188 - D[PO-Cy]
Day_P31_DECOPPLE_H1_MED CD₂Cl₂ /x/av400pas/data/eq_o/nmr e.mothoso 13

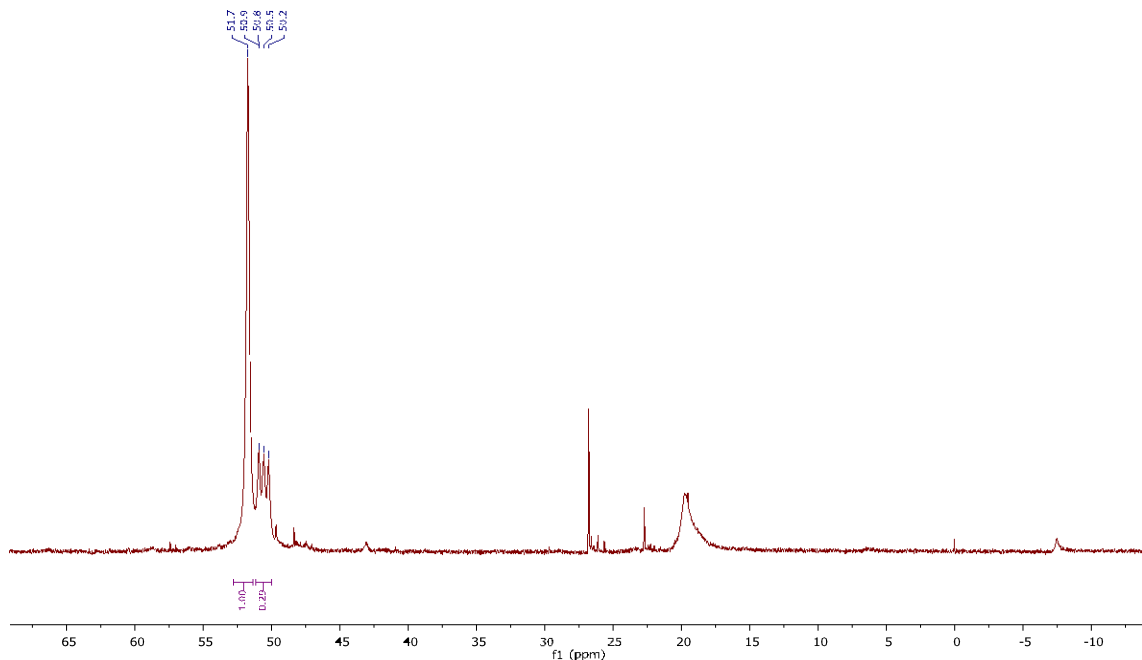


Figure S36. $^{31}\text{P}\{^1\text{H}\}$ NMR spectrum for compound **D[PO-Cy]** at 298 K in CD_2Cl_2

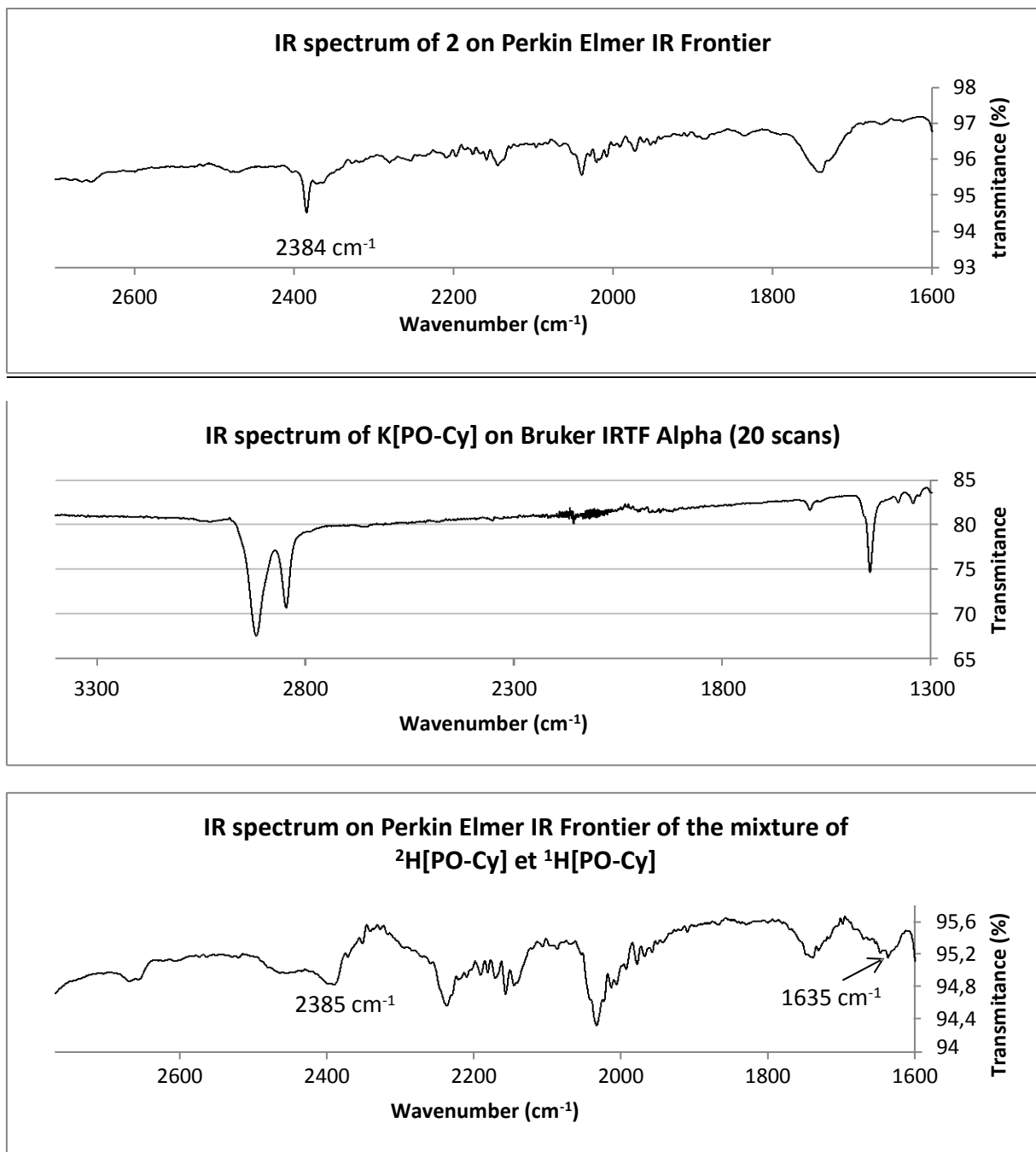


Figure S37. Powder ATR IR for compound 2.

NMR and IR Spectra of compound 3

analyse RMN500/RMN-31P{1H}298K
31P{1H} 298K

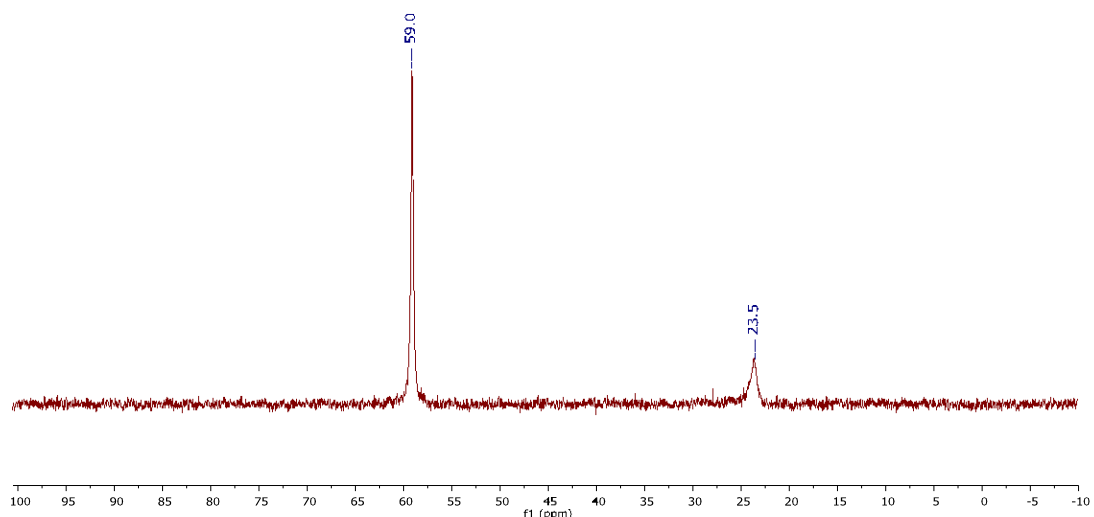


Figure S38. $^{31}\text{P}\{^1\text{H}\}$ NMR spectra for compound 3 at 298 K in CD_2Cl_2

analyse RMN500/RMN-31P{1H}213K
31P{1H} 213K

analyse RMN500/RMN-31P{1H}233K
31P{1H} 233K

analyse RMN500/RMN-31P{1H}253K
31P{1H} 253K

analyse RMN500/RMN-31P{1H}273K
31P{1H} 273K

analyse RMN500/RMN-31P{1H}298K
31P{1H} 298K

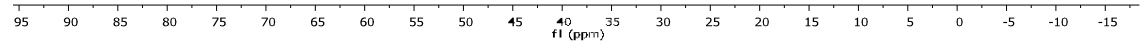


Figure S39. Variable temperature $^{31}\text{P}\{^1\text{H}\}$ NMR spectra for compound 3 from 298 K to 213 K in CD_2Cl_2

osbG170608.2.fid
 Sample: EMM171
 Probe: 3.2mm Vr = 16kHz
 31P CP

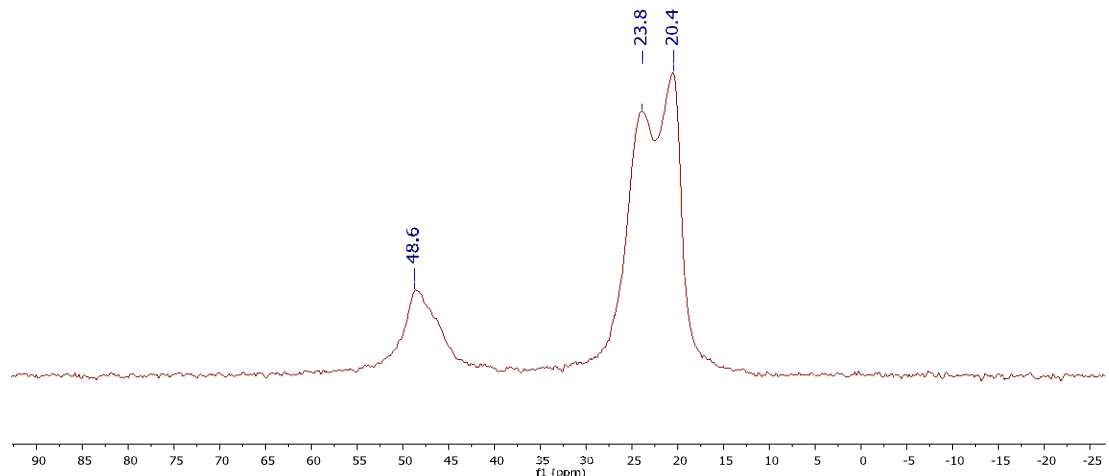
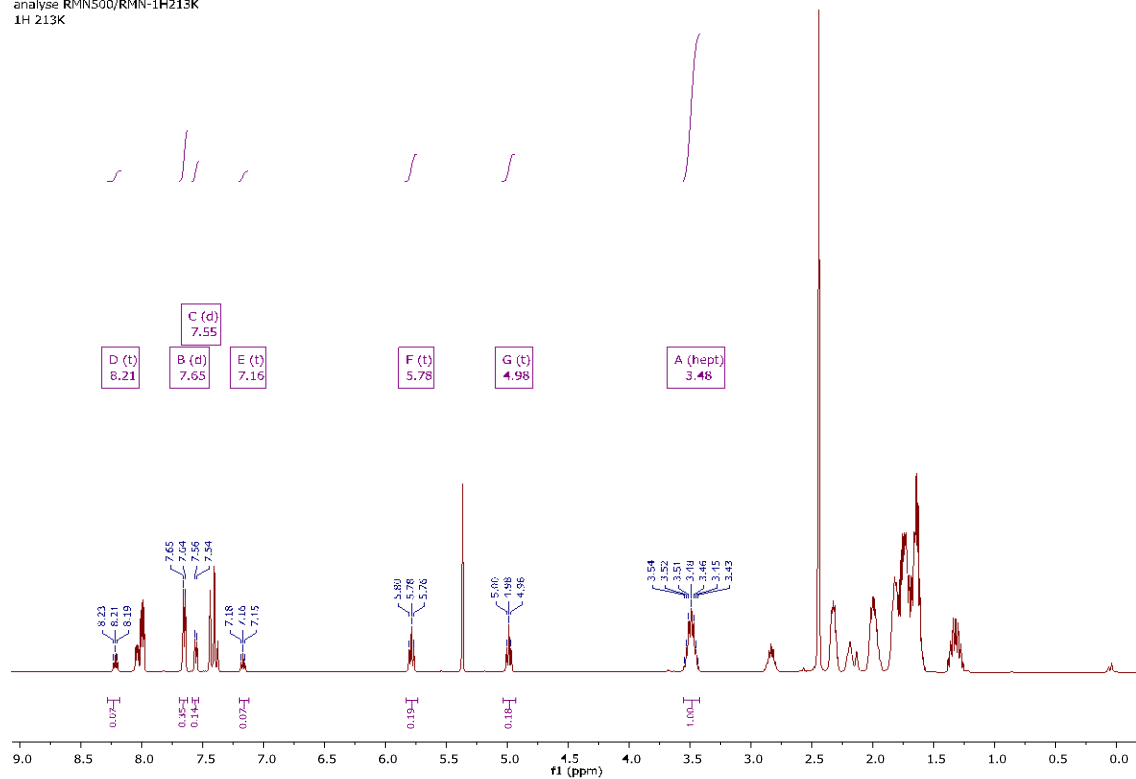


Figure S40. Solid state CPMAS ^{31}P NMR spectrum for compound 3

analyse RMN500/RMN-1H213K
 1H 213K



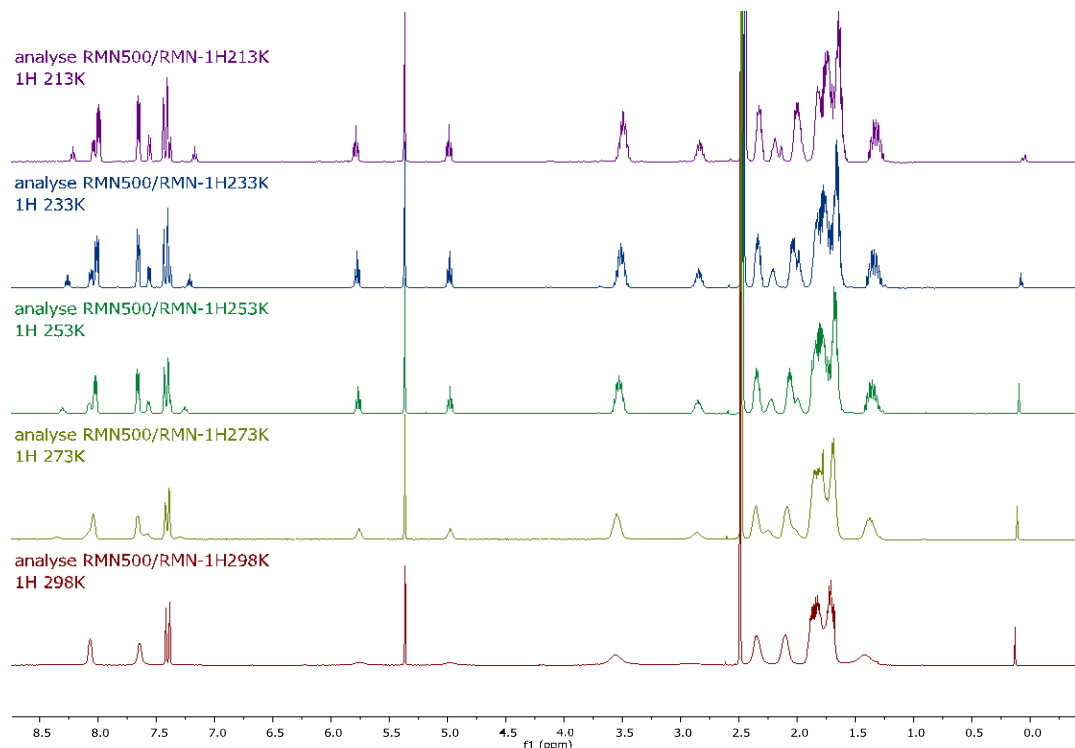


Figure S42. Variable temperature ^1H NMR spectra for compound **3** from 298 K to 213 K in CD_2Cl_2

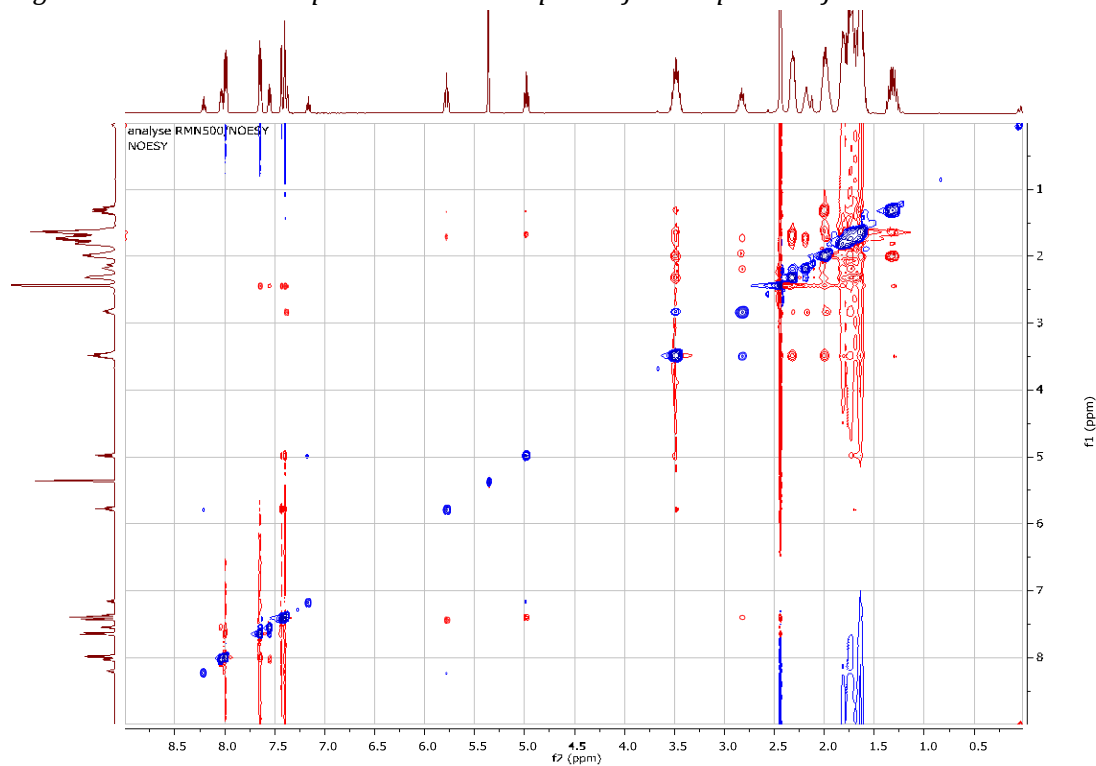


Figure S43. NOESY $^1\text{H}/^1\text{H}$ spectrum for compound **3** at 213 K in CD_2Cl_2

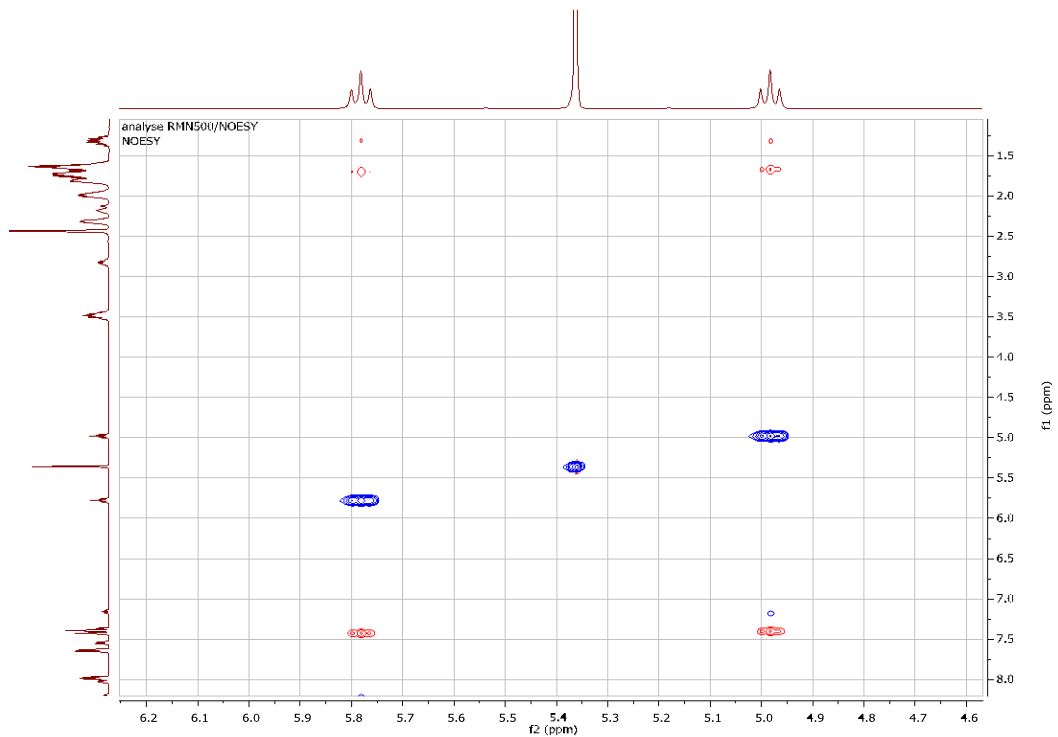


Figure S44. NOESY $^1\text{H}/^1\text{H}$ spectrum for compound **3** at 213 K, zoom on H-P form 1 in CD_2Cl_2

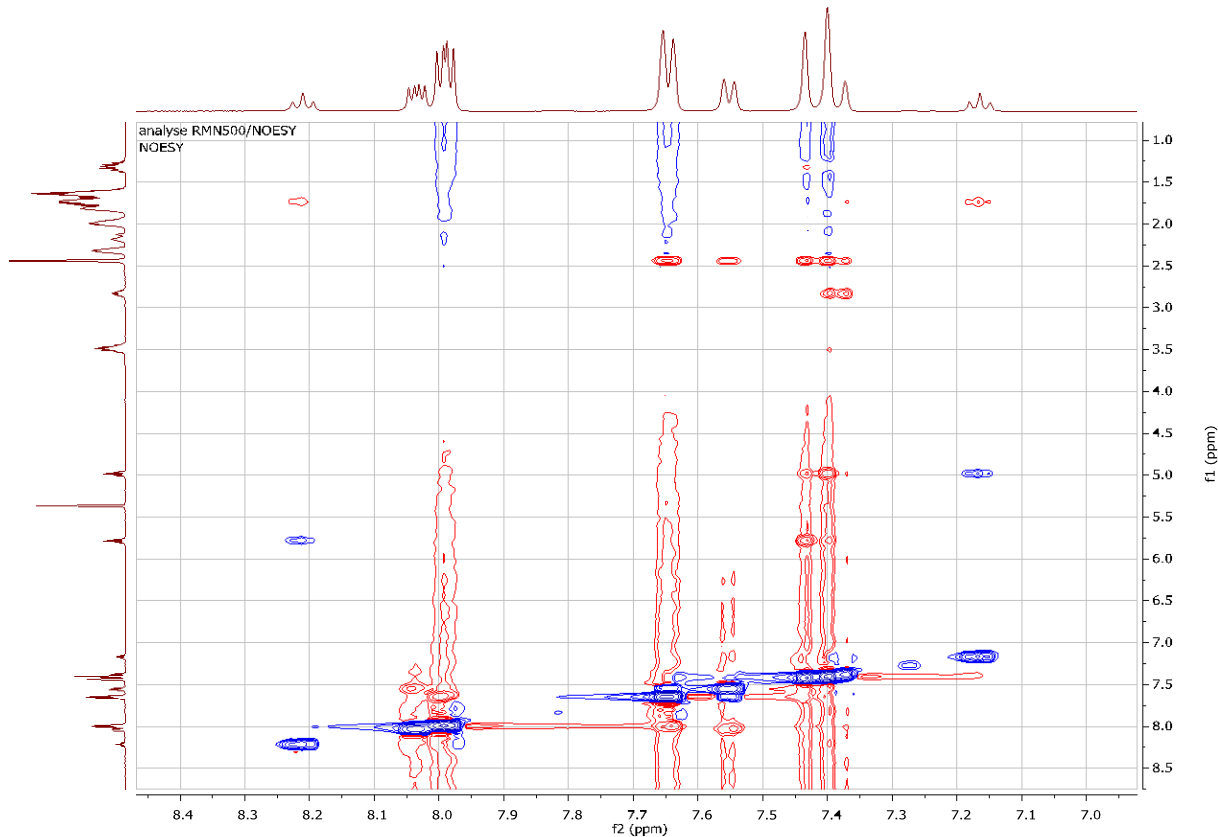


Figure S45. NOESY $^1\text{H}/^1\text{H}$ spectrum for compound **3** at 213 K, zoom on H-P form 2 in CD_2Cl_2

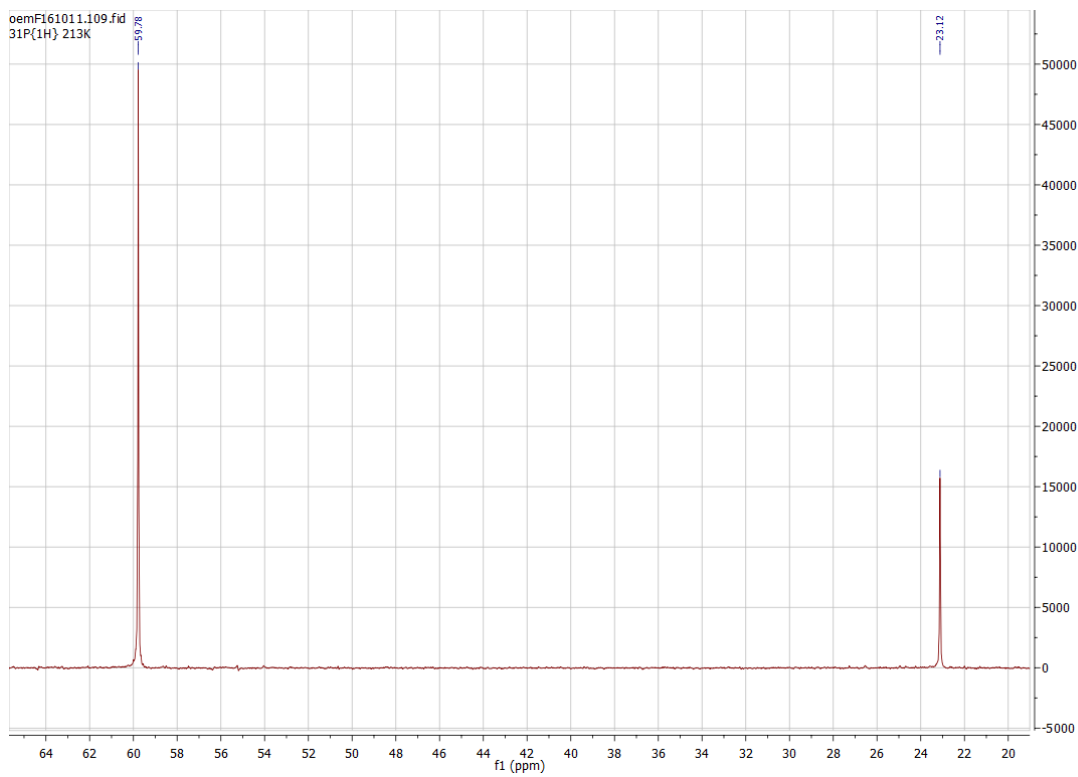


Figure S46. $^{31}\text{P}\{\text{H}\}$ NMR spectra for compound **3** at 213 K in CD_2Cl_2

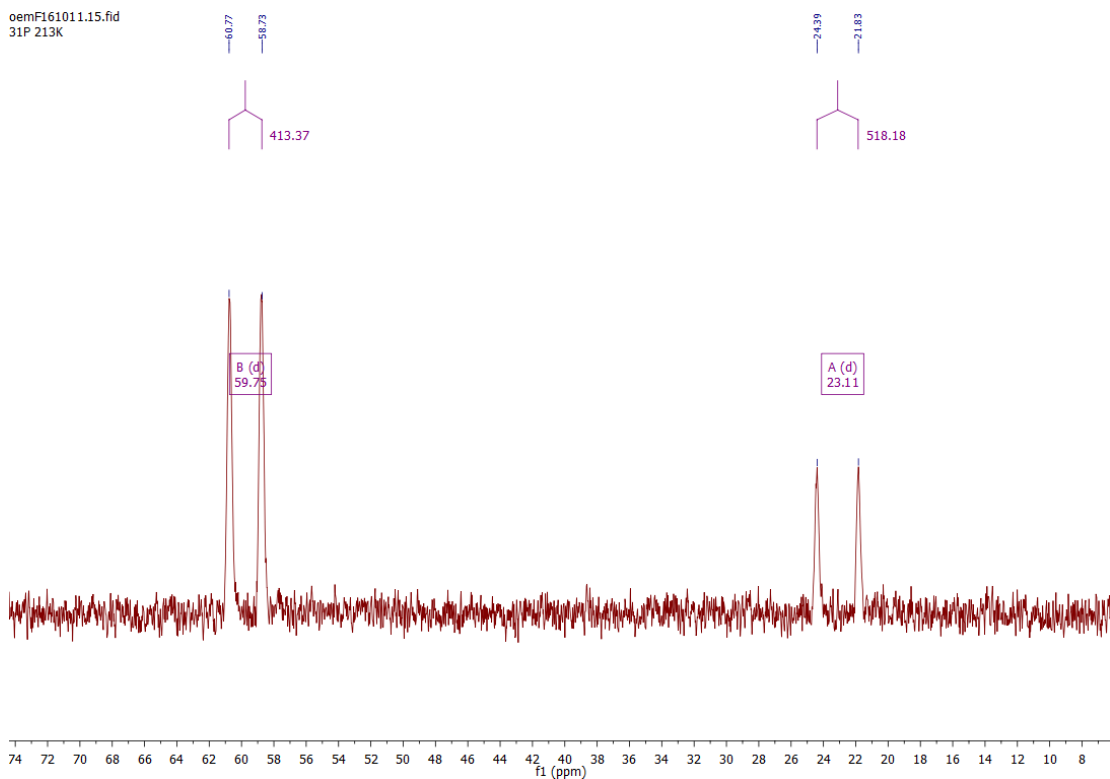


Figure S47. ^{31}P NMR spectra for compound **3** at 213 K in CD_2Cl_2

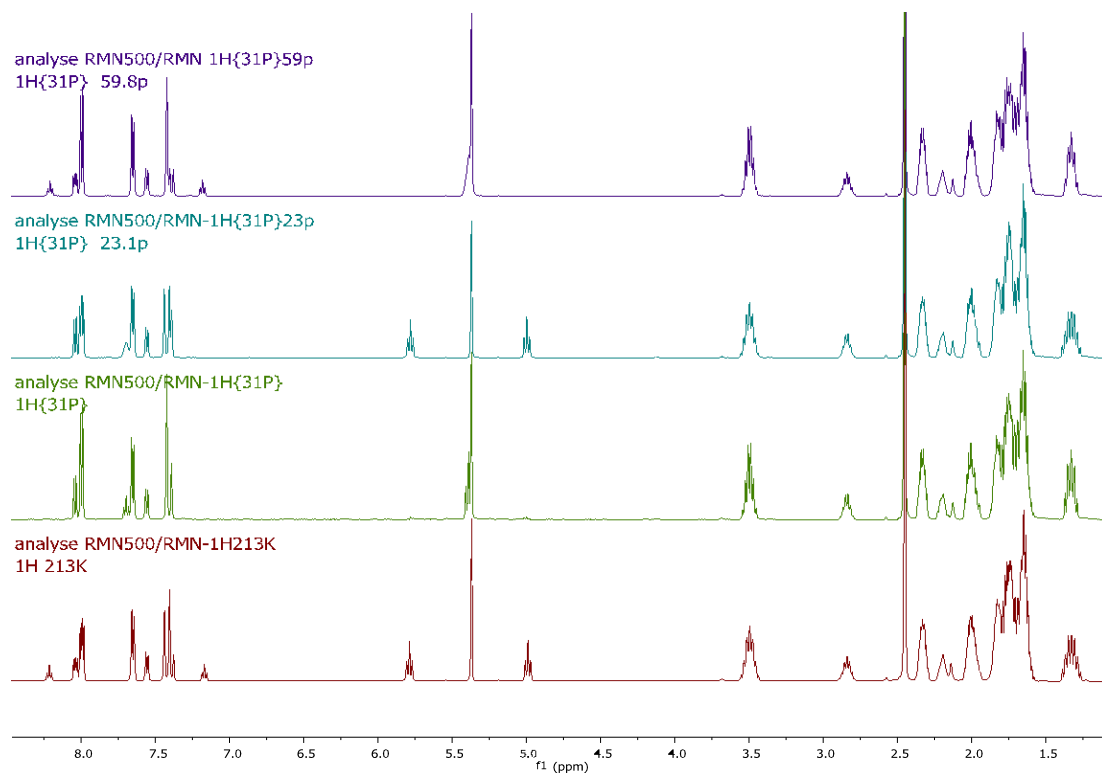


Figure S48. ^1H NMR analysis of compound **3** at 213 K in CD_2Cl_2 , from bottom to top: no ^{31}P decoupling, broad band ^{31}P decoupling, selective ^{31}P decoupling at 23 ppm, selective ^{31}P decoupling at 59 ppm.

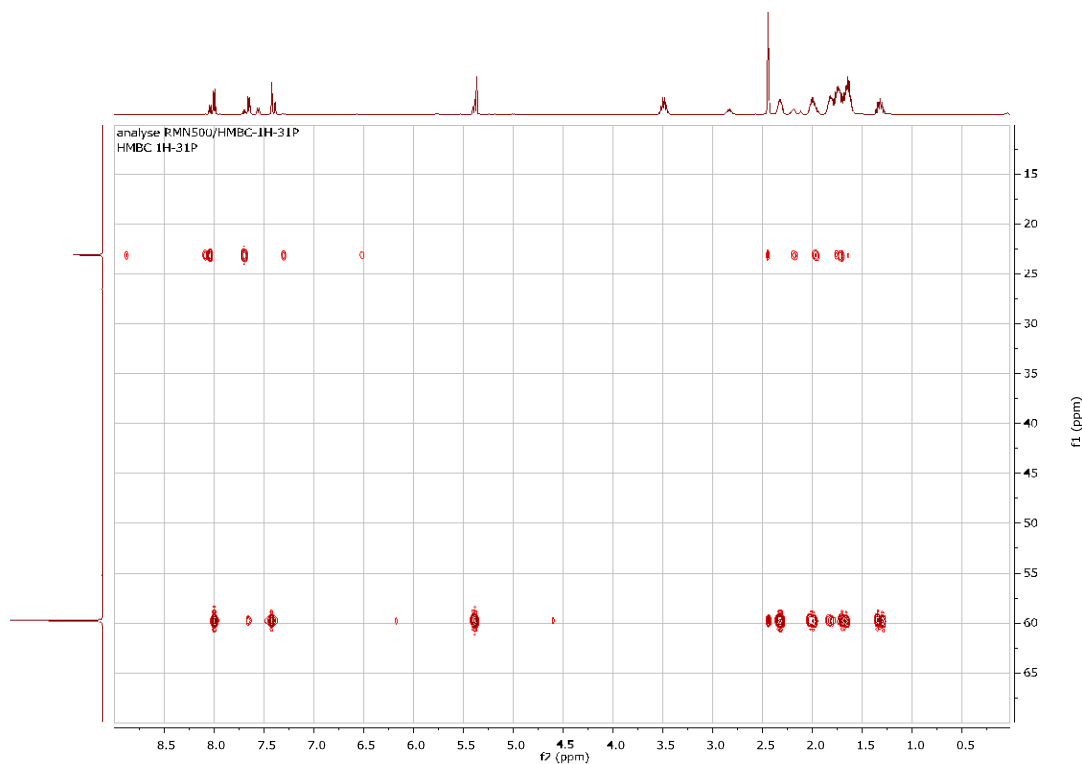


Figure S49. ^1H / $^{31}\text{P}\{^1\text{H}\}$ NMR HMBC experiment at 213 K for compound **3** in CD_2Cl_2

analyse RMN500/RMN-13C{1H}
13C{1H}

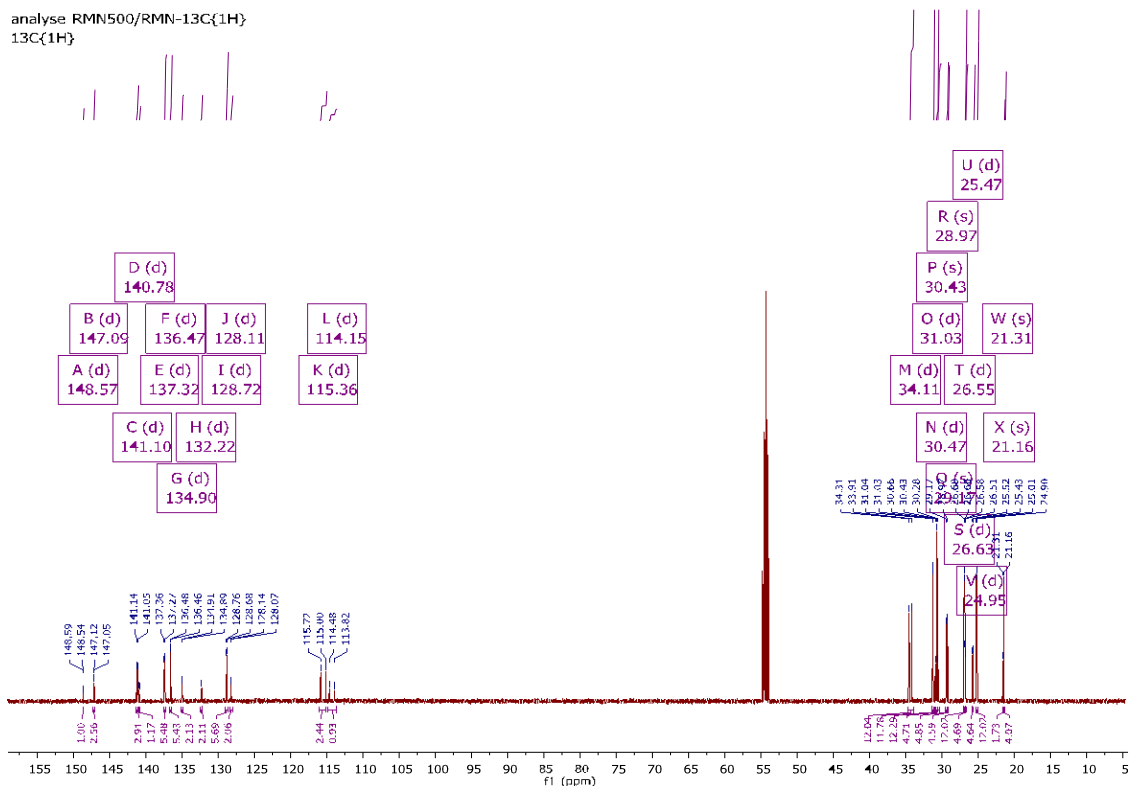


Figure S50. $^{13}\text{C}\{^1\text{H}\}$ NMR spectrum at 213 K for compound 3 in CD_2Cl_2

analyse RMN500/RMN-13C{1H}
13C{1H}

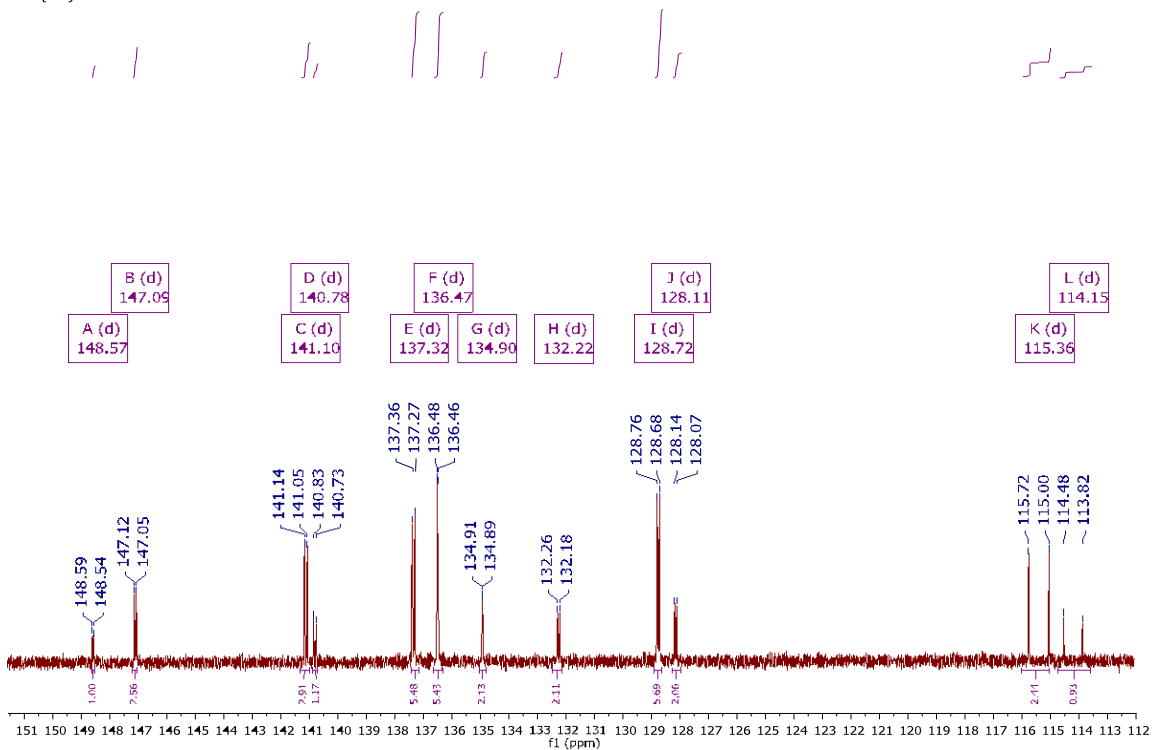


Figure S51. $^{13}\text{C}\{^1\text{H}\}$ NMR spectrum at 213 K in CD_2Cl_2 for compound 3, 152 to 112 ppm window.

analyse RMN500/RMN-13C{1H}
13C{1H}

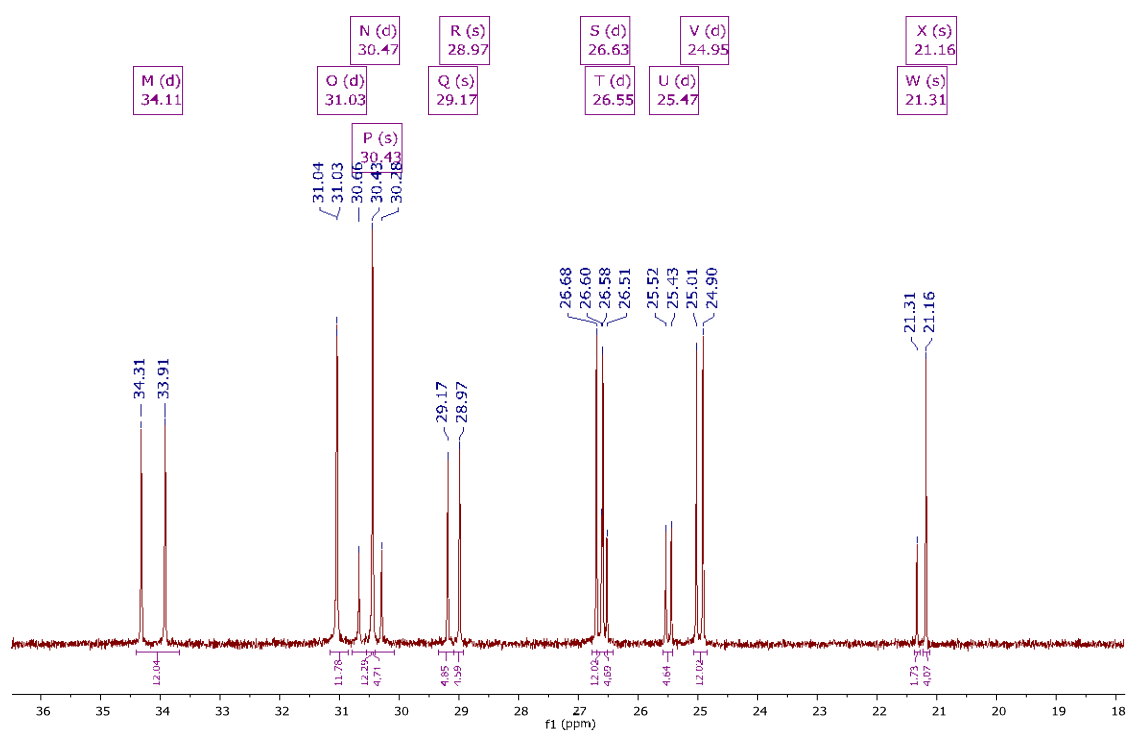
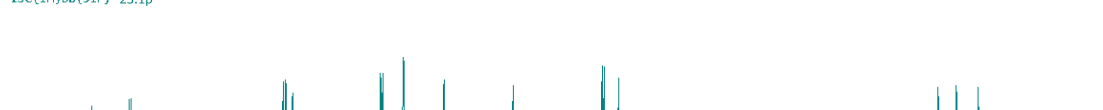


Figure S52. $^{13}\text{C}\{^1\text{H}\}$ NMR spectrum at 213 K in CD_2Cl_2 for compound 3, 36 to 18 ppm window.

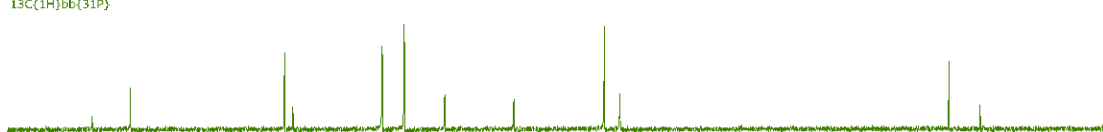
analyse RMN500/RMN-13C{1H}bb{31P}59p
13C{1H}bb{31P} 59.8p



analyse RMN500/RMN-13C{1H}bb{31P}23p
13C{1H}bb{31P} 23.1p



analyse RMN500/RMN-13C{1H}bb{31P}
13C{1H}bb{31P}



analyse RMN500/RMN-13C{1H}
13C{1H}

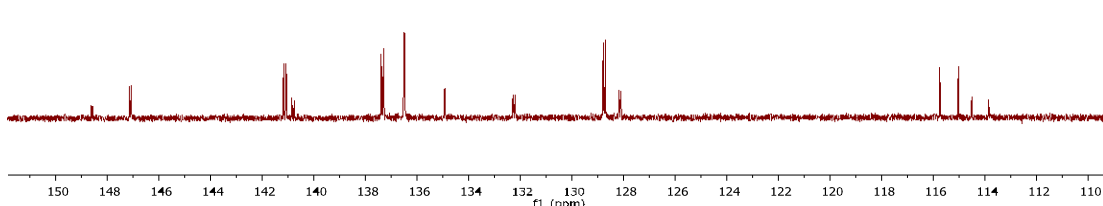


Figure S53. $^{13}\text{C}\{^1\text{H}\}$ NMR analysis of compound 3 at 213 K in CD_2Cl_2 , from bottom to top: no ^{31}P decoupling, broad band ^{31}P decoupling, selective ^{31}P decoupling at 23 ppm, selective ^{31}P decoupling at 59 ppm.

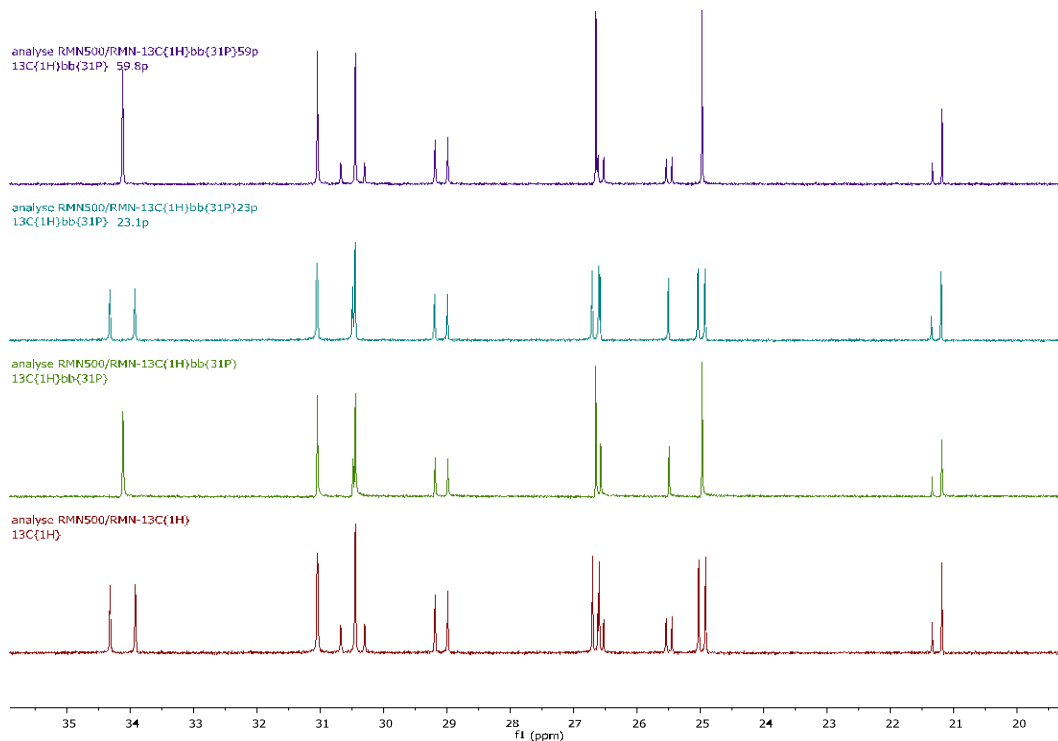


Figure S54. $^{13}\text{C}\{^1\text{H}\}$ NMR analysis of compound **3** at 213 K in CD_2Cl_2 , from bottom to top: no ^{31}P decoupling, broad band ^{31}P decoupling, selective ^{31}P decoupling at 23 ppm, selective ^{31}P decoupling at 59 ppm, 36 to 18 ppm window.

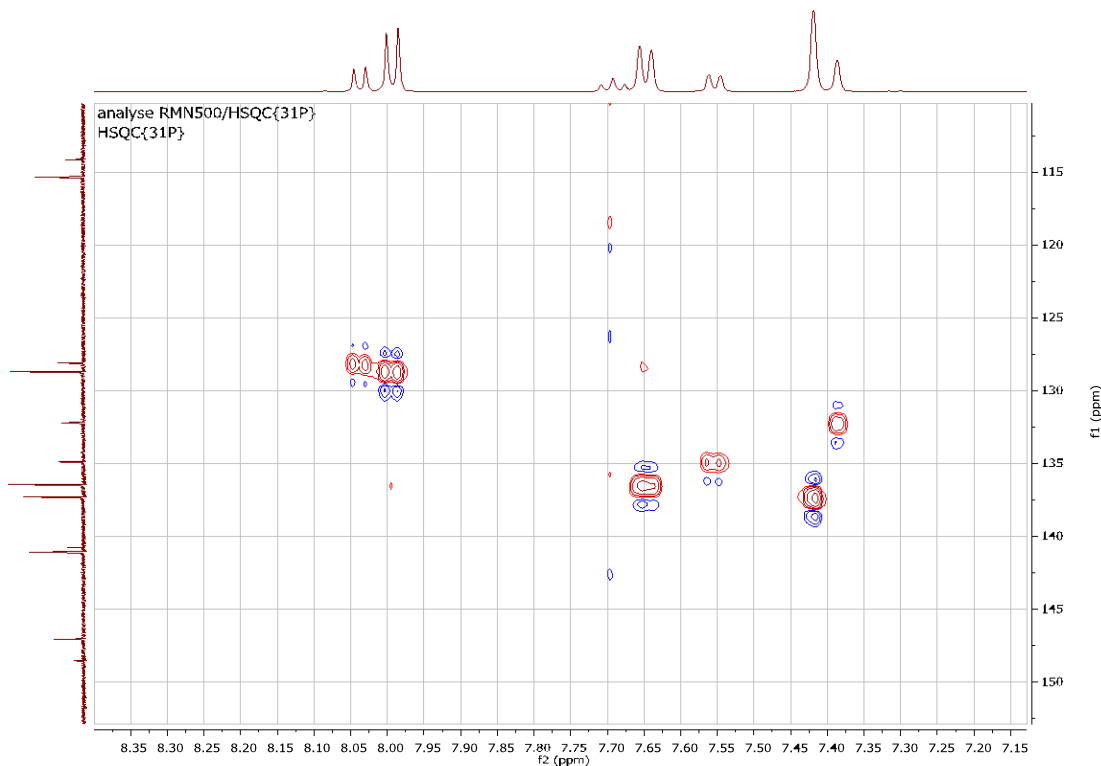


Figure S55. $^1\text{H} / ^{13}\text{C}\{^1\text{H}\}$ NMR HSQC experiment at 213 K in CD_2Cl_2 for compound **3**.

emoL0021.2.fid
H1_INT
EMM184 : K[PO-Cyp]

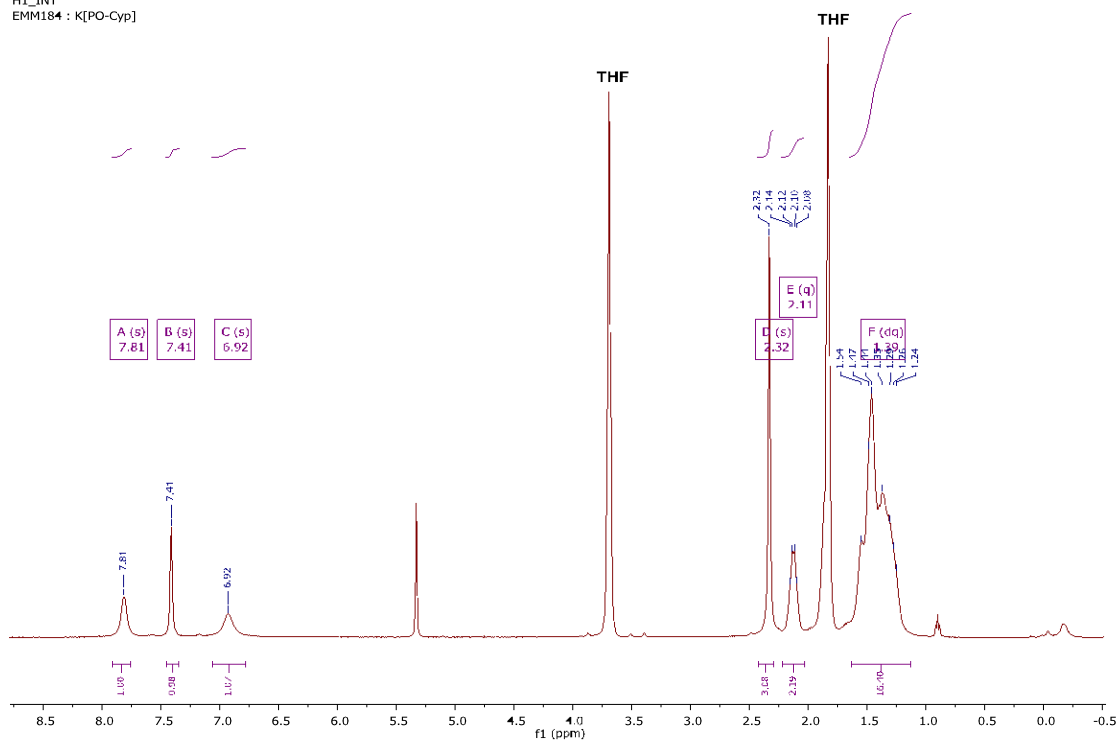


Figure S56. ¹H NMR spectrum for compound K[PO-Cyp] at 298 K in CD₂Cl₂

emoL0021.3.fid
P31_DECOPPLE_H1
EMM184 : K[PO-Cyp]

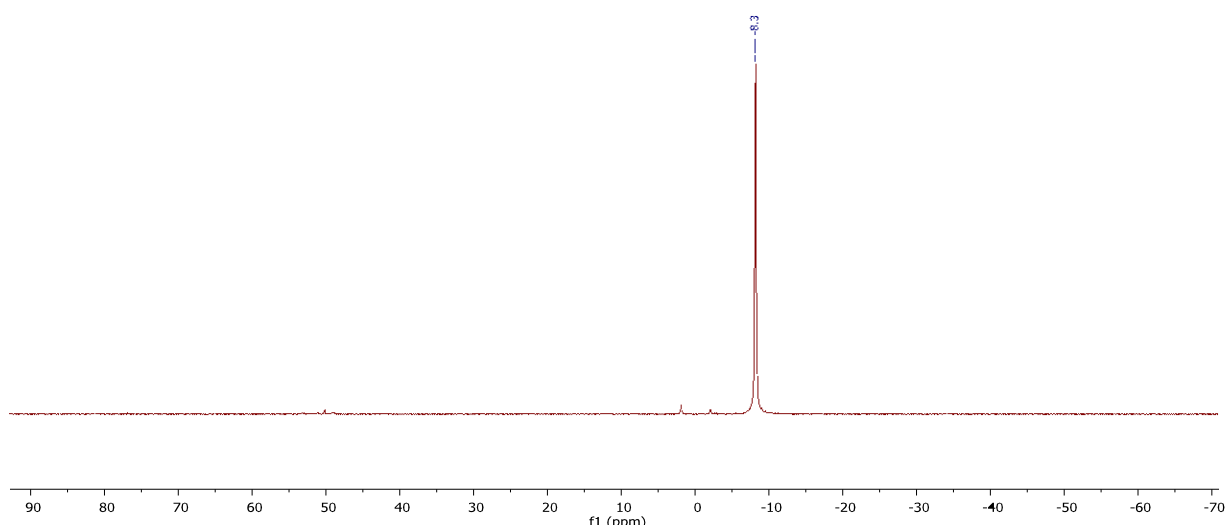


Figure S57. ³¹P{¹H} NMR spectrum for compound K[PO-Cyp] at 298 K in CD₂Cl₂

EMM184 - K[PO-Cyp]
C13_DECOPPLE_H1 THF /x/av400hd/data/eq_o/nmr e.mothess 3

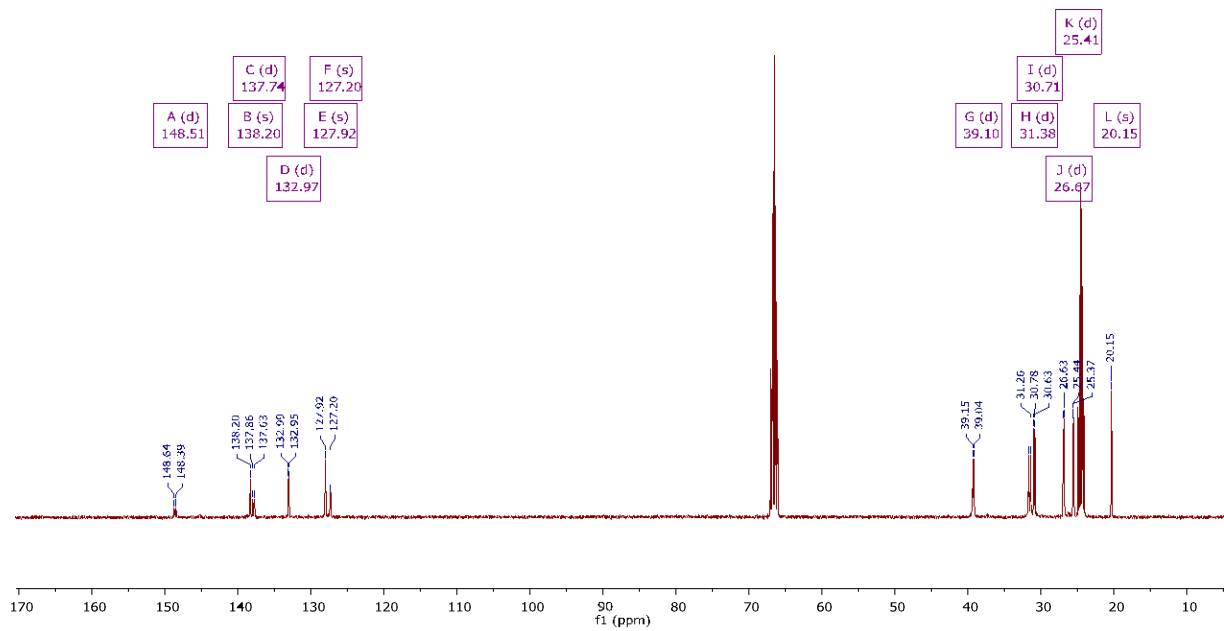
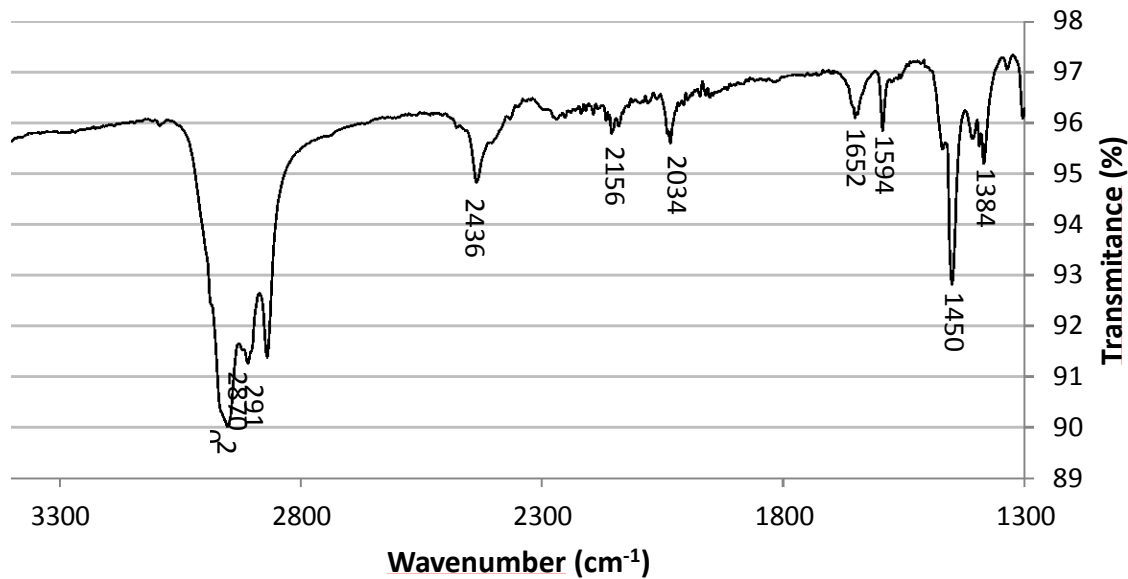


Figure S58. $^{13}\text{C}\{^1\text{H}\}$ NMR spectrum for compound **K[PO-Cyp]** at 298 K in $\text{THF}-d_8$

IR spectrum of compound 3 on Perkin Elmer IR Frontier (4 scans)



IR spectrum of K[PO-Cyp] on Bruker IRTF Alpha (20 scans)

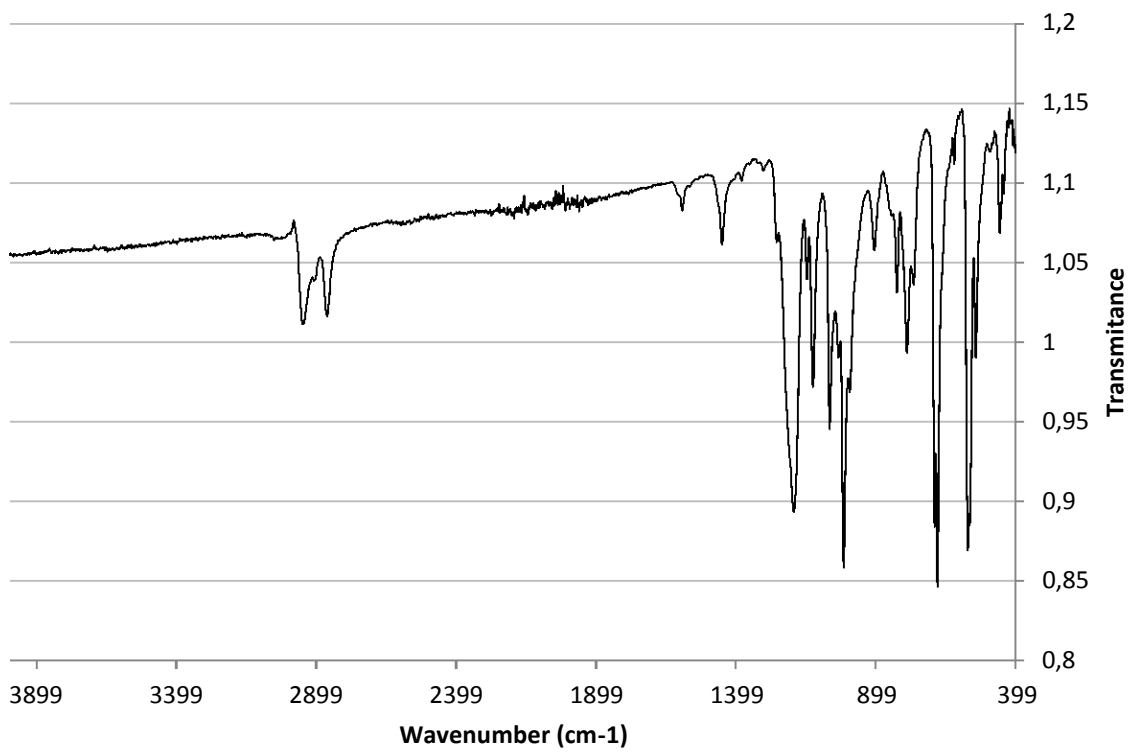


Figure S59. Powder IR analysis for compound 3 and K[PO-Cyp].

NMR and IR Spectra of compound 4

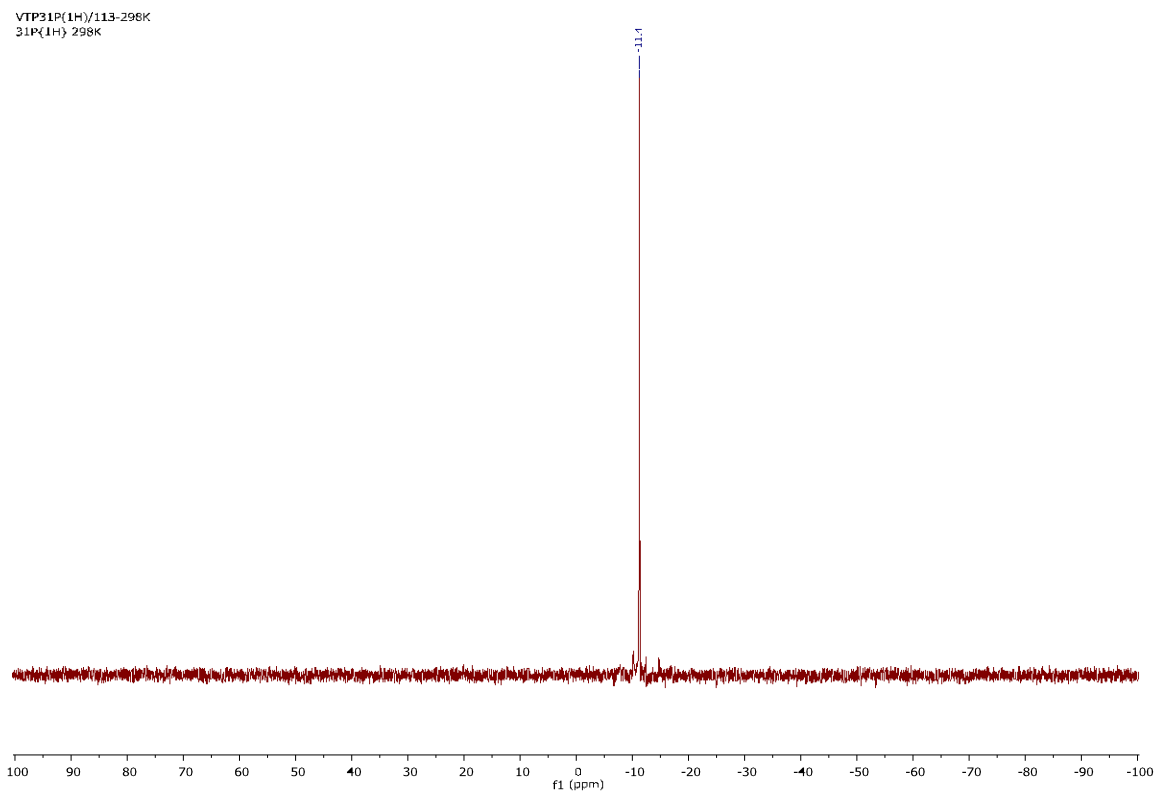


Figure S60. $^{31}\text{P}\{^1\text{H}\}$ NMR spectra for compound **4** at 298 K in CD_2Cl_2

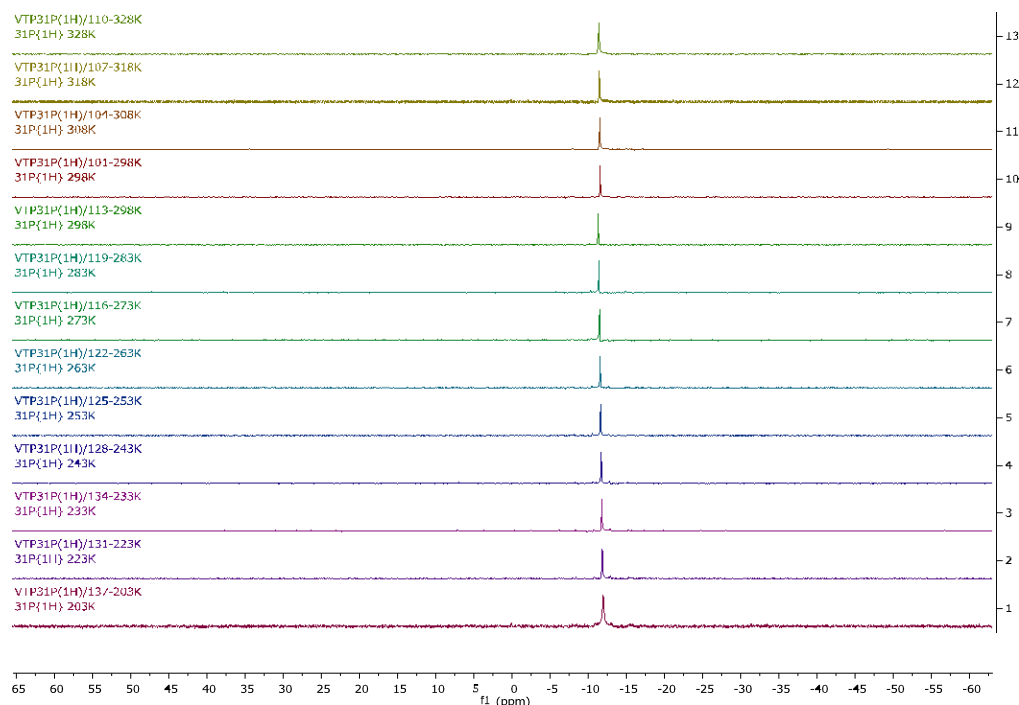


Figure S61. Variable temperature $^{31}\text{P}\{^1\text{H}\}$ NMR spectra for compound **4** from 203 K to 328 K in CD_2Cl_2 (exp 1 to 9) and CDCl_3 (exp 10 to 13)

osbG170712.2.fid
Sample: EMM181
Probe: 3.2mm Vr = 16kHz
31P CP

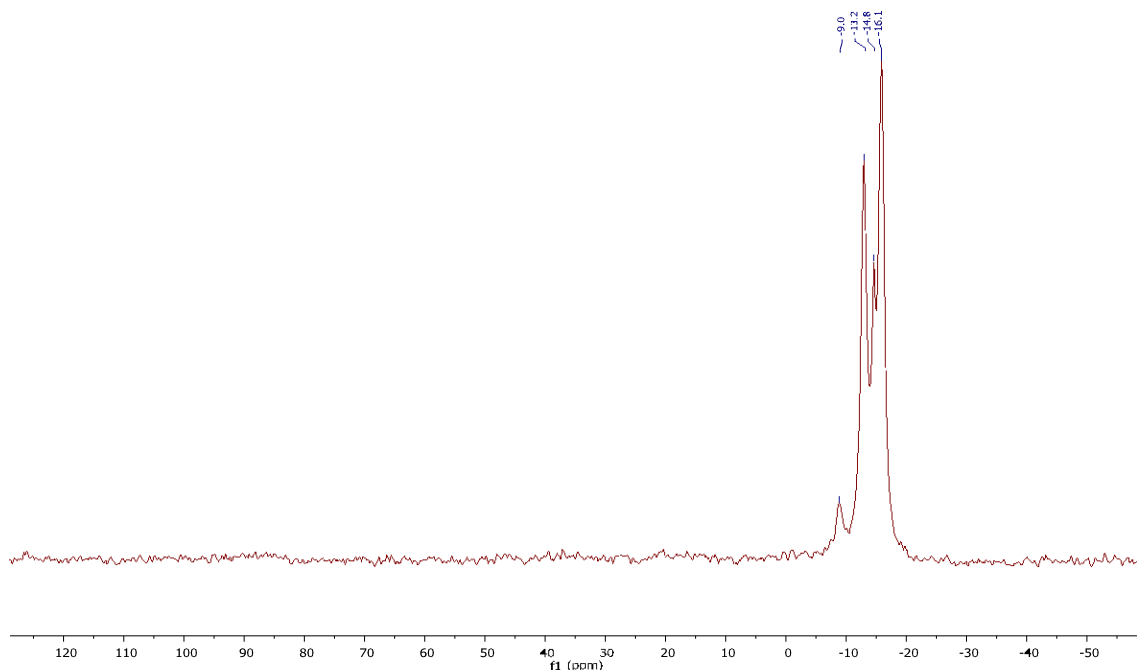


Figure S62. Solid state CPMAS ^{31}P NMR spectrum for compound 4

VTP1H/112-298K
1H 298K

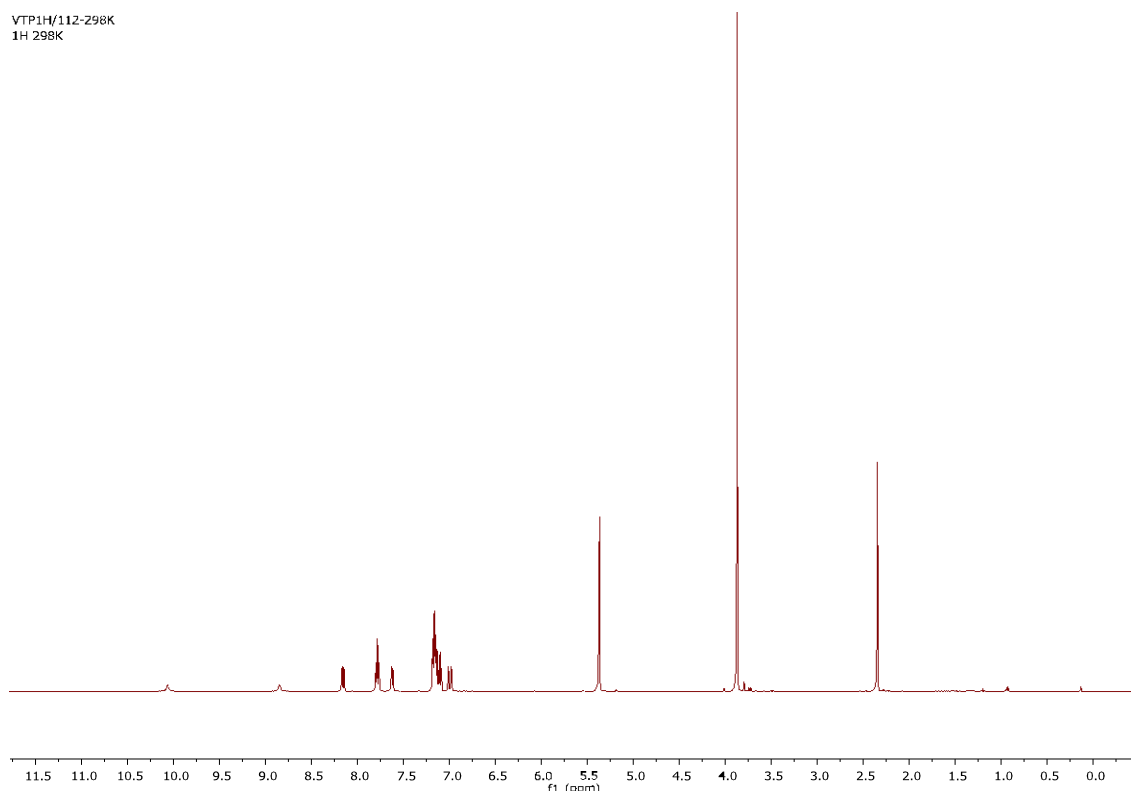


Figure S63. ^1H NMR spectrum for compound 4 at 298 K in CD_2Cl_2

oemF170720-RMN500MHz/3-1H{³¹P}298K
1H{³¹P} 298K

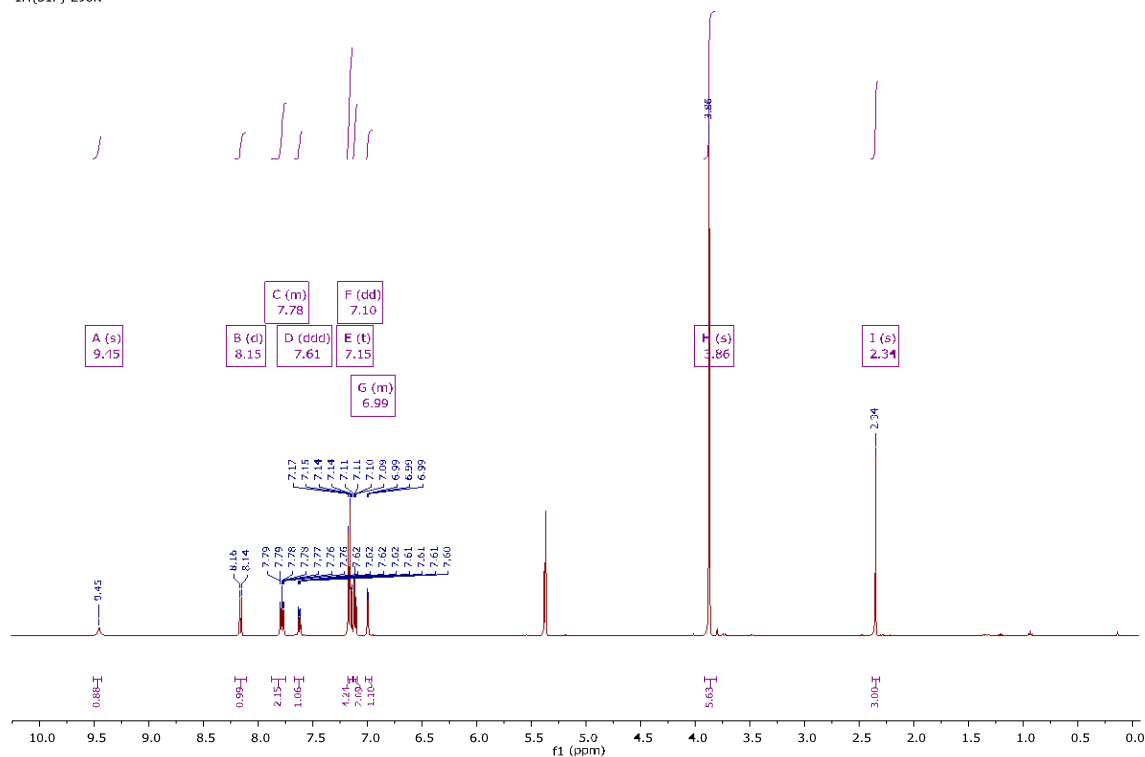


Figure S64. ¹H{³¹P} NMR spectrum for compound 4 at 298 K in CD_2Cl_2

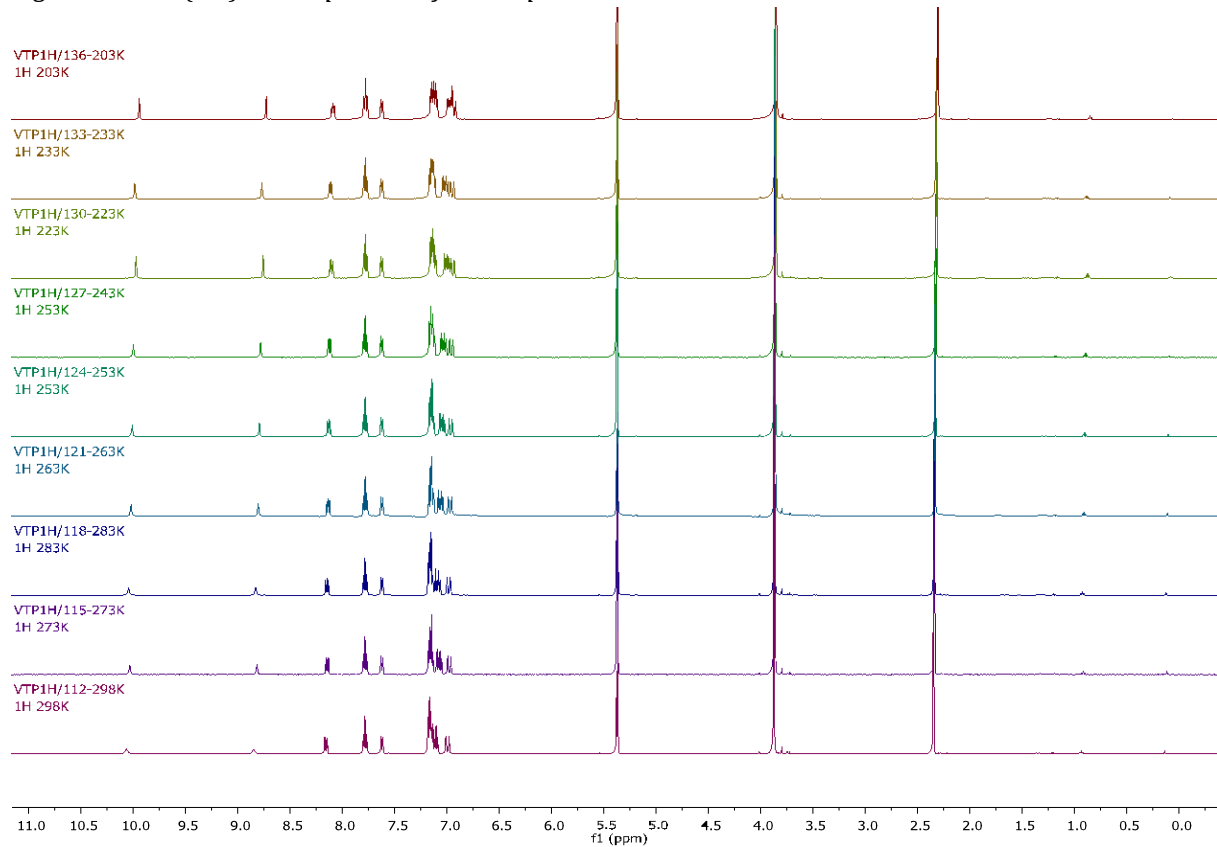


Figure S65. Variable temperature ¹H NMR spectra for compound 4 from 203 K to 298 K in CD_2Cl_2

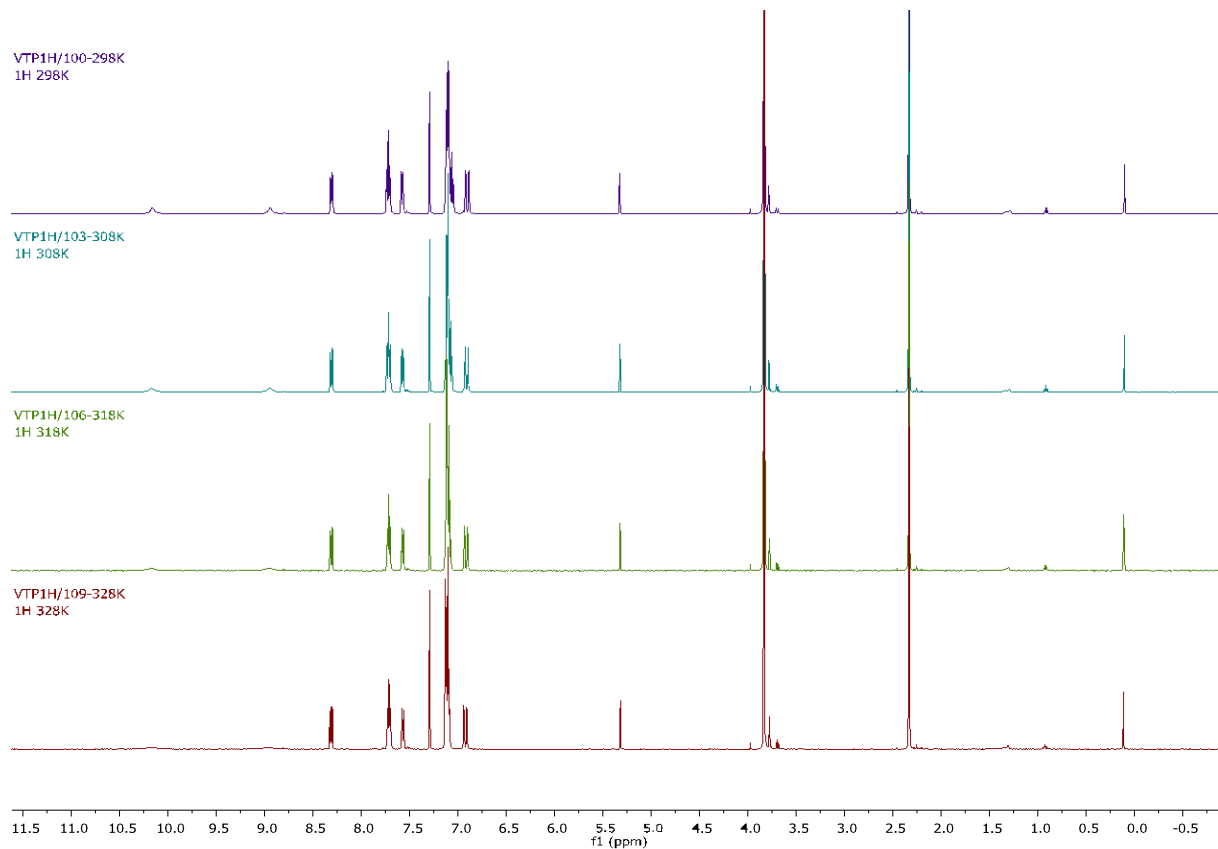


Figure S66. Variable temperature ^1H NMR spectra for compound 4 from 298 K to 328 K in CDCl_3

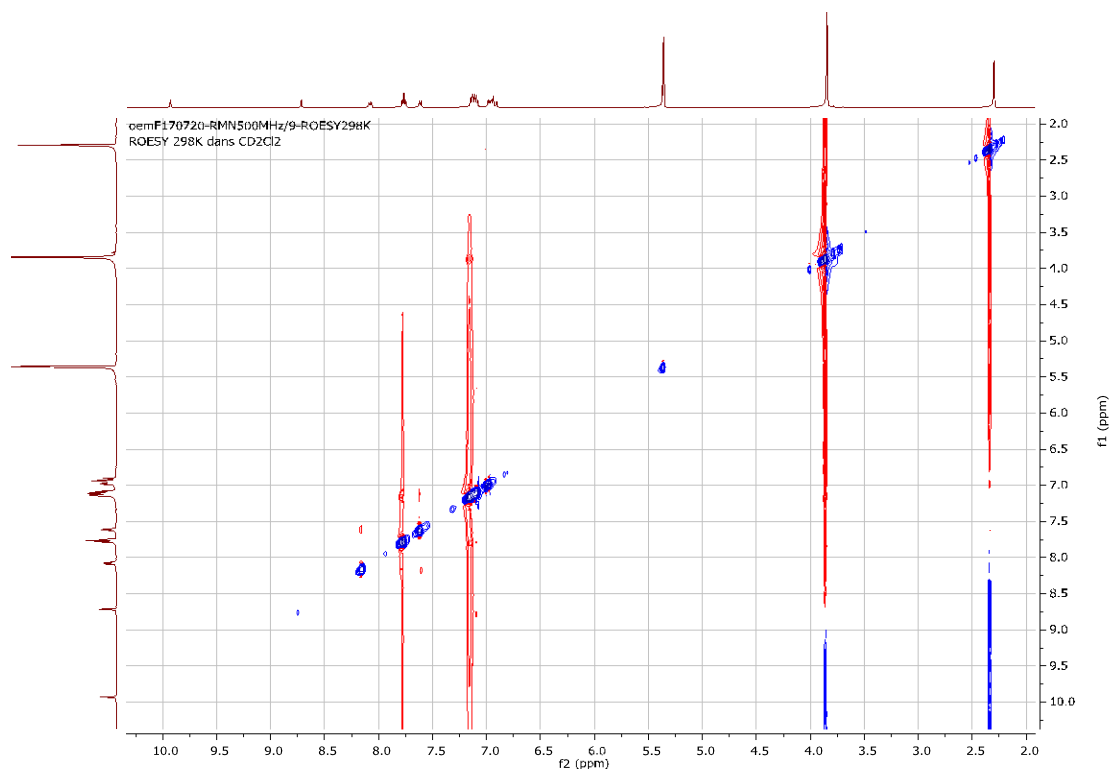


Figure S67. NOESY $^1\text{H}/^1\text{H}$ spectrum for compound 4 at 298 K in CD_2Cl_2

oemF170720-RMN500MHz/7-13C(1H)298K
13C(1H) 298K dans CD₂Cl₂

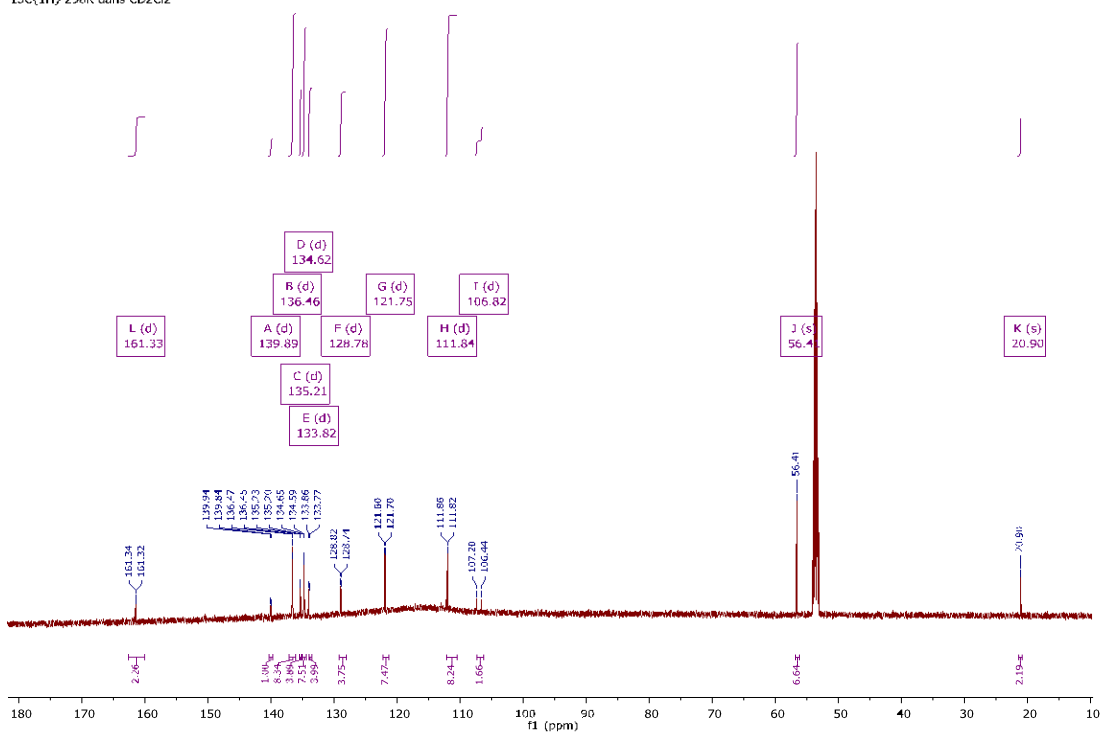


Figure S68. ¹³C{¹H} NMR spectrum at 298 K for compound **4** in CD₂Cl₂

emok0171.2.fid
EMM187 - K[PO-PhOMe]
H1_INT THF-x/av400hd/data/eq_o/nmr emotheso 5

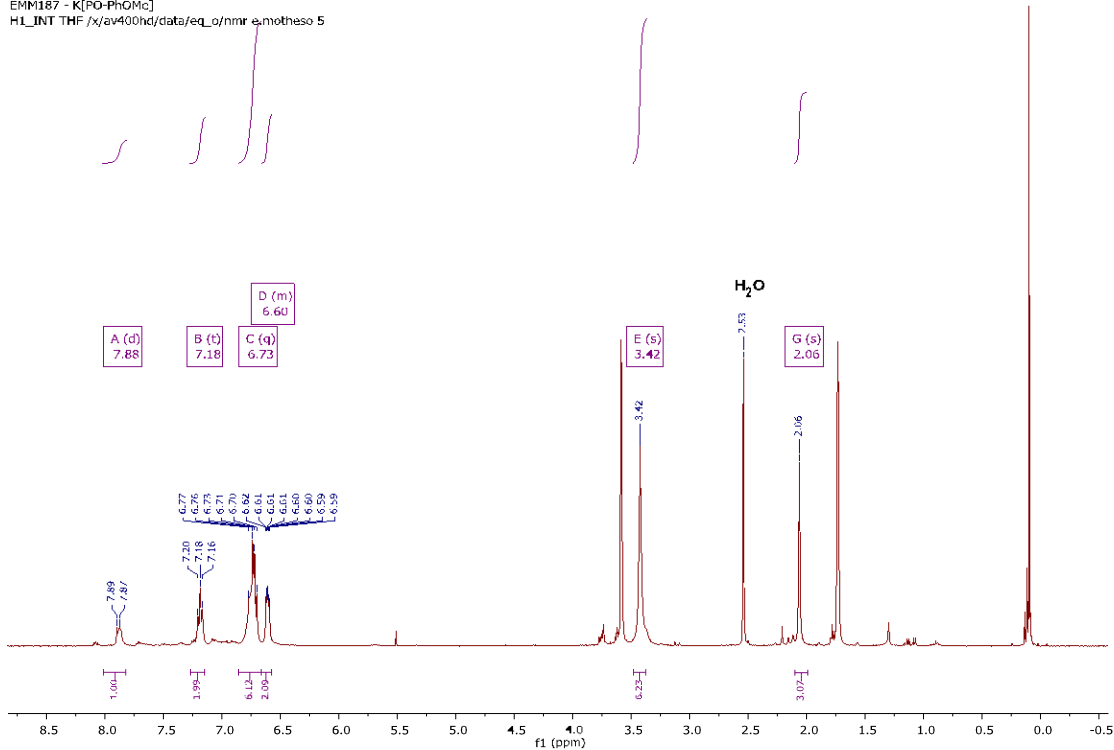


Figure S69. ¹H NMR spectrum for compound **K[PO-OMe-Ph]** at 298 K in THF-d₈

emoK0171.3.fid
EMM187 - K[PO-PhOMe]
P31_DECOPPLE_H1 THF /x/av400hd/data/eq_o/nmr e.mothese 5

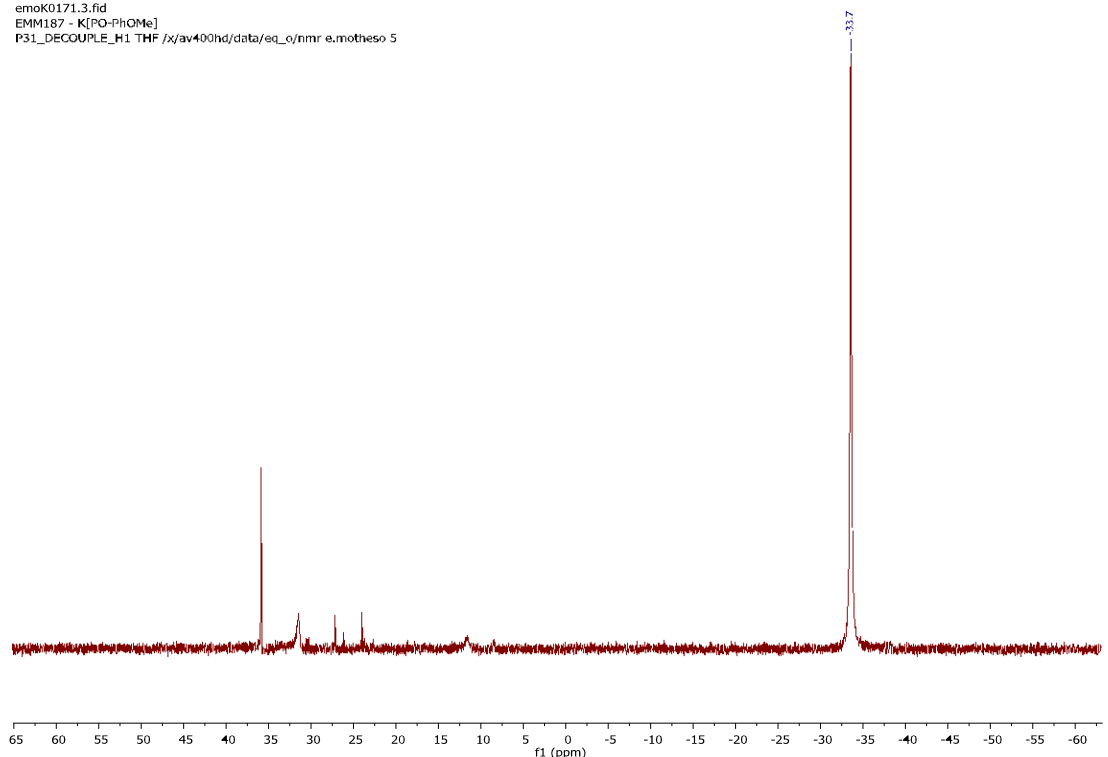


Figure S70. $^{31}\text{P}\{\text{H}\}$ NMR spectrum for compound **K[PO-OMe-Ph]** at 298 K in $\text{THF}-d_8$

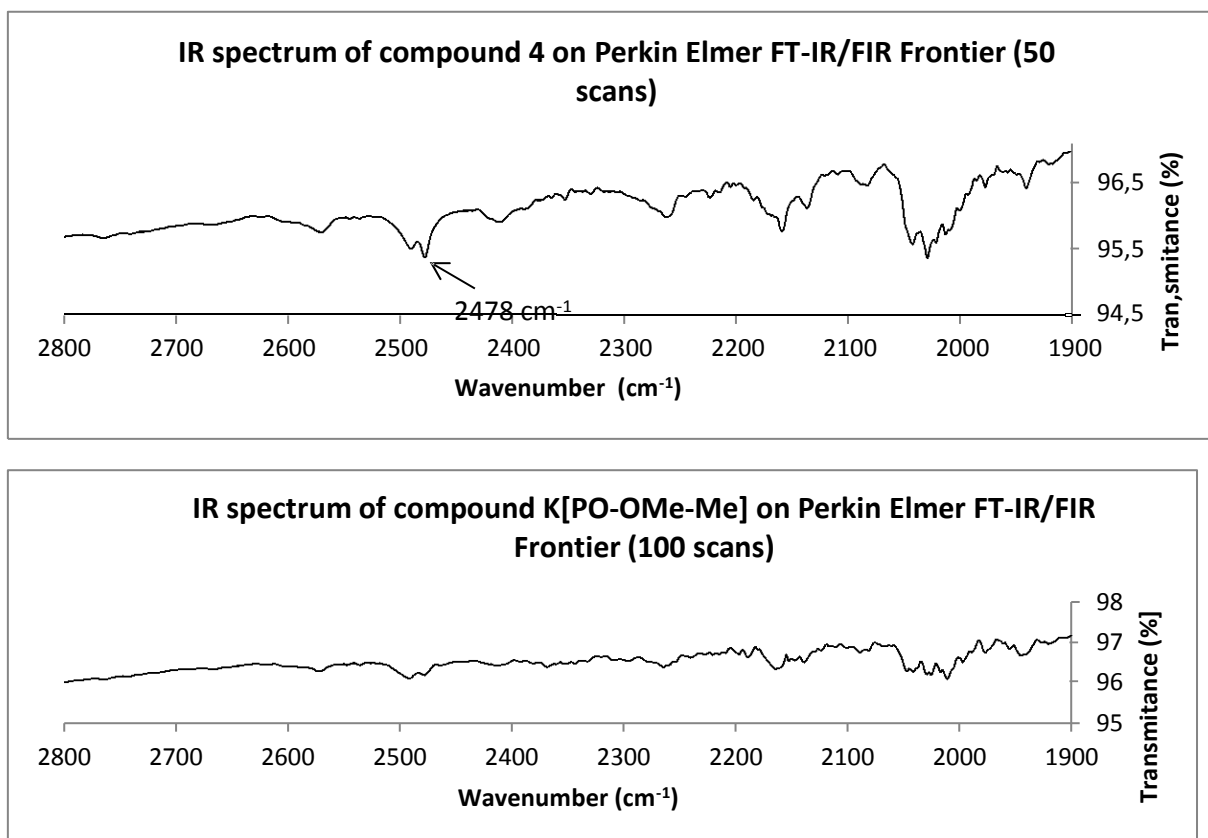


Figure S71. Powder ATR IR for compound **4** and **K[PO-OMe-Me]**

Dynamic exchange between the exo and endo form in solution for 1-3

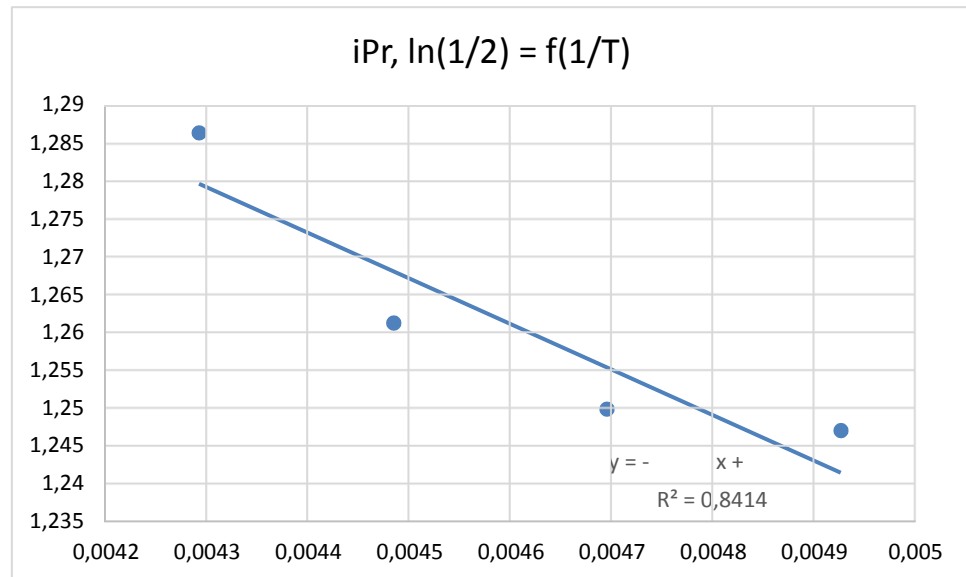
Thermodynamic data

The van't Hoff plot affords ΔG_0 according to the following equation:

$$\ln k = \frac{\Delta G}{RT} \quad (1)$$

Compound 1 H[PO-iPr]

T (K)	Integral Form 1	Integral Form 2	$\ln(1/2)$	1/T
233	3,62	1	1,28647403	0,00429185
223	3,53	1	1,26129787	0,0044843
213	3,49	1	1,24990174	0,00469484
203	3,48	1	1,24703229	0,00492611



$$\Delta H_0 = -(60.315) * 8.31 \cdot 10^{-3} = 501.21765 \cdot 10^{-3} \text{ kJ.mol}^{-1}$$

$$\Delta S_0 = 1.5386 * 8.31 \cdot 10^{-3} = 12.785766 \text{ J.mol}^{-1}$$

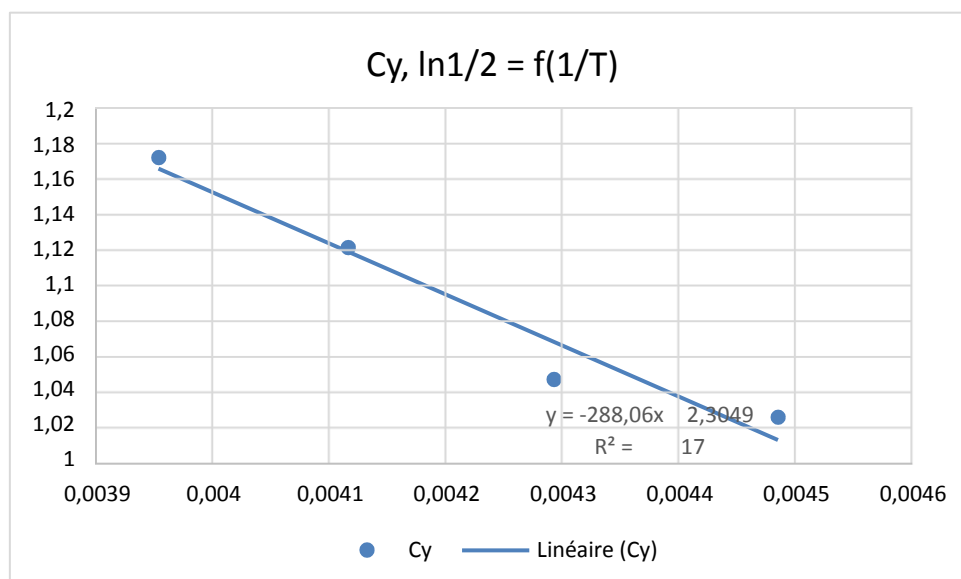
With $\Delta G_0 = \Delta H_0 - T\Delta S_0$

$$\Delta G_0^{298} = -3.31 \text{ kJ.mol}^{-1}$$

$$\Delta G_0^{213.15} = -2.22 \text{ kJ.mol}^{-1}$$

Compound 2 H[PO-Cy]

T (K)	Integral Form 1	Integral Form 2	ln(1/2)	1/T
253	3,23	1	1,17248214	0,00395257
243	3,07	1	1,12167756	0,00411523
233	2,85	1	1,04731899	0,00429185
223	2,79	1	1,0260416	0,0044843



$$\Delta H_0 = 2393.8 \cdot 10^{-3} \text{ kJ.mol}^{-1}$$

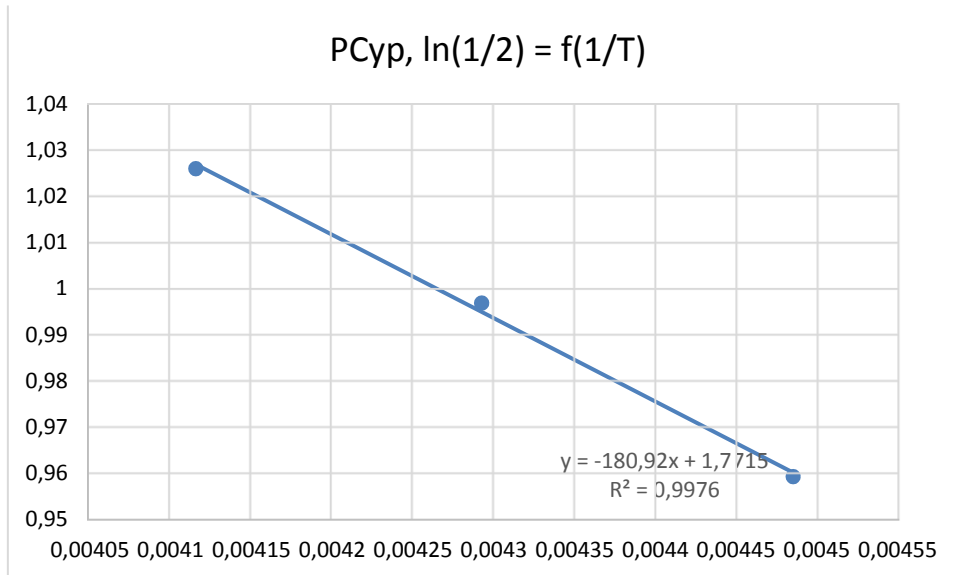
$$\Delta S_0 = 19.15 \text{ J.mol}^{-1}$$

$$\Delta G_0^{298} = -3.31 \text{ kJ.mol}^{-1}$$

$$\Delta G_0^{213.15} = -1.69 \text{ kJ.mol}^{-1}$$

Compound 3 H[PO-Cyp]

T	Integral Form 1	Integral Form 2	ln(1/2)	1/T
243	2,79	1	1,0260416	0,00411523
233	2,71	1	0,99694863	0,00429185
223	2,61	1	0,95935022	0,0044843



$$\Delta H_0 = 1503.45 \cdot 10^{-3} \text{ kJ.mol}^{-1}$$

$$\Delta S_0 = 14.709 \text{ J.mol}^{-1}$$

$$\Delta G_0^{298} = -2.88 \text{ kJ.mol}^{-1}$$

$$\Delta G_0^{213.15} = -1.63 \text{ kJ.mol}^{-1}$$

Kinetic data

The activation parameters for the equilibrium have been determined according to equation (2), from the Eyring equation (1).

$$k = x \frac{k_B T}{h} e^{-\Delta G / RT} \quad (1)$$

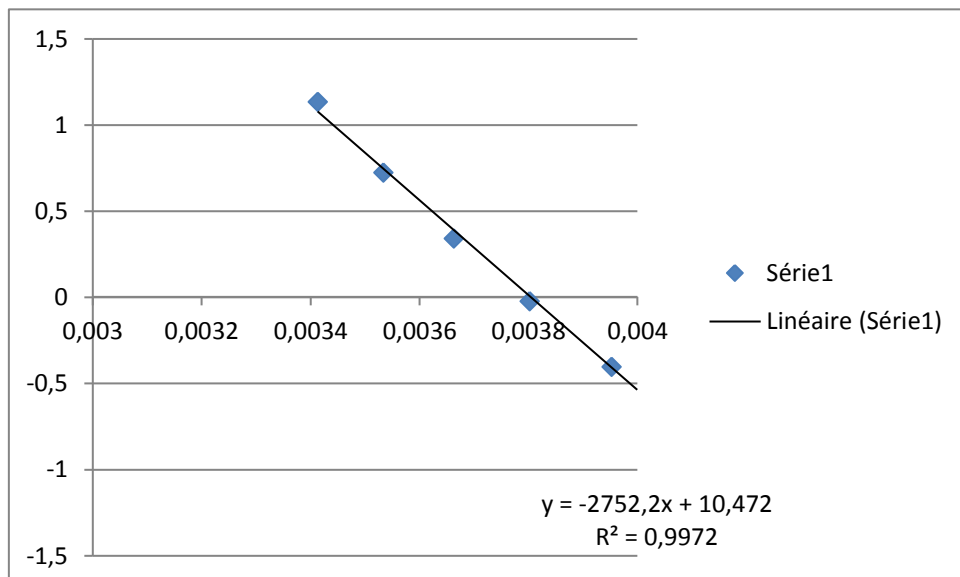
$$\log \frac{k}{T} = 10,32 - \frac{\Delta H}{4,58 T} + \frac{\Delta S}{4,58} \quad (2)$$

The rate constant k has been determined with DNMR software from Topspin 1.3

Compound 1 H[PO-iPr]

T (Kelvin)	k (s ⁻¹)
233	10
243	40
253	100
263	250
273	600
283	1500
293	4000

$$\log \frac{k}{T} = f\left(\frac{1}{T}\right) \text{ below}$$



$$-\frac{\Delta H}{4,58} = -2752,2$$

$$\Delta H = 12605 \text{ cal/mol}$$

$$\frac{\Delta S}{4,58} + 10,32 = 10,47$$

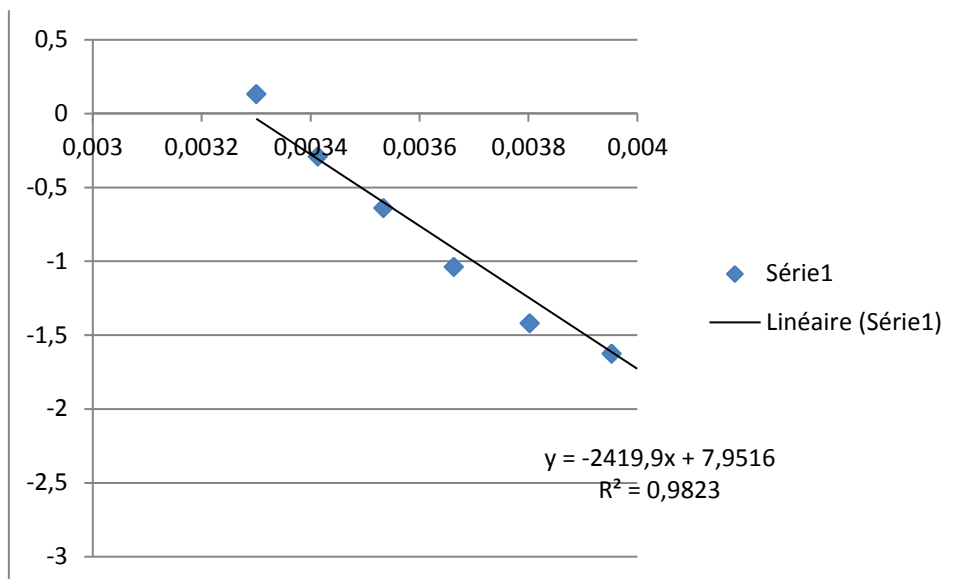
$$\Delta S = 0,69 \text{ cal/mol}$$

At 293 K: $\Delta G = 12605 - 293 (0,69) = 12,4 \text{ Kcal/mol} = 51.9 \text{ KJ/mol}$

Compound 2 H[PO-Cy]

T (Kelvin)	k (s^{-1})
233	1
243	3
253	6
263	10
273	25
283	65
293	150
303	410

$\log \frac{k}{T} = f\left(\frac{1}{T}\right)$ below



$$-\frac{\Delta H}{4,58} = -2419,9$$

$$\Delta H = 11083 \text{ cal/mol}$$

$$\frac{\Delta S}{4,58} + 10,32 = 7,95$$

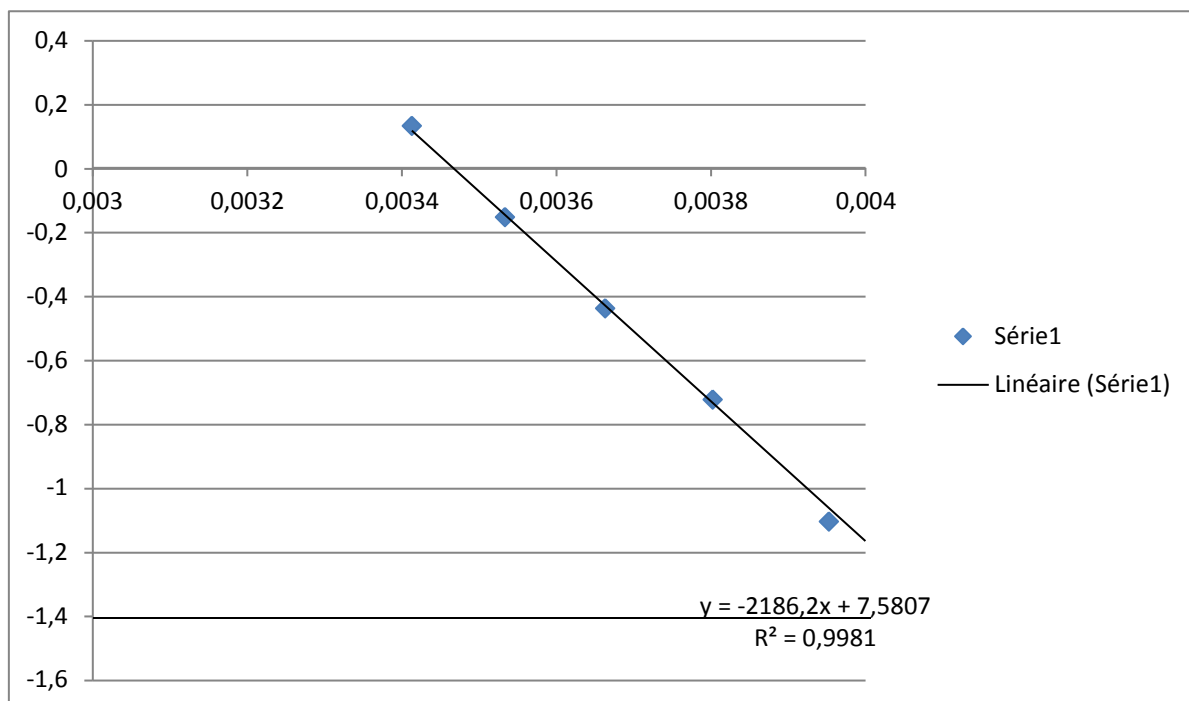
$$\Delta S = -10,85 \text{ cal/mol}$$

At 293 K: $\Delta G = 11083 - 293 (-10,85) = 14,3 \text{ Kcal/mol} = 59.8 \text{ KJ/mol}$

Compound 3 H[PO-Cyp]

T (Kelvin)	k (s ⁻¹)
243	10
253	20
263	50
273	100
283	200
293	400

$$\log \frac{k}{T} = f\left(\frac{1}{T}\right) \text{ below}$$



$$-\frac{\Delta H}{4,58} = -2186,2$$

$$\Delta H = 10013 \text{ cal/mol}$$

$$\frac{\Delta S}{4,58} + 10,32 = 7,58$$

$$\Delta S = -12,55 \text{ cal/mol}$$

At 293 K: $\Delta G = 10013 - 293 (-12,55) = 13,7 \text{ Kcal/mol} = 57.3 \text{ KJ/mol}$

X-Ray Analyses and Structural Figures

Data for **2** (CCDC 1846730), **3** (CCDC 1846732) and **4** (CCDC 1846731) were collected at low temperature (100 K) on a *Bruker Kappa Apex II* diffractometer using a microsource with a Mo-K α radiation ($\lambda = 0.71073\text{\AA}$) and equipped with an *Oxford Cryosystems Cryostream Cooler Device*.

The structures have been solved by Direct Methods using either SIR92 [1] or SHELXS97 [2], and refined by means of least-squares procedures on a F^2 with the aid either of the program SHELXL2016 [2] included in the softwares package WinGX version 1.63 [3] or with the software Crystals [4]. The Atomic Scattering Factors were taken from International tables for X-Ray Crystallography [5]. All hydrogens atoms were placed geometrically, and refined by using a riding model, except for the Hydrogen atom bonded to the Phosphorus atom which was located for each structure by Fourier differences. All non-hydrogens atoms were anisotropically refined. Drawing of molecules were performed with the program ORTEP32 [6] with 30% probability displacement ellipsoids for non-hydrogen atoms.

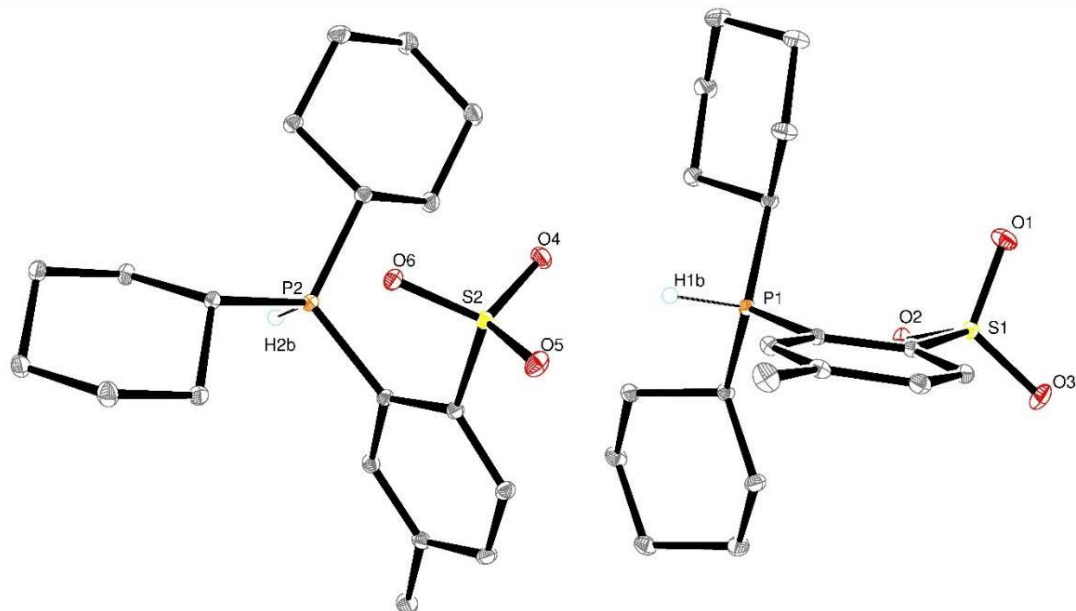


Figure S72. Molecular structure of **2**

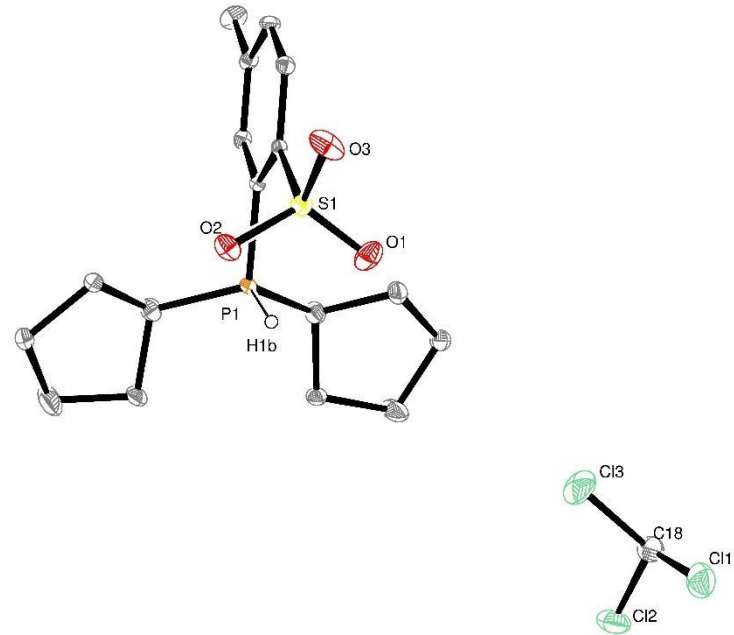


Figure S73. Molecular structure of 3

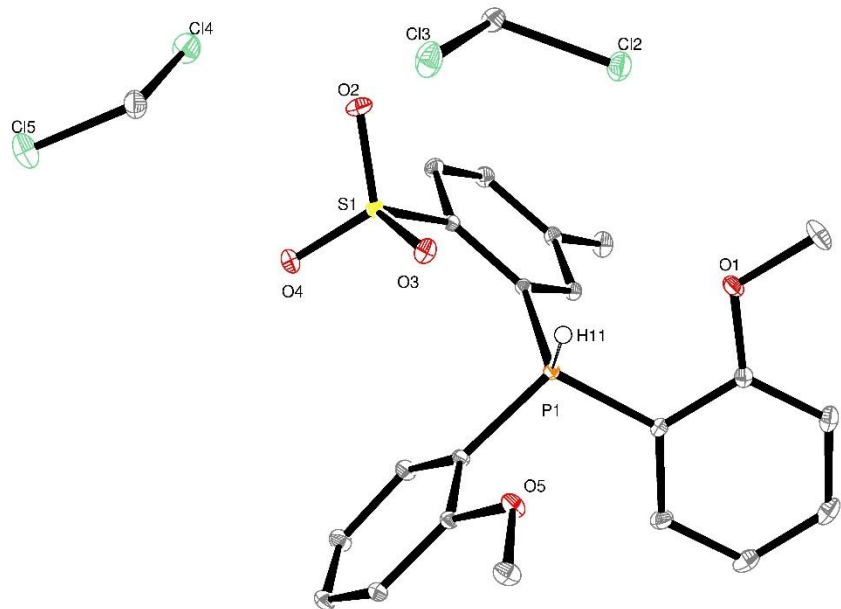


Figure S74. Molecular structure of 4

References

1. SIR92 - A program for crystal structure solution. A. Altomare, G. Cascarano, C. Giacovazzo and A. Guagliardi, *J. Appl. Crystallogr.* **1993**, *26*, 343-350.
2. WINGX - 1.63 Integrated System of Windows Programs for the Solution, Refinement and Analysis of Single Crystal X-Ray Diffraction Data. L.Farrugia, *J. Appl. Crystallogr.* **1999**, *32*, 837 - 838.
3. SHELX&SHELXTL programms - G. M. Sheldrick, *Acta Crystallogr., Sect. A: Found. Crystallogr.*, **2008**, *64*, 112-122.
4. CRYSTALS, P. W. Betteridge, J. R. Carruthers, R. I. Cooper, K. Prout and D. J. Watkin, *J. Appl. Crystallogr.*, **2003**, *36*, 1487.
5. INTERNATIONAL tables for X-Ray crystallography, **1974**, Vol IV, Kynoch press, Birmingham, England.
6. ORTEP3 for Windows - L. J. Farrugia, *J. Appl. Crystallogr.* **1997**, *30*, 565.